Functional analysis of the zebrafish caudal fin regeneration

Minshuo Lin

Thesis submitted to the Faculty of Graduate and Postdoctoral Studies
in partial fulfillment of the requirements for the degree

Master of Science

Department of Biology
Faculty of Science
University of Ottawa

Abstract

The caudal fin of zebrafish (*danio rerio*) is often used to study regeneration thanks to its extraordinary regenerative ability, easy access, and relative simplicity in structure. Branching morphogenesis is observed in many organs, including lungs and salivary glands in mammals, as well as the fin rays in zebrafish and is thought to follow unifying principles. An important developmental gene, *sonic hedgehog a (shha),* has been shown in other studies to play an essential role in the branch formation. Previous studies in our lab have shown that the transient depletion of the *shha*-expressing cells following laser ablation of the *shha*-expressing cells in the regenerating caudal fin results in a delay of fin rays branch formation. In order to study the long-term effect of ablating the *shha*-expressing cells, I generated a new zebrafish transgenic line (*Tg*)*(2.4shha:CFP-NTR-ABC)* to perform a conditional cell ablation using the Metronidazole/Nitroreductase (Mtz/NTR) system. Preliminary data suggest that cell ablation using the Mtz/NTR system is successful in the *Tg(2.4shha:CFP-NTR-ABC)* embryos. In addition, short-term ablation of the *shha*-expressing cells through Mtz/NTR system delays branch formation during caudal fin regeneration of the *Tg(2.4shha:CFP-NTR-ABC)* adult fish. Further work will involve the analysis of the effects of the long-term ablation of the *shha*-expressing cells and the involvement of other signaling pathways in the ray branching formation during zebrafish caudal fin regeneration. This study can provide insights into understanding of the molecular mechanisms underlying branching morphogenesis in various organs.

During the course of the above project, I have observed an organ-wide response to local injury in the zebrafish caudal fin. In this study, I have shown, for the first time, an immediate organ-wide response to partial fin amputation characterized by the damage of blood vessels,

nerve fibers and the activation of inflammatory response in the non-amputated tissues. I established that the adult zebrafish caudal fin serves as an excellent model for the study of the organ-wide response to local injury, and such study may provide new insights into the field of regenerative medicine in which stimulating regeneration locally may trigger responses in unintended locations.

Résumé

La nageoire caudale du poisson zèbre (*danio rerio*) est souvent utilisée pour étudier les mécanismes de régénération à cause de son extraordinaire capacité de régénération, son accès facile, et sa relative simplicité structurale. La morphogenèse de branches est observée dans plusieurs organes incluant les poumons et les glandes salivaires chez les mammifères ainsi que les rayons des nageoires du poisson zèbre et est supposée suivre des principes communs. Un important gène de développement, *sonic hedgehog a* (*shha*), joue un rôle essentiel dans la formation des branches. Des études précédentes effectuées dans notre laboratoire ont montré que l'absence transitoire des cellules exprimant *shha* dans des expériences d'ablation au rayon laser induit un délai de la formation des branches dans les rayons au cours de la régénération de la nageoire caudale. Afin d'étudier les effets de l'ablation à long terme des cellules exprimant *shha*, j'ai fait un nouvelle lignée transgénique de poisson zèbre *Tg(2.4shha:CFP-NTR-ABC)* pour effectuer une ablation cellulaire conditionnelle à l'aide du système Métronidazole / Nitroréductase (Mtz/NTR). Mes données préliminaires suggèrent que l'ablation cellulaire à l'aide du système Mtz/NTR fonctionne sur les embryons *Tg(2.4shha:CFP-NTR-ABC).* De plus, l'ablation à court terme des cellules exprimant *shha* à l'aide du système Mtz/NTR induit un délai de la formation des branches au cours de la régénération des rayons la nageoire caudale des poissons adultes *Tg(2.4shha:CFP-NTR-ABC).* Des études supplémentaires incluront l'analyse des effets de l'ablation à long terme des cellules exprimant *shha* et le rôle d'autres cascades de signalisation dans la formation des branches des rayons au cours de la régénération de la nageoire caudale du poisson zèbre. Cette étude pourrait fournir des informations concernant la compréhension des mécanismes moléculaires sous-jacents à la formation de branches dans des organes variés.

Au cours de l'étude décrite ci-dessus, j'ai fait l'observation d'une réponse globale de toute la nageoire caudale à une blessure locale. Dans cette étude, j'ai montré pour la première fois, une réponse immédiate et globale après amputation partielle de la nageoire. Cette réponse est caractérisée par des lésions des vaisseaux sanguins, des fibres nerveuses et par l'activation d'une réponse inflammatoire dans les tissus non-amputés. J'ai établi que la nageoire caudale du poisson zèbre adulte est un excellent modèle pour l'étude de la réponse globale d'un organe à une lésion locale. Une telle étude pourrait fournir de nouvelles informations pertinentes à la médecine régénérative qui, en visant à stimuler la régénération de façon locale, peut entraîner des réponses dans des domaines non voulus.

Table of Content

List of Figures

List of Abbreviations

Bmp	Bone morphogenetic protein
CFP	Cyan Fluorescent Protein
Col10	Type X Collagen
DEPC	diethylpyrocarbonate
Dhh	Desert hedgehog
DMSO	Dimethyl sulfoxide
DNA	Deoxyribonucleic Acid
Dpa	Days post amputation
EGFP	Enhanced Green Fluorescent Protein
Fgf	Fibroblast growth factor
Fgfr	Fibroflast growth factor receptor
GFP	Green Fluorescent Protein
Hh	Hedgehog
hpa	Hours post amputation
Ihh	Indian hedgehog
ISH	*In situ* hybridization

IHC	Immunohistochemistry
Mtz	Metronidazole
mM	Millimolar
mpa	Minutes post amputation
mRNA	Messenger Ribonucleic Acid
mpx	Myeloperoxidase
NTR	Nitroreductase
PCR	Polymerase Chain Reaction
PBS	Phosphate Buffered Saline
PBST	Phosphate Buffer Saline/ 0.1%Tween-20
PFA	Paraformaldehyde
Ptch	Patched
Runx	Runt-related transcription factor
Shha	Sonic hedgehog
Spry	Sprouty
Smo	Smoothened
Tg	Transgenic line

Twhh	Tiggy-winkle hedgehog
WT	Wild type
ZPA	Zone of polarizing activity

Acknowledgement

Firstly, I would like to thank my supervisor Dr. Marie-Andrée Akimenko and the advisory committee members: Dr. Marc Ekker and Dr. Anne-Gaelle Rolland-Lagan for their advice and help. The special thank goes to Jing Zhang, for the technical support and research advice in the lab as well as tremendous help outside the lab. To Ali Al-Rewashdy, Daniel Moses, Stephanie McKay, Rob Lalonde, Shahram Eisa-Beygi, Raymond Kwong, Shengrui Feng, Abid Ismail, Siavash Darbandi, Rafael Godoy, Sandra Noble, Lei Xing, Eglantine Heude, Vishal Saxena, I appreciate your kindness, hard work and cooperation. I would also like to thank temporary researchers who have helped me in the lab: Suzanne Gerdis, Rémi Blais, Tim Xu, Weishi Liu, Jordan Albino, Alyssa Kositpaiboon, Yan Li, Léa Guinot, Samuel Drapeau, Wenyu Wu, and Kewen Li. To my girlfriend Moxi Zhang, thank you for your love and support. In addition, I am willing to extend my thanks to Dr. Zilong Wen (Hong Kong University of Science and Technology), Dr. Augustine Choi (Harvard Medical School) for the gift of the transgenic fish and Dr. Jennifer Moss (Duke University), Dr. Robert Tanguay (Oregon State University) for the help in the experimental protocols. Finally, I would like to express my deep and sincere respect and gratitude to zebrafish; I wish humans could benefit from the knowledge of the regenerative medicine acquired from zebrafish as soon as possible.

Preamble

This thesis contains three chapters that are under a broad research topic of regeneration. The first chapter is a general introduction on adult zebrafish caudal fin regeneration. In this chapter, I demonstrate the importance of regeneration studies, and I explain reasons why zebrafish and zebrafish caudal fin are chosen as my research models. In addition, I describe regeneration processes of the adult zebrafish caudal fin.

Chapter II is about the project of the functional analysis of *shha*-expressing cells during zebrafish caudal fin regeneration. My gene of interest is *shha*, which has proved to be an essential regulator in the branch formation of various organs. Researchers in our lab have previously shown that transient ablation of *shha*-expressing cells results in a branch delay of fin rays. However, the effects of the long-term ablation of *shha*-expressing cells have not been analyzed. Hence, I took over this project from a former MSc student (Shirine Jeradi). My aims were to establish a transgenic line for the durably ablation of the *shha*-expressing cells, and analyze the effects of ablation of the *shha*-expressing cells in the regenerating caudal fin.

Chapter III is the analysis of the consequences of a local injury of the caudal fin on the rest of the fin. This project was undertaken when, in the course of the project described in Chapter II, I observed an organ-wide response to local injury in the zebrafish caudal fin. -No one had previously examined whether partial or local injury of the zebrafish caudal fin induces an organ-wide injury response. My aims were to characterize this organ-wide injury response after local injury in the zebrafish caudal fin, with the help of various available zebrafish transgenic lines.

Chapter I: General Introduction

1.1 Regeneration

All animals are prone to injury. Injury can trigger coordinated cellular and molecular responses that will initiate the regeneration processes such as cell recruitment, cell proliferation, and immunological responses, which allow the partial or complete replacement of the lost tissues/organs (Rennert *et al.,* 2012). Key goals of regeneration studies are to understand the injury response and the cellular events that lead to the regenerative repair, which may foster the broad new field of regenerative medicine (Poss, 2010).

Regeneration has been divided into two categories: the epimorphic regeneration and the morphallactic regeneration (Morgan, 1901). Epimorphic regeneration requires cell proliferation and the formation of the blastema (a proliferative mass of undifferentiated precursor cells); whereas, morphallactic regeneration is mainly processed by remodeling of the pre-existing tissues and does not require cell proliferation (Morgan, 1901).

The term "Regenerative Medicine" was first used about two decades ago (Kaiser, 1992). Since then, regenerative medicine has become an intriguing research field that appeals to many developmental and molecular biologists. The overall aim for researchers in this field is to identify strategies to repair tissues or organs that cannot be naturally regenerated in humans, because humans lack the regenerative ability in essential systems such as the central nervous system (e.g. brain) and limbs (Alvarado, 2012; Nachtrab and Poss, 2012; Tal *et al.*, 2010). Some invertebrate and vertebrate organisms, such as planarian and zebrafish, respectively, have better regenerative capacity (Alvarado 2012; Nachtrab and Poss, 2012). There are two hypothese as to why species have different regenerative ability (Alvarado,

2012; Johnson and Voss, 2013; Seifert and Voss, 2013). One hypothesis is that all animals had the capacity to regenerate but this regenerative capacity has been lost during during evolution in certain species. Another hypothesis is that the regenerative capacity is not evolutionarily ancestral, meaning that certain species somehow acquire the regenerative capacity (Alvarado, 2012). No matter how regenerative ability evolved among species, it is believed that we can identify the mechanisms driving regeneration and improve the regenerative ability in humans, so that we can find strategies to repair lost tissues or organs for the human health (Andersson and Lendahi, 2009; Alvarado 2012).

1.2 Animal models for regeneration study

1.2.1 Available animal models

There are several vertebrate and invertebrate animal models and plant models for the study of regeneration (Figure 1.1; Nachtrab and Poss, 2012). Freshwater planarian is an excellent invertebrate animal model due to its remarkable regenerative ability for all of its tissues, including tissues derived from endoderm, mesoderm and ectoderm. Furthermore, planarians share with vertebrates all of the major developmental signaling pathways that are essential for the formation of the bilateral body plan, making an ideal model in regeneration study (Almuedo-Castillo *et al.*, 2012; Alvarado, 2004; Elliott and Alvarado, 2012). Urodele amphibians (including axolotl and salamander) or anuran amphibians (including frog tadpoles) are excellent vertebrate animal models for regeneration study. Axolotls and salamanders have remarkable regenerative ability as they are able to regenerate their limbs, tail, lens, retina, and heart tissues at any time of their life cycle (Han *et al.*, 2005; Yokoyama, 2008). In contrast, the regenerative ability of limbs in frogs undergoes an ontogenic decline; the regenerative ability is stage-dependent as younger animals regenerate better than older ones (Lin *et al.*,

2013). Due to this stage-dependent regenerative ability, frogs serve as an ideal animal system to study the progressive loss of regenerative ability (Beck *et al.*, 2009).

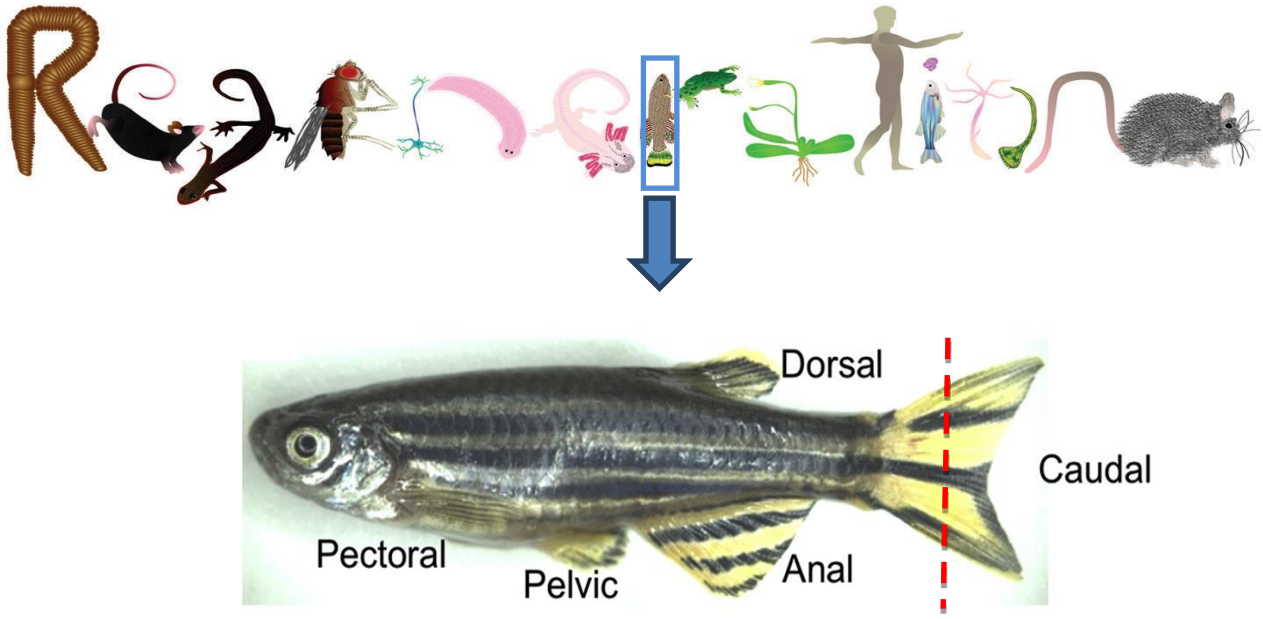
Dorsal
Caudal
Pectoral
Pelvic
Anal

Figure 1.1 Animal and plant models used for the study of regeneration (Modified from Nachtrab and Poss, 2012; Nachtrab *et al.*, 2011).

A: From left to right: Annelid, mouse, newt, *Drosophila*, planarian, axolotl, killifish, *Xenopus*, *Arabidopsis*, human, zebrafish, Hydra, *Stentor coeruleus*, African spiny mouse. B: Five types of fins in the adult zebrafish, including a pair of pectoral fins, a pair of pelvic fins, the dorsal fin, the anal fin and the caudal fin. The red dotted line on the caudal fin indicates the amputation plane. Permission to reproduce obtained from publisher.

1.2.2 Zebrafish model

The zebrafish (*Danio rerio*) is a small freshwater teleost fish that was originally found in slow streams and rice paddies in the Ganges region in Eastern India. In 1981, a publication in the journal Nature demonstrated methods for mutational and genetic analysis of zebrafish embryos, which opened the world of zebrafish research (Streisinger *et al.*, 1981). Zebrafish have many advantages for embryonic and genetic analyses that surpass other animal models, including the high fertility rate (each pair can lay hundreds of eggs per day), the low maintenance cost, the rapid external development, and the transparent embryos. These characteristics make the zebrafish amenable to genetic and cellular manipulations, making it a powerful model to assess gene function *in vivo*. For example, the rapid external development and the transparency of zebrafish embryos make it possible to directly observe the developmental processes in the organism. More importantly, the use of transgenic zebrafish that contains fluorescent reporter genes, allows *in vivo* analysis of the spatial and temporal expression of genes. Similarly, fins of adult zebrafish being very thin, fluorescent reporters can easily be used for *in vivo* analysis as the fin regenerates. Furthermore, the full genome of the zebrafish has been sequenced. Genome sequence analysis indicates that 70% of the human genes have a counterpart in zebrafish. These advantages have made the zebrafish a very popular and valuable vertebrate research model for the study of developmental biology over the past three decades (Westerfield, 2000; Detrich *et al.*, 1999; Howe *et al.*, 2013).

Aside from being a great model for the developmental biology, the zebrafish has an extraordinary regenerative ability throughout its life that makes it an ideal animal model for the study of regeneration. So far, many studies have shown that zebrafish are able to regenerate scales, optic nerves, heart, retina, kidney, spinal cord, brain, pancreas, sensory hair

cells, liver and all types of fins (Tal *et al.*, 2010; Vrieze *et al.*, 2011; Poss *et al.*, 2002; Raya *et al.*, 2004; Johnson and Weston, 1995; Akimenko *et al.*, 2003; Bernhardt *et al.*, 1996; Becker and Becker, 2002; Sadler *et al.*, 2007; López-Schier and Hudspeth, 2005; Becker *et al.*, 2004; Sire *et al.*, 2000; Reimschuessel, 2001; Kizil *et al.*, 2012; Zupanc, 2001; Zupanc and Sîrbulescu, 2013; Moss *et al.*, 2009; Andersson *et al.*, 2012).

1.3 Fin Regeneration

1.3.1 Zebrafish fins morphology

Zebrafish have five types of fins, including a pair of pectoral fins, a pair of pelvic fins, one dorsal fin, one anal fin and one caudal fin. All fins have the capability to regenerate after injury (Figure 1.1; Nachtrab *et al.*, 2011). The caudal fin is often used to study regeneration, mainly due to its many advantages: it is easily accessible, fin amputation does not impair the survival of the fish, the fin rapidly regenerates (the injured fin can fully regenerate lost tissues in three weeks at 28.5°C) and it has a relatively simple structure (Akimenko *et al.*, 2003).

Each fin is made of fin rays. Fin rays are the major exoskeleton components of the adult zebrafish fins. The adult zebrafish caudal fins contain 16 to 18 fin rays. Each fin ray (lepidotrichia) is composed of two hemirays that are concave dermal bones facing each other, enclosing the intraray mesenchyme that contains fibroblasts, blood vessels, axons and glial cells, osteoblasts, bone matrix, and pigment cells (Figure 1.2; Santamaria *et al.*, 1992; Johnson and Weston, 1995; Huang *et al.*, 2003; Tu and Johnson, 2011; Akimenko *et al.*, 2003). Each hemiray is made of a succession of bone segments, and the sequential addition of new segments of bone to the distal end of each fin ray ensures the growth of the fin in length throughout the life of the zebrafish (Figure 1.2; Becerra *et al.*, 1983; Haas,1962; Akimenko *et*

al., 2003). In teleost fish, the distal border of the tail fin is supported by rigid unmineralized fibrils, named actinotrichia and composed of collagen and actinodin (Figure 1.2; Becerra *et al.*, 1983; Akimenko *et al.*, 2003; Zhang *et al.*, 2010).

During the growth of the zebrafish caudal fin, each fin ray can form successive bifurcations except the two most lateral rays. During the formation of the bifurcation, one fin ray forms two sister fin rays from the bifurcation point or the origin of bifurcation, and two sister fin rays have the same component as the fin ray before the formation of the bifurcation (Figure 1.2; Akimenko *et al.*, 2003; Poss *et al.*, 2003).

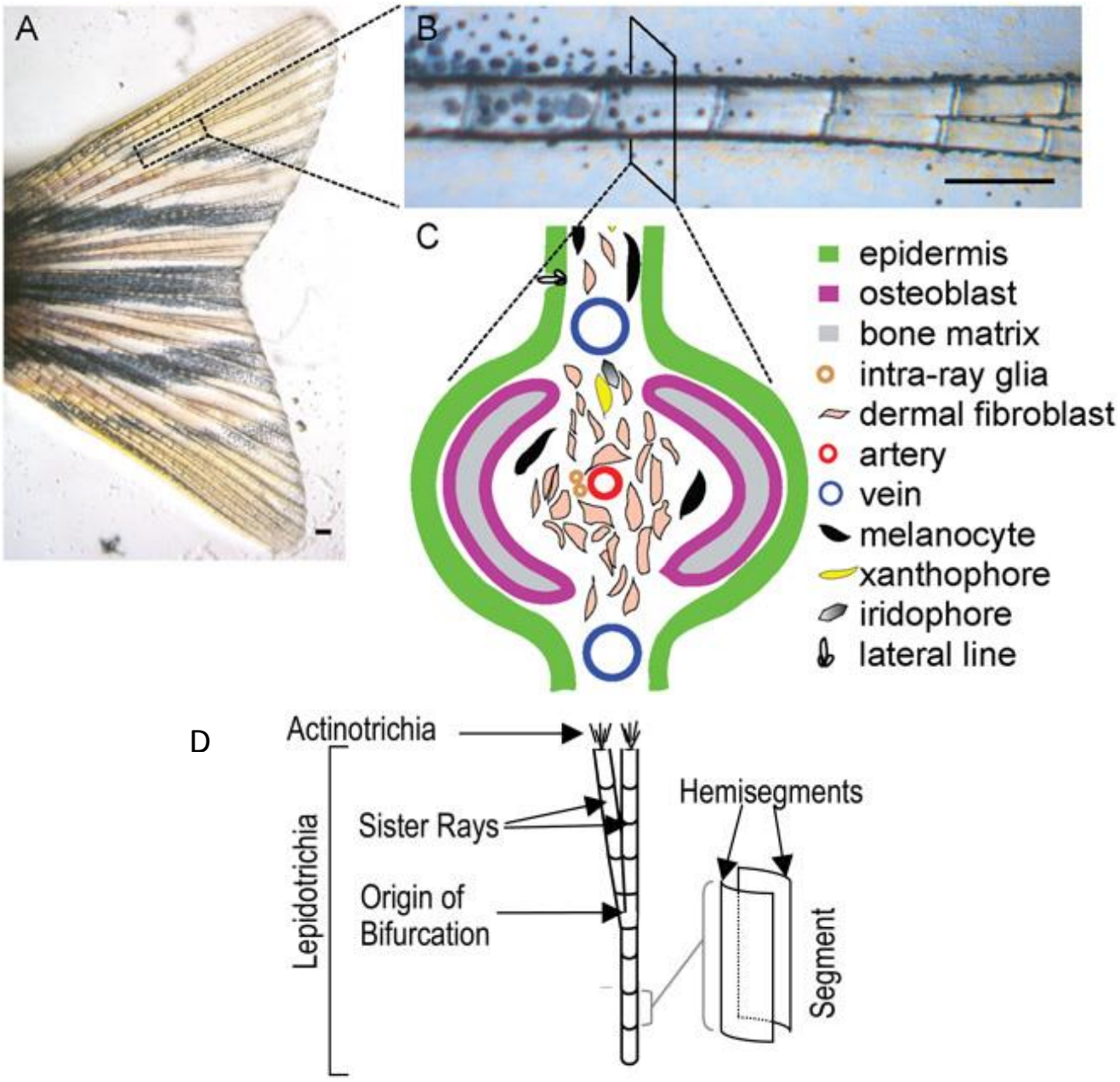
A
B
C
epidermis
osteoblast
bone matrix
intra-ray glia
dermal fibroblast
artery
vein
melanocyte
xanthophore
iridophore
lateral line
D
Actinotrichia
Lepidotrichia
Sister Rays
Origin of
Bifurcation
Hemisegments
Segment

Figure 1.2 Anatomy of the caudal fin and fin rays and schematic representation of the cell types in the zebrafish caudal fin (Adapted from Tu and Johnson, 2011; Akimenko *et al.*, 2003).

A: Adult zebrafish caudal fin. B: Close-up of one fin ray in the caudal fin. The fin ray (lepidotrichia) is made of a succession of bone segments. Scale bars, 0.2 mm. C: Schematic representation of the cross section of a single fin ray showing the different cell types. D: Schematic representation of the dermal skeleton of a zebrafish fin ray. The lepidotrichia is made of two concave hemirays. Hemirays are composed of hemisegments, facing each other. Actinotrichia are located between the distal-most hemisegments of the lepidotrichia. During fin growth and regeneration, fin rays bifurcate, forming two sister rays. Permission to reproduce obtained from publisher.

1.3.2 Zebrafish caudal fin regeneration

Upon amputation of the caudal fin, regenerative mechanisms are activated and the complete regeneration process takes about three weeks at 28°C (Akimenko *et al.*, 2003). The regeneration process has three steps, starting from wound healing in the first 0-12 hours post amputation (hpa), followed by blastema formation at 12-48 hpa and regenerative outgrowth after 48 hpa (Figure 1.3; Poss *et al.*, 2003).

The wound is healed by the migration of epithelial cells to the wound and these cells form the epithelial cap (or wound epidermis) (Figure 1.4; Poss *et al.*, 2003). Bromodeoxyuridine (BrdU) incorporation assays show that this response does not involve cell proliferation (Poleo *et al.*, 2001).

Between 12 and 24 hpa, the wound epidermis thickens, becomes multi-layered, and completely covers the amputation site (Figure 1.4; Poleo *et al.*, 2001; Akimenko *et al.*, 2003). This process is dominated by disorganization and migration events from the mesenchymal tissue underneath the wound epidermis, not by cell proliferation (Poss *et al.*, 2003). Meanwhile, various cell types in the mesenchymal tissue, such as osteoblasts (also known as scleroblasts, the bone-forming cells), undergo dedifferentiation and these cells migrate distally (Tu and Johnson, 2011; Knopf *et al.*, 2011). These cells form the blastema, which is a group of undifferentiated cells. Between 24-48 hpa, un-differentiated cells accumulate to the fin blastema, which is newly formed distal to the amputation plane. These blastema cells can proliferate (Figure 1.4; Akimenko *et al.*, 2003) and the formation of the blastema in the caudal fin represents the hallmark of epimorphic regeneration. The blastema is divided in two compartments: the proximal blastema that is composed of highly proliferative cells and the

distal blastema that is composed of non- or slow- proliferative cells (Figure 1.4; Poleo *et al.*, 2001; Akimenko *et al.*, 2003; Poss *et al.,* 2003).

The regenerative outgrowth process, after 48 hpa, involves massive proliferation and differentiation of blastemal cells to replace the missing tissues (Akimenko *et al.*, 2003; Poss *et al.,* 2003). Recent studies have shown that the blastema cells are not multipotent, meaning that one type of cell in the blastema is not able to give rise to all cell types (Tu and Johnson, 2011). The blastemal cells' lineages retain fate restriction, meaning that one type of cell that dedifferentiate and migrate to contribute to the blastemal cell, can only re-differentiate into the same cell type of its own lineage (Tu and Johnson, 2011; Knopf *et al.*, 2011). For example, mature osteoblasts undergo dedifferentiation and migration to the blastema during the phase of the blastema formation, and then those un-differentiated cells proliferate and can only give rise to osteoblasts in the fin regenerate during the phase of the regenerative outgrowth, indicating that osteoblasts do not change their fate during regeneration (Knopf *et al.*, 2011). As the regenerative outgrowth continues, the blastema grows distally and regenerating rays are visible by 3 dpa (Figure 1.4; Akimenko *et al.*, 2003). By 6 dpa, each ray is regenerating at a differential rate according to its position in the fin. The longest fin rays (normally the dorsal and the ventral fin ray No. 3) regenerate at the fastest rate and central fin rays (normally the dorsal or the ventral fin rays No. 8 or No. 9) regenerate at the slowest rate (Figure 1.4; Akimenko *et al.*, 2003).

Zebrafish fin rays are dermal bones and the regeneration of the dermal bones involves the differentiation zone, which is located proximal to the proximal blastema. The differentiation zone has a moderate proliferative activity. Osteoblasts are re-differentiated in a proximo-

distal manner (Poss *et al.*, 2003). Dermal bones are also known as intramembranous bones. They are formed without a cartilage intermediate. During the formation of the intramembranous bones, intramembranous ossification is initiated from mesenchymal condensation. Mesenchymal progenitor cells differentiate into osteoblasts, secreting the bone matrix and bone matrix will mineralize and form the intramembranous bones (Avaron *et al.*, 2006). The regeneration of zebrafish caudal fin rays follows in a unidirectional manner (Akimenko *et al.*, 2003).

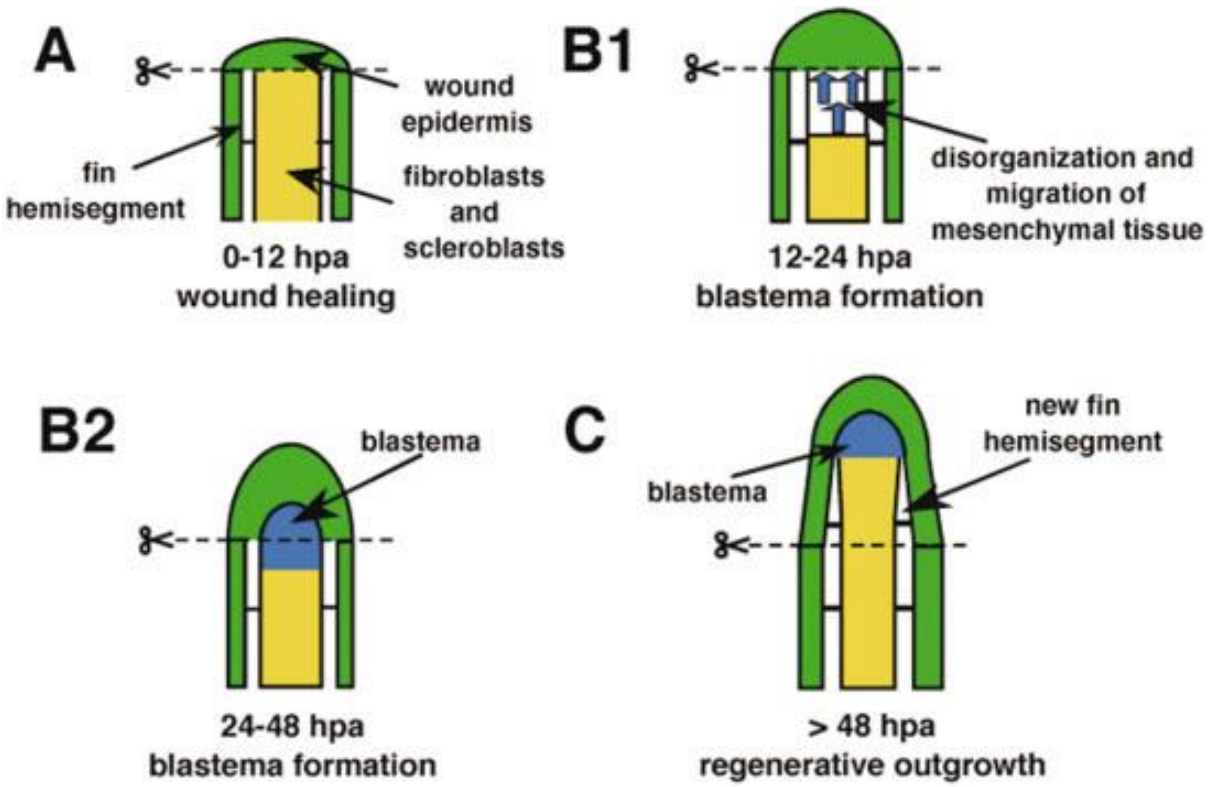
A
wound
epidermis
fin
hemisegment
fibroblasts
and
scleroblasts
0-12 hpa
wound healing
B1
disorganization and
migration of
mesenchymal tissue
12-24 hpa
blastema formation
B2
blastema
24-48 hpa
blastema formation
C
new fin
hemisegment
blastema
> 48 hpa
regenerative outgrowth

Figure 1.3 Schematic representation of stages of fin regeneration depicted as longitudinal sections through a caudal fin (Adapted from Poss *et al.*, 2000).

The distal end of the fin ray is at the top. The amputation plane is shown by the dashed line. A: Wound healing process: The wound is closed within 12 hours post amputation (hpa) by migrating epithelial cells. B1: Blastema formation, disorganization of mesenchymal tissue: Between 12-24 hpa, the wound epidermis thickens, mesenchymal tissue between hemirays disorganizes, and cells migrate distally. B2: Blastema formation: Between 24-48 hpa, the blastema, a mass of undifferentiated and proliferative mesenchymal cells, is formed distal to the amputation plane. C: Regenerative outgrowth: Blastemal cells proliferate and differentiate to replace missing structures. Permission to reproduce obtained from publisher.

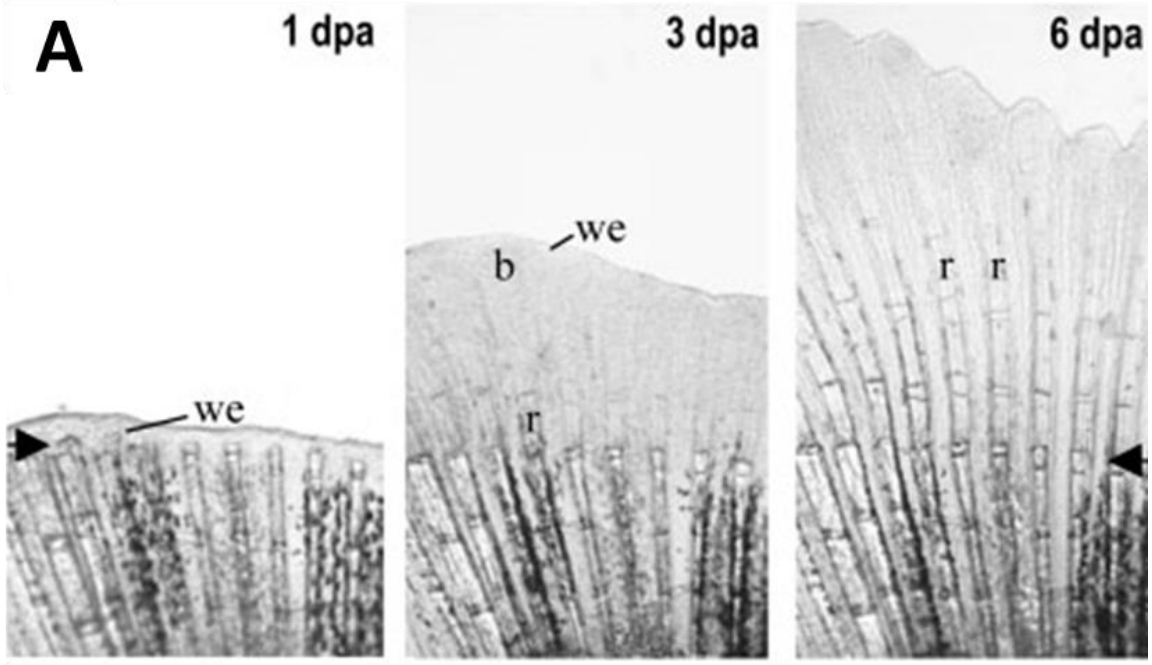
A
1 dpa
3 dpa
6 dpa
we
we
b
r
r r

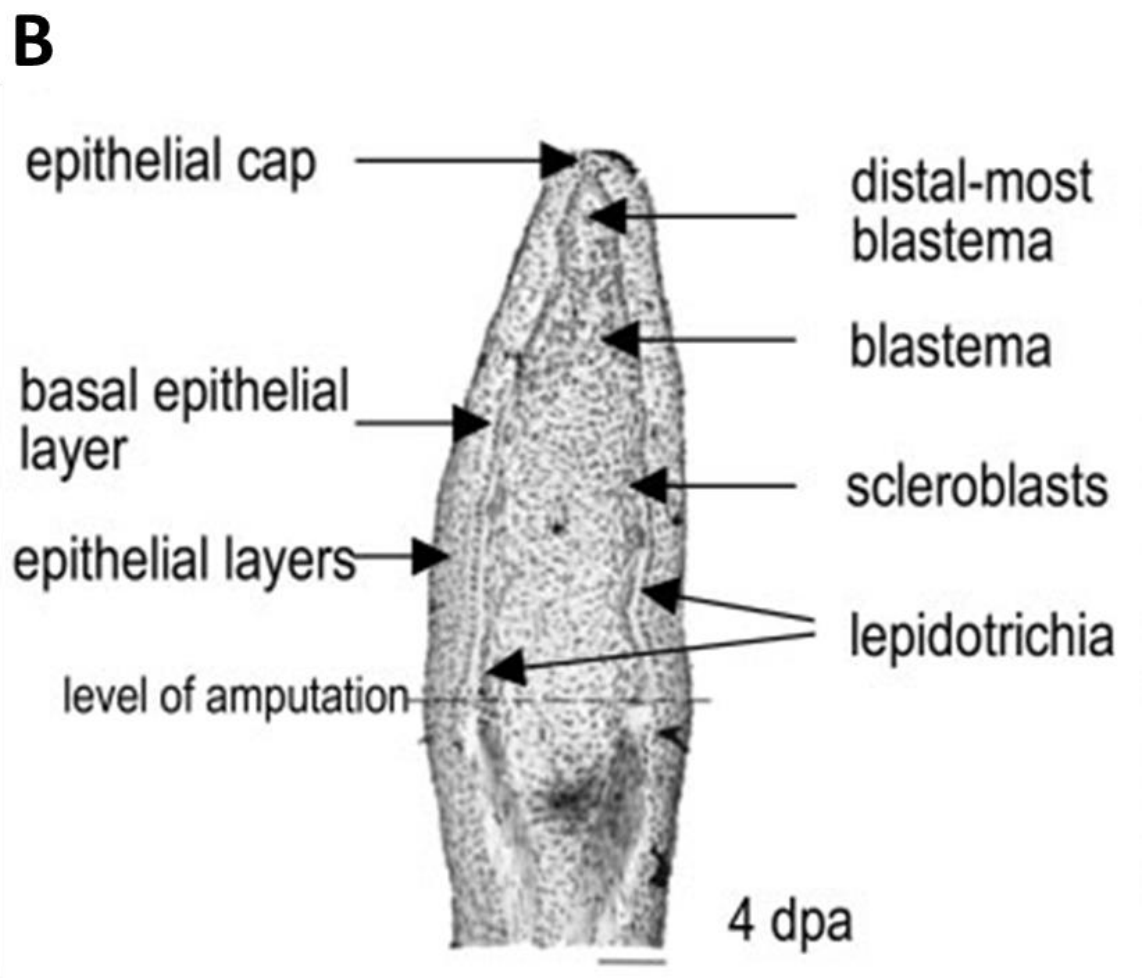
B
epithelial cap
distal-most blastema
blastema
basal epithelial layer
scleroblasts
epithelial layers
lepidotrichia
level of amputation
4 dpa

Figure 1.4 A regenerating adult zebrafish caudal fin at various time points following amputation (Adapted from Akimenko *et al.*, 2003; Poleo *et al.*, 2001).

A: Whole-mounts of the same caudal fin regenerate at 1, 3, 6 days post amputation (dpa). The arrows indicate the amputation plane. The wound epidermis (we) completely covers the amputation site by 1 dpa. By 3 dpa, the blastema grows distally and regenerating rays are visible. Rays are separated by soft tissue in the interray region. By 6 dpa, each ray is regenerating at a differential rate according to its position in the fin. Central rays are already shorter than lateral rays in accordance with the caudal fin pattern that will be produced. B: Proximodistal section of a 4 dpa caudal fin regenerate stained with hematoxylin. The epithelial cap is at the most distal region of each regenerating fin ray and above the distal-most blastema and blastema. In the proximal part of the regenerate underneath the blastema, cell differentiation has already started. Osteoblasts line the lepidotrichial bone matrix on its inner surface in the distal part of the regenerate and are distributed on the inner and outer surfaces of the bone in the proximal part of the regenerate (not visible at this magnification). Permission to reproduce obtained from publisher.

Every fin ray is vascularized. One artery is running in the center of each fin ray and two veins run along the lateral sides of the ray; the intervessel commissures within one fin ray connect the artery to veins as well as veins to veins; the interray vessels connect veins to veins of adjacent rays (Figure 1.5; Huang *et al.*, 2003). *In vivo* analysis of blood vessel regeneration during caudal fin regeneration has been described using the reporter transgenic fish line *Tg(fli1:EGFP*), in which the regulatory region of the *fli1* gene, drives the expression of the fluorescent reporter, enhanced green fluorescent protein (EGFP) (Lin, 2000; Lawson and Weinstein, 2002; Huang *et al.*, 2003). *fli1* is a known endothelial cell marker in mouse (Melet *et al.*, 1996) and is also expressed during vascular development in zebrafish embryos (Thompson *et al.*, 1998). *Tg(fli1:EGFP*) recapitulates the endogenous *fli1* expression pattern in endothelial cells throughout normal development and fin regeneration (Brown *et al.*, 2000; Lawson and Weinstein, 2002; Huang *et al.*, 2003).

Upon amputation the caudal fin, the morphogenetic mechanisms for blood vessels regeneration are activated, including vessel healing in 1 dpa, artery–vein anastomosis during 1-2 dpa, plexuses formation and remodeling during 3-4 dpa, intervessels pruning during 4-8 dpa, and late regenerative angiogenesis after 8 dpa, leading to the blood vessels network observed in the intact fin (Figure 1.5; Risau, 1997; Huang *et al.*, 2003).

Immediately after injury in the caudal fin, little bleeding is seen when the severed ends of arteries and veins are opened. Bleeding stops within an hour by blood clot. By 1 dpa, injured vessels are healed and appeared to be rounded at the vessels ends suggesting the close-off of the severed vessels. By 2 dpa, anastomoses between the wounded arteries and veins occur. Blood vessels in the amputated fin rays show reconnecting bridges between arteries and veins and blood flow resumes in all the anastomotic bridges. By 4 dpa, sprouts at the newly formed

bridge extend distally, forming the vascular plexuses. The vascular plexuses show numerous connections with neighboring vessels, suggesting the active blood vessels regeneration. However, arteries and veins cannot be identified in those early regenerating vascular plexuses because there is no clear morphological difference. By 8 dpa, intervessel pruning removes excess intervessel commissures during early plexus formation. Meanwhile, the unstructured regenerating vessels are gradually remodeled to form arteries and veins at more proximal levels. Following remodeling, blood can flow distally in the newly regenerated arteries and veins, indicating that basic vein–artery–vein architecture is reestablished in fin regenerates. In addition, no plexuses are present in distal regenerates at 8 dpa. After 8 dpa, sprouts still actively extend distally and blood vessels continue to regenerate until the normal vasculature pattern is regenerated (Figure 1.5; Huang *et al.*, 2003).

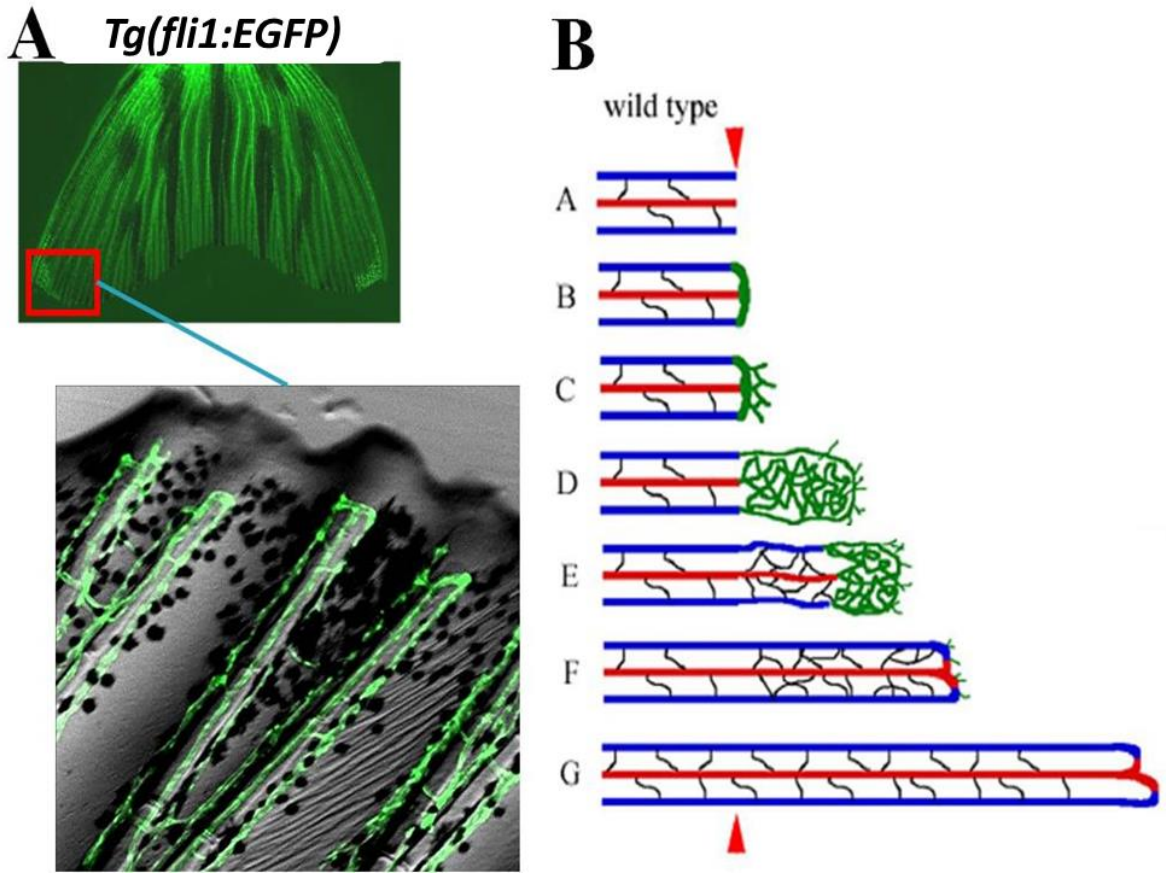
A
Tg(fli1:EGFP)
B
wild type
A
B
C
D
E
F
G

Figure 1.5 Blood vessels distribution and regeneration processes after amputation.

A: *Tg(fli1:EGFP)* labels the endothelium of the blood vessels of the caudal fin, where one artery is running in the center of each ray and two veins are along the side of the fin. B: Summary cartoon of stages of blood vessel regeneration process after fin amputation (Adapted from Huang *et al.*, 2003). The red triangle indicates the amputation plane. The red and blue lines depict arteries and veins, respectively. Black lines depict inter-vessel commissures. (A) After amputation, the regenerating vessels heal their ends by 1 dpa. (B) By 2 dpa, anastomosis or the bridge formation between the artery and the veins occurs. Blood flow to the wound site is restored. (C, D) Blood vessels outgrow to form plexuses and plexuses undergo remodeling from the 3-4 dpa. (E) The newly formed arteries and veins appear to have denser intervessel commissures than non-regenerating vessels. New vessels undergo intervessel pruning from 4 dpa onward (E–G). The regenerating blood vessels stop plexus formation at around 8 dpa but continue to grow by late regenerative angiogenesis (F). By about 35 dpa, the density of intervessel commissures has returned to the normal level (G). Permission to reproduce obtained from publisher.

Chapter II: Functional Analysis of *shha*-expressing Cells in Zebrafish Caudal Fin Regeneration

2.1 Introduction

2.1.1 Hedgehog signaling pathway and role of Shh during embryonic development

The Hedgehog (Hh) signaling pathway was first identified in *Drosophila melanogaster* in the early 1990s (Nusslein-Volhard and Wieschaus, 1980; Lee *et al.*, 1992; Mohler and Vani, 1992; Tabata *et al.*, 1992; Tashiro *et al.*, 1993). Hh proteins are intercellular signaling proteins that play important roles in many fundamental processes during embryonic development, including the growth, patterning, and morphogenesis of many different regions of vertebrates and invertebrates (Ingham and McMahon, 2001).

In mammals, Hh proteins are Sonic Hedgehog (SHH), Indian Hedgehog (IHH) and Desert Hedgehog (DHH). They are secreted proteins that activate signaling pathways initiated by their binding to receptors, Patched 1 (PTCH1) and Patched 2 (PTCH2), the 12-transmembrane proteins (Echelard *et al.*, 1993). Mutation or deletion of the extracellular domains of PTCH reduces or abolishes the responsiveness of cells to Hh (Mullor and Guerrero, 2000; Briscoe *et al.*, 2001). In *Drosophila melanogaster*, Hh proteins binding to their receptors, can induce a conformational change of PTCH, releasing the inhibition of the seven-transmembrane protein Smoothened (SMO) and subsequent activation of the zinc finger transcription factor Cubitus interruptus (Ci) (Ho and Alman, 2010). The Hh signaling

pathway causes the dissociation of the Ci complex from microtubules and the simultaneous inhibition of Ci cleavage, which converts Ci from a transcriptional repressor to a transcriptional activator, which subsequently activates or represses target genes (Figure 2.1; Ingham and McMahon, 2001; Robbins *et al.*, 2012). The Ci homologous proteins in mammals are Gli1, Gli2 and Gli3 transcription factors (Figure 2.1; Burglin, 2008; Fuse *et al.*, 1999; Katoh and Katoh, 2006; Robbins *et al.*, 2012). Gli1 lacks the proteolytic cleavage site, and can only act as a transcriptional activator (Hynes *et al.*, 1997; Aza-Blanc *et al.*, 2000). Gli2 and Gli3 can either be stabilized under their full-length form to act as transcription activators, or be cleaved to act as transcriptional repressors (Sasaki *et al.*, 1999). The three hedgehog genes share a high degree of homology but the different expression patterns suggest that SHH, IHH, and DHH play different roles during development (Ho and Alman, 2010)

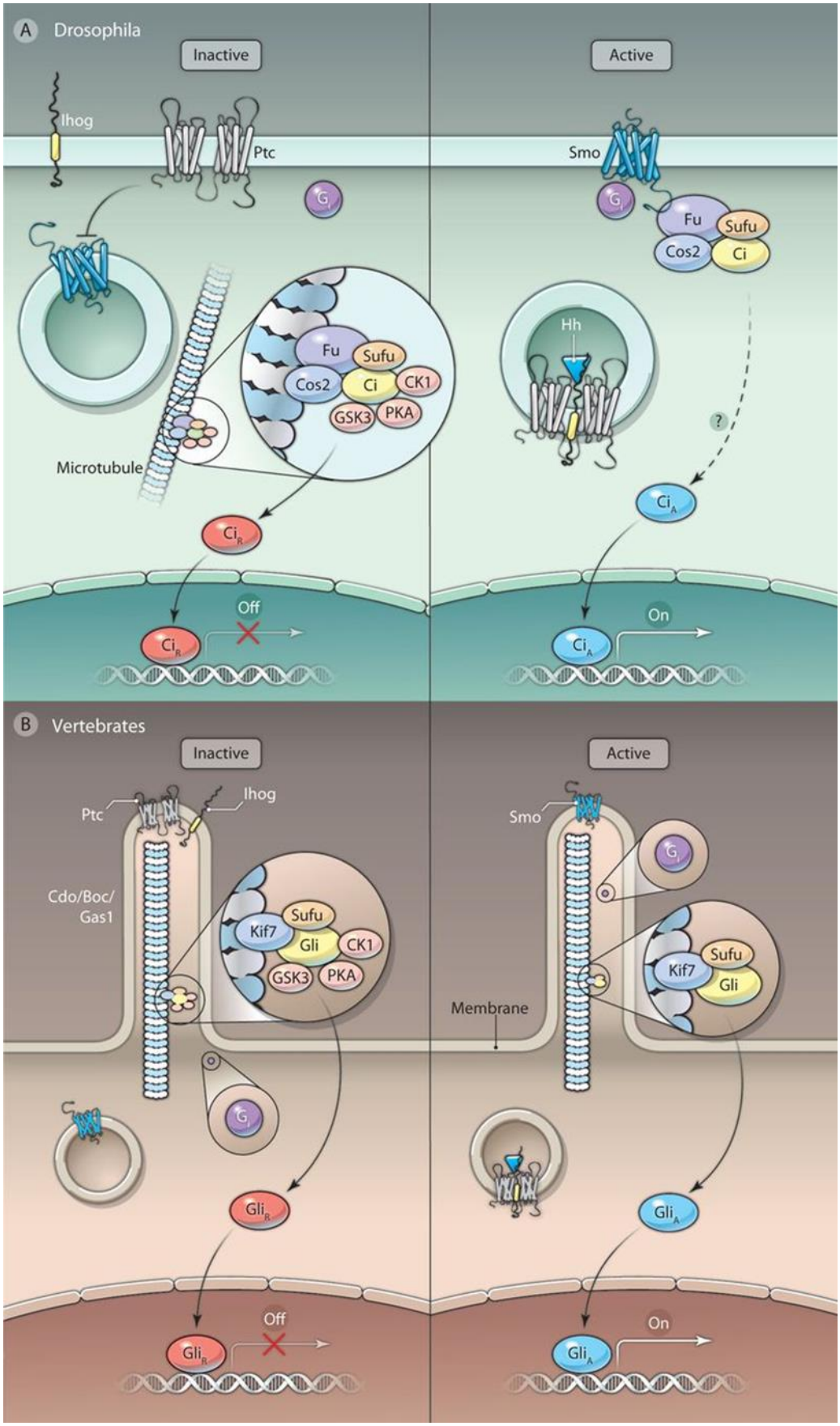
A Drosophila
Inactive
Active
Ihog
Ptc
Smo
Fu
Sufu
Cos2
Ci
CK1
GSK3
PKA
Hh
Microtubule
?
Off
On
B Vertebrates
Inactive
Active
Ptc
Ihog
Smo
Cdo/Boc/
Gas1
Kif7
Gli
Membrane
Off
On

Figure 2.1 The Hh signaling pathway (from Robbins *et al.*, 2012).

(A) Hh signaling in *Drosophila*. In the absence of Hh (left), Ptc prevents Smo membrane localization and activation so that Smo is retained on intracellular vesicles. In this context, full-length Ci (yellow, indicating partial activity) is held in a microtubule-associated complex containing the kinesin-like protein Costal2 (Cos2), the kinase Fused (Fu), and Suppressor of Fused (Sufu), which promotes phosphorylation of Ci by PKA, GSK3, and CK1 and its partial proteasomal processing into a transcriptional repressor form (Ci_R, red). Binding of Hh to the receptor complex composed of Ptc and an Ihog co-receptor (Ihog or Boi, right) results in internalization of the ligand-receptor complex and phosphorylation and translocation of Smo to the plasma membrane, where it interacts with Cos2 to partially disrupt the microtubule-associated complex, leading to release of Ci and activation of the heterotrimeric G_i protein. Ci is subsequently converted into a fully active labile transcriptional activator (Ci_A, blue) by an unknown mechanism. (B) Hh signaling in vertebrates. Hh signaling in vertebrates is similar to Hh signaling in *Drosophila*, with the important distinction that signaling takes place on primary cilia. When a Hh ligand binds to the receptor complex formed by Ptc and an Ihog co-receptor (Cdo, Boc, or Gas1), Smo translocates to both the plasma membrane and to the primary cilium, where it regulates Gli processing and activation. Permission to reproduce obtained from publisher.

Due to whole-genome duplication and further rearrangements, zebrafish have five members in the hedgehog family, including *sonic hedgehog a* (*shha*) and *shhb* (previously named *tiggy-winkle hedgehog* (*twhh*)), *indian hedgehog a* (*ihha*), and *ihhb* (previously named *echidna hedgehog* (*ehh*)), and *desert hedgehog (dhh). Shha* and *shhb* are both orthologs of the mammalian *Shh* gene; *ihha* and *ihhb* are both orthologs of the mammalian *Ihh* gene (Roelink *et al.*, 1994; Ekker *et al.*, 1995; Currie and Ingham, 1996; Avaron *et al.*, 2006; Jaillon *et al.* 2004).

In mice, extensive research has been done on the expression of *Shh* and its role during development. SHH acts as a morphogen that is essential for the development of various organs (Ming *et al.*, 1998). *Shh* is expressed in the notochord, the floor plate cells of the neural tube, and the zone of polarizing activity (ZPA) in the developing limbs during early embryogenesis (Varjosalo and Taipale, 2008). The ZPA is the region that is located in the posterior mesenchyme in the limb and fin buds and controls anterior-posterior (AP) limb bud patterning (Bénazet and Zeller, 2009). SHH expression in the ZPA establishes a gradient along the anterior-posterior axis of the limb bud, which is essential for the establishment of correct digit patterns (Scherz *et al.*, 2007). Furthermore, SHH is shown to be the key inductive signal in patterning of the ventral neural tube (Echelard *et al.*, 1993; Roelink *et al.*, 1994) and the ventral somites (Johnson *et al.*, 1994). SHH is critical for the determination of interneuron progenitor fate and the differential specification of cortical interneurons in the central nervous system (Xu *et al.*, 2010), as well as in floor plate specification (Ribes *et al.*, 2010). In addition, SHH plays a role in cell proliferation by regulating other factors to mediate the proliferation of the growing digits in mice (Towers *et al.*, 2008), and the differentiation of osteoblasts through the Runx2-independent pathway (Yuasa *et al.*, 2002; Zunich *et al.*, 2009). Since the SHH orthologs, and their functional properties in mice and

zebrafish, are highly conserved (Marigo *et al.*, 1995; Marigo *et al.*, 1996), it is possible to use the zebrafsih as an animal model to study the roles of Shh.

2.1.2 Role of *Shha* in the branching morphogenesis

Branched structures are seen in many organs, including the nervous system, the vasculature, kidney, lungs and many internal glands (Ochoa-Espinosa and Affolter, 2012). Each of these organs has its own evolutionary history but it is suggested that the developmental programs regulating the branching morphogenesis of various organs have a shared mechanism (Ochoa-Espinosa and Affolter, 2012). Branching morphogenesis depends on interactions between epithelial and mesenchymal cells (Affolter *et al.*, 2009; Gjorevski and Nelson, 2010; Gray *et al.*, 2010; Harunaga *et al.*, 2011). Increased evidence supports the notion that SHH plays a role in the branching morphogenesis in various organs, including the salivary gland and the lung (Affolter *et al.*, 2009).

In mice, during lung development, *Shh* is expressed throughout the lung epithelium but with highest expression levels in the distal tips of epithelial buds at embryonic age of 11.5 days (E11.5) (Bellusci *et al.*, 1996). The receptor of SHH, PTCH1 is expressed in the mesenchyme with highest levels at the distal branch points mirroring epithelial *Shh* expression (Grindley *et al.*, 1997). *Shh* knockout mice show a significantly reduced expression of *Ptch1* and a severely disrupted branching morphogenesis by E12.5 (Pepicelli *et al.*, 1998). Using a gene overexpression approach, it has been shown that SHH in the epithelial bud of the lung tip can negatively regulate the expression of the *fibroblast growth factor 10* (*Fgf10*) in the distal mesenchyme, which is essential for the formation of the epithelial bud tip and directional outgrowth of the branches; FGF10 in the distal mesenchyme can activate the FGF signaling pathway in the epithelium by activating Fgf receptor 2B (FGFR2B) located in the distal

epithelium (Figure 2.2); activation of FGF signaling in the epithelium increases the expression of *sprouty 2* (*Spry2*), which encodes a Sprouty family receptor tyrosine kinase inhibitor that can negatively regulate FGF signaling in the epithelium and stop branching morphogenesis in the distal lung epithelial bud tips cells (Figure 2.2). The negative effect of SPRY2 on branching morphogenesis is confirmed by *Spry2* null mutant mice. *Spry2* mutant mice have shown an increasing number of lateral branches during lung development (Bellusci *et al.*, 1997; Pepicelli *et al.*, 1998; Minowada *et al.*, 1999; Hacohen *et al.*, 1998; Affolter *et al.*, 2009; Metzger *et al.*, 2008). Furthermore, *Fgf10* expression in the distal mesenchyme can be negatively regulated by the mesenchymal bone morphogenetic protein 4 (BMP4) signaling, which results in the enhancement of local branching morphogenesis in the distal bud tip cells (Figure 2.2; Tefft *et al.*, 1999; Mailleux *et al.*, 2001; Affolter *et al.*, 2009; Metzger *et al.*, 2008; Gjorevski and Nelson, 2010; Miller *et al.*, 2004).

In mice, the branching morphogenesis for the three pairs of major salivary glands (the sublingual, the submandibular, and the parotid) share common mechanisms (Denny *et al.*, 1997). During the development of the mice salivary glands, SHH is expressed in the epithelium at the terminal bud (Harunaga *et al.*, 2011; Jaskoll *et al.*, 2004). Exogenous SHH peptides enhance branching morphogenesis, whereas abrogation of the hedgehog (HH) signaling by cyclopamine treatment (inhibit HH signaling) results in a significant decrease of branching morphogenesis (Jaskoll *et al.*, 2004).

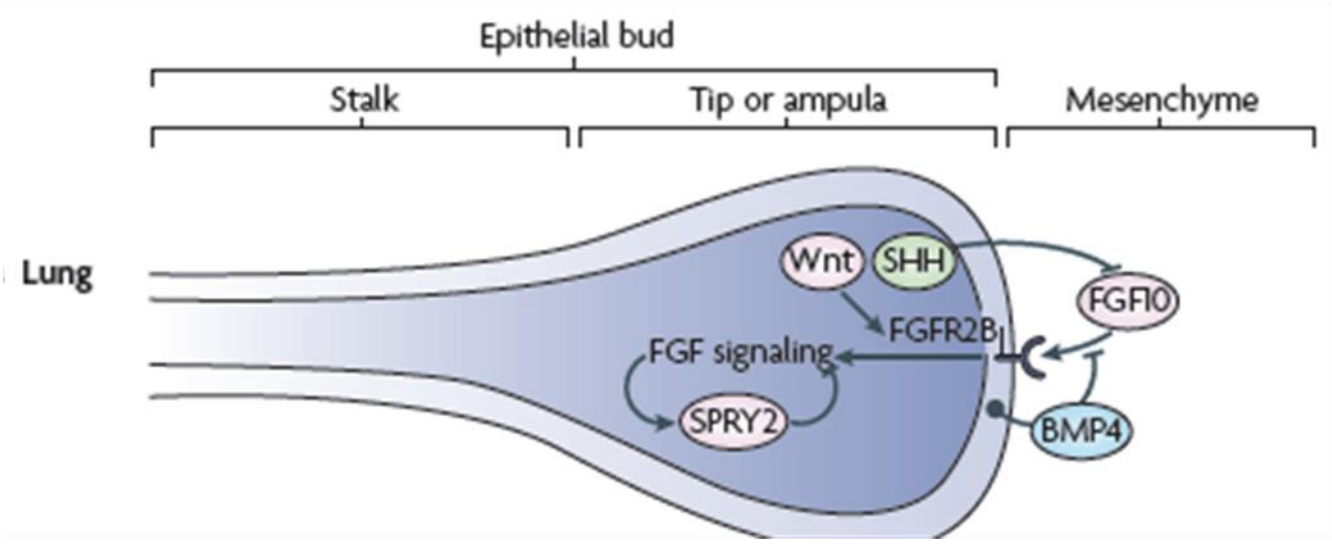
Epithelial bud
Stalk
Tip or ampula
Mesenchyme
Lung
Wnt
SHH
FGF10
FGFR2B
FGF signaling
SPRY2
BMP4

Figure 2.2 Molecular regulation of lung branching morphogenesis (Adapted from Affolter *et al.*, 2009).

Fibroblast growth factor 10 (FGF10) in the distal mesenchyme signals to FGF receptor 2B (FGFR2B) in the distal epithelium and this FGF signal transduction increases sprouty 2 (SPRY2) expression, which, in turn, controls branching by limiting the proliferation and migration of distal tip cells. In addition, sonic hedgehog (SHH) and bone morphogenetic protein 4 (BMP4) signaling by the tip epithelium restrict FGF signal transduction and branching, whereas mesenchymal BMP4 enhances local branching (not shown). Furthermore, Canonical Wnt signaling reinforces FGFR2B expression in the epithelium. Permission to reproduce obtained from publisher.

2.1.3 Shha signaling during zebrafish caudal fin regeneration

2.1.3.1 Expression of *shha*

The *shha* gene expression pattern in zebrafish embryos was described and shown to be similar to that observed in other vertebrate species (Krauss *et al.*, 1993; Johnson and Tabin, 1995; Goodrich and Scott, 1998; Chuang and Kornberg, 2000; Bardet *et al.*, 2010; Odent *et al.*, 1999; Martí *et al.*, 1995; Pepicelli *et al.*, 1998; Ingham and McMahon, 2001). During the early development of the zebrafish, *shha* is expressed in the notochord and floor plate cells of the neural tube at 11.5 hpf. After 24 hpf, *shha* expression in the notochord is progressively lost in a rostral to caudal manner but its expression is maintained in the floor plate. Furthermore, *shha* expression is also detected in the pectoral fin buds. In the developing fins, *shha* is expressed in the distal part of each fin ray (Laforest *et al.*, 1998).

During zebrafish caudal fin regeneration, *shha* gene expression starts at 30 hpa in a few dispersed cells covering the distal tips of each ray (Laforest *et al.*, 1998; Avaron *et al.*, 2000). Whole mount *in situ* hybridization (ISH) shows a strong expression of *shha* as one expression domain in the distal region of each fin ray at 48 hpa (Figure 2.3; Laforest *et al.*, 1998). *in situ* hybridization (ISH) on transverse sections shows that *shha* is expressed in a subset of cells of the basal layer of the epidermis, and this subset of cells remains confined to the distal end of the regenerate throughout the regeneration process (Figure 2.3; Laforest *et al.*, 1998). . The expression of *shha* in the basal layer of the epidermis is adjacent to the differentiating osteoblasts. *Ptch1*, the Hh receptor and Hh transcriptional downstream target, is expressed in the same cells as *shha* and in the newly differentiated osteoblasts, suggesting that the expressions of *shha* and *ptch1* may be involved in epithelial-mesenchymal interactions (Laforest *et al.*, 1998; Avaron *et al.*, 2006). *Ihha,* known for its role during endochondral

bone formation, is also expressed in the newly differentiated osteoblasts adjacent to *shha*-expressing cells, suggesting the potential role of Ihha in osteoblast differentiation in fin regenerate. By 4 dpa, the single expression domain of *shha* splits into two discrete cell populations in each hemiray, and the fin ray bifurcates following the splitting of *shha* expression, suggesting that *shha*-expressing cells play a role in the patterning or the branching morphogenesis of the regenerating fin rays (Figure 2.3; Laforest *et al.*, 1998). Similar expression patterns of *shha* are observed by GFP expression of the *Tg(2.4shha:GFP-ABC)*. In this transgenic line, 2.4*shha* contains the promoter of *shha*; GFP is the green fluorescent protein; ABC corresponds to the ArA, ArB and ArC enhancers located in the introns of the *shha* gene (Muller *et al.*, 1999). During fin regeneration, expression of GFP of the *Tg(2.4shha:GFP-ABC)* recapitulates the endogenous expression of *shha* (Figure 2.3; Zhang *et al.*, 2012). In addition, this pattern can be observed in all fin rays except the lateral-most rays that do not form bifurcations (Laforest *et al.*, 1998; Avaron *et al.*, 2006).

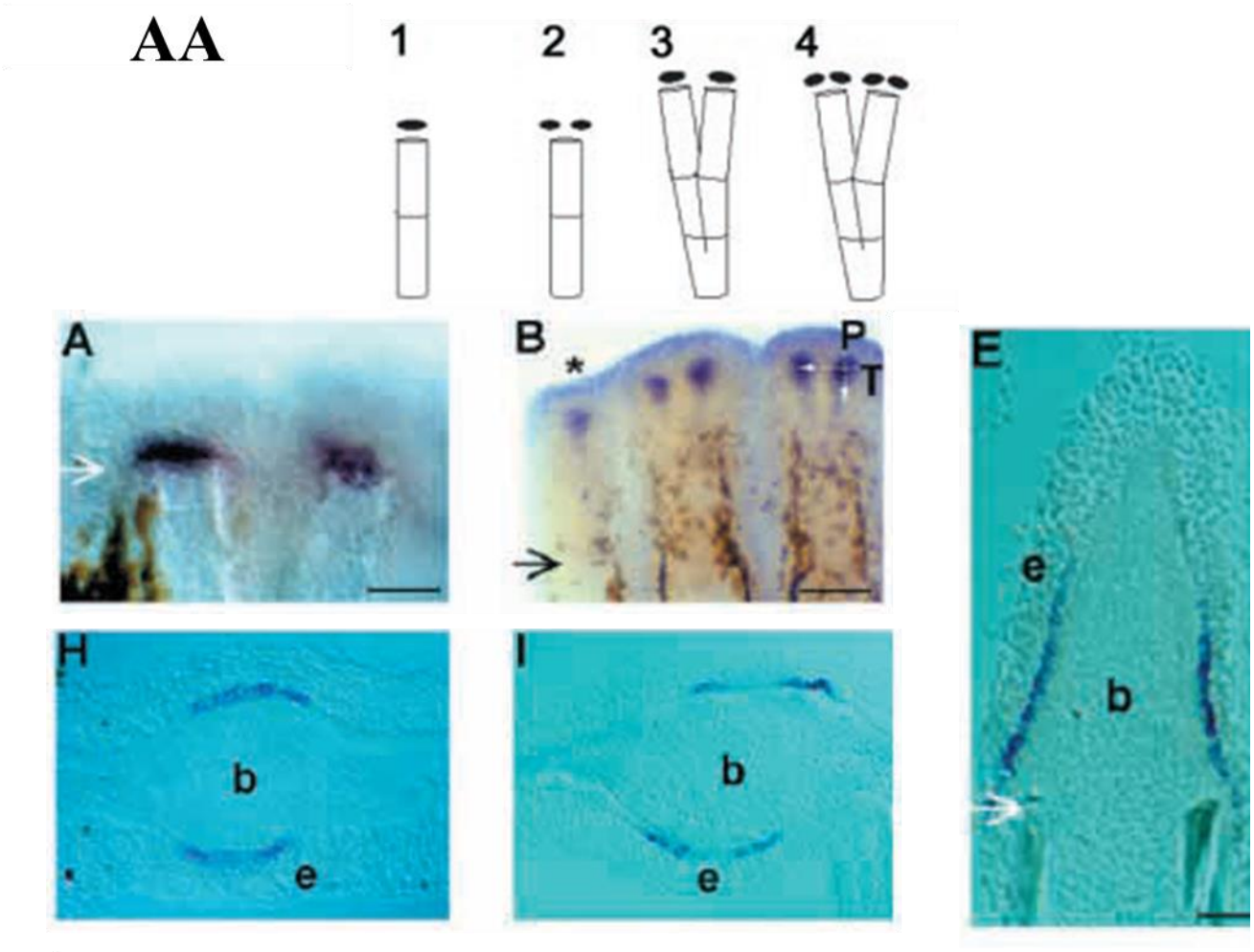
AA
1
2
3
4
A
B
P
T
*
E
e
b
H
b
e
I
b
e

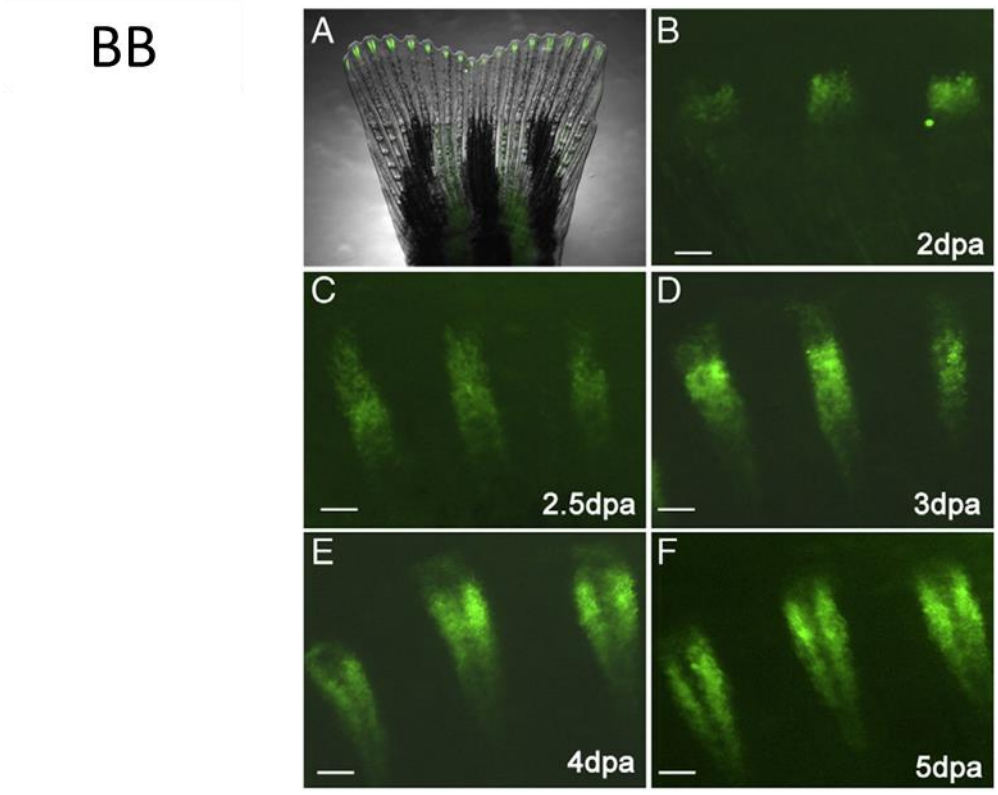
BB
A
B
2dpa
C
2.5dpa
D
3dpa
E
4dpa
F
5dpa

Figure 2.3 *shha* gene expression patterns during zebrafish caudal fin regeneration (Adapted and modified from Laforest *et al.*, 1998; Quint *et al.*, 2002; Zhang *et al.*, 2012).

AA: Induction of *shha* expression during caudal fin regeneration. A) Schematic representation of *shha* expression patterns (black dots) during branching morphogenesis of a regenerating fin ray. A1: *shha* is expressed in one domain in the distal blastema at 2 dpa. A2: *shha* expression splits in two domains by 4-5 dpa, previous to the phenotypic appearance of the two sister rays. A3: Two newly formed sister rays each exhibit one *shha* expression domain. A4: The process repeats itself as *shha* expression splits in two domains in each sister ray. B-F) *shha* expression was shown at 2 dpa (B, D, and E) and at 4 dpa (C, F). B, D) *shha* is expressed in one subset of cells in the basal layer of the epidermis in each fin ray at 2 dpa. C) *Shha* is expressed in two subsets of cells in each fin ray at 4 dpa. H) Transverse section of a regenerating caudal fin at 2 dpa shows *shha* is expressed in a broad domain when no bifurcation is forming. F) Transverse section of a regenerating caudal fin at 4 dpa shows that *shha* is expressed in two subsets of cells on one side of the fin ray preceding the formation of a bifurcation of the fin rays. The arrows in B, C and D indicate the level of amputation. The plane of the transverse section is indicated in C; b, blastema; e, epidermis; Scale bars, B, C, 80 mm; D-F, 30 mm.

BB: GFP expression shows the *shha* expression pattern during the caudal fin regeneration of the *Tg(2.4shha:GFP-ABC).* (A) Merged bright field and fluorescent image of the regenerating caudal fin. (B–F) Higher magnification of whole-mount images show three fin rays from the same fin at different stages of regeneration. (B) At 2 dpa, GFP is expressed in a few cells at the level of the blastema. (C) At 2.5 dpa, GFP expression is restricted to one single domain. (D) At 3 dpa, cleavages start to appear at the proximal end of the GFP-expressing domain and in some rays these cleavages are extending distally. (E) At 4 dpa, a

clear bifurcation of the expression domain is visible, and it is more prominent at 5 dpa when two *shha* expression domains are clearly observed (F). Scale bars: 100 μm. Permission to reproduce obtained from publisher.

2.1.4 Functional analysis of the *shha*-expressing cells

Functional analysis of the *shha*-expressing cells further support that these cells play a role in patterning or branching morphogenesis of bony fin rays during zebrafish fin regeneration.

2.1.4.1 Cyclopamine treatment to block Hh signaling

Treatment of fish during fin regeneration with cyclopamine, the pharmacological drug that can block Hh signaling, has been shown to reduce the expression of *ptch1* and inhibit the fin outgrowth in a dose-dependent manner (Figure 2.4; Quint *et al.*, 2002). After cyclopamine treatment, cell proliferation in the blastema is highly reduced (Quint *et al.*, 2002). However, since cyclopamine interacts with Smo and blocks the signal transduction of the Hh signaling, it is difficult to distinguish the specific role of Shha and other members in the Hh family such as Ihha, during caudal fin regeneration. The growth defects in the fin regenerate after cyclopamine treatment indicate that Shha and/or Ihha play a role in cell proliferation and/or differentiation of osteoblasts in the blastema, and highlight the importance of the Hedgehog pathway during fin regeneration (Quint *et al.*, 2002).

2.1.4.2 Ectopic expression of Shha

By *in vivo* local gene transfection methods (plasmid DNA transfection) to express genes of interest locally, Quint and colleagues studied the effects of the ectopic expression of Shha between ray branches where *shha* is normally not expressed, and found that ectopic expression of Shha led to a fusion of the branches. Furthermore, the fusion of sister rays shows the ectopic bone deposition in the space between the basal epidermal layer and the mesenchymal cells of the interray. These results indicate that ectopic expression of Shha

disrupts the normal patterning of regenerating rays and induce ectopic bone deposition of the fin regenerate (Figure 2.4; Quint *et al.*, 2002).

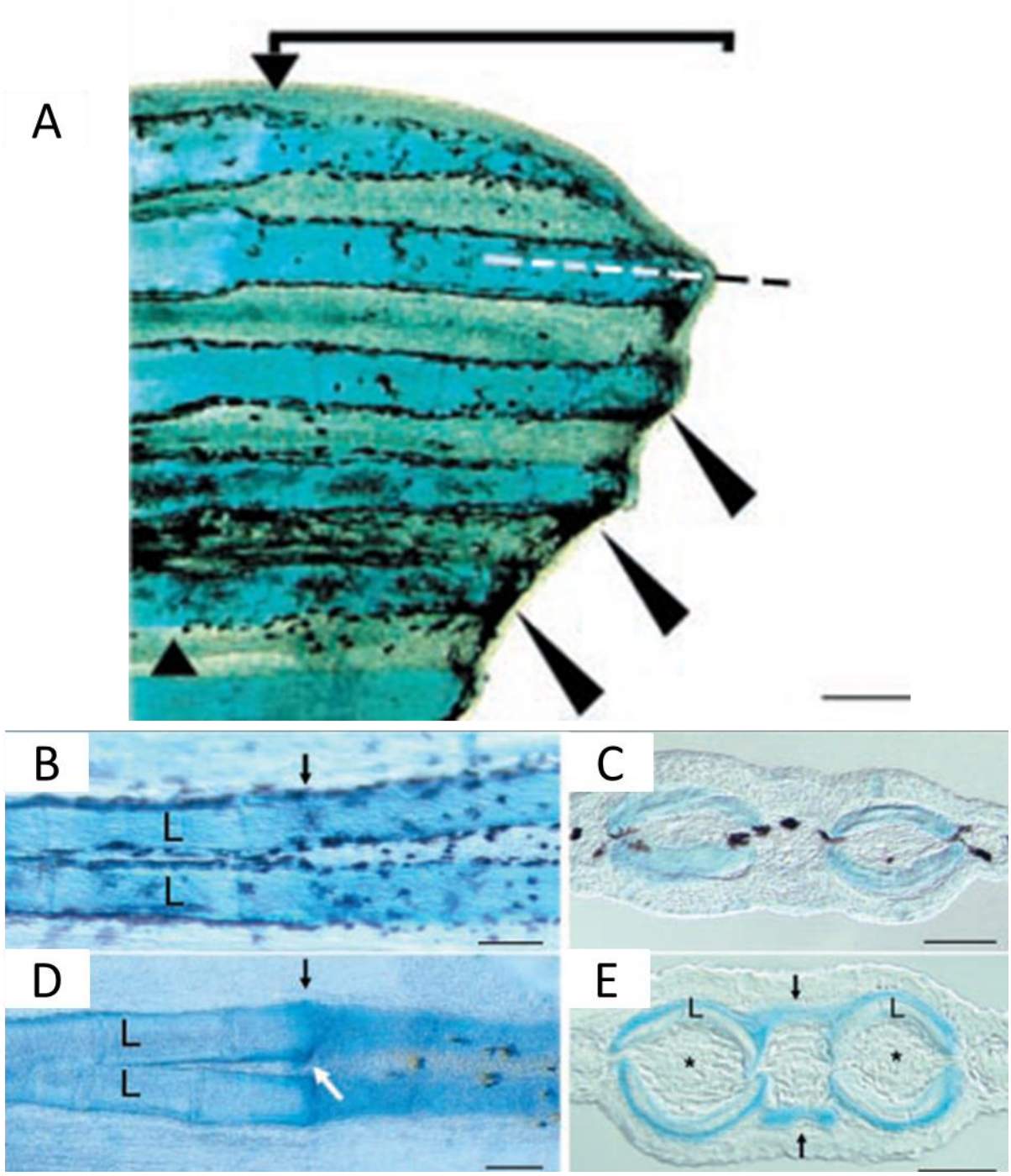
A
B
L
L
C
D
L
L
E
L
L

Figure 2.4 Effects of cyclopamine (blocking of Hh signaling pathway) and ectopic expression of Shha in zebrafish caudal fin regenerates (Adapted from Quint *et al.*, 2002). A: 2dpa zebrafish fin regenerates are exposed to 5 M cyclopamine for 5 days and stained with Alcian blue. Treatment of cyclopamine results in the growth arrest of the fin regenerate, the accumulation of melanocytes in the distal stumps of the rays (large arrowheads), and the absence of the blastema. Small arrowhead indicates the level of fin amputation. B-C: Normal bifurcation in the caudal fin regenerate stained with Alcian blue. D-E: Ectopic expression of Shha through transfection with a *shha*-expressing plasmid results in the fusion of rays in the fin regenerate. Local gene transfection is conducted in the region indicated by the white arrow (D). C and E are cryosections in the region of normal bifurcation in B and fusion in D, respectively. Arrows in E indicate the region of ectopic bone matrix deposition. No ectopic bone deposition occurs in the mesenchyme interior of the lepidotrichia (L) as marked with asterisks. Scale bars: 100 μm. Permission to reproduce obtained from publisher.

2.1.5 Conditional ablation of the *shha*-expressing cells during zebrafish caudal fin regeneration

2.1.5.1 Laser ablation of the *shha*-expressing cells

Using the *Tg(2.4shha:GFP-ABC)* line, laser ablation of the *shha*-expressing cells was conducted on five fin rays on one lobe while the five fin rays of the other lobe were used as internal controls. As a result, a significant delay of the fin ray bifurcation was observed after laser ablation of the *shha*-expressing cells during fin regeneration (Figure 2.5; Zhang *et al.*, 2012). Furthermore, it has been shown that splitting of the *shha* expression domains during branching morphogenesis correlates with the distribution of proliferating osteoblasts, indicating that the *shha*-expressing cells may play a role in mediating directed osteoblast proliferation (Zhang *et al.*, 2012). In addition, the splitting of *shha* expression domains preceded the separation of osteoblasts and subsequent branch formation of fin rays. These results support the hypothesis that *shha*-expressing cells play a role during the branching morphogenesis in zebrafish fin regeneration (Zhang *et al.*, 2012; Chin *et al.*, 2007; Ferrari and Kosher, 2002; Zhu and Bendall, 2009; Padhi *et al.*, 2004).

However, laser ablation only caused transient ablation of the *shha*-expressing cells which can regenerate almost immediately. Furthermore, laser ablation of one *shha* expression domain is time-consuming (about 15 mins). Therefore, this method did not make it possible to examine the effects of the prolonged absence of the *shha*-expressing cells on the fin regenerate. In order to analyze the long-term effect of the absence of the *shha*-expressing cells on the fin regenerate, we decided to use a different approach that will be discussed in the following section.

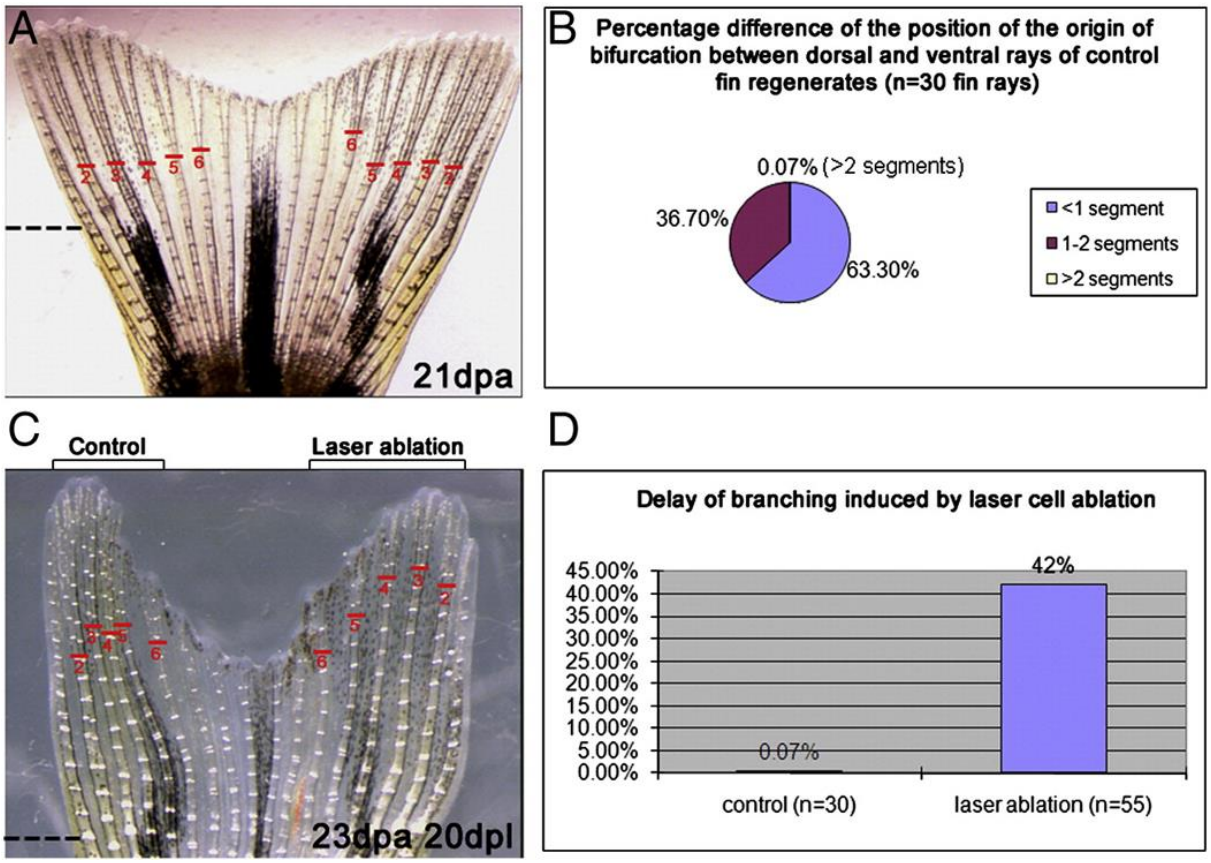
A
21dpa
B
Percentage difference of the position of the origin of bifurcation between dorsal and ventral rays of control fin regenerates (n=30 fin rays)
0.07% (>2 segments)
36.70%
63.30%
<1 segment
1-2 segments
>2 segments
C
Control
Laser ablation
23dpa 20dpl
D
Delay of branching induced by laser cell ablation
45.00%
40.00%
35.00%
30.00%
25.00%
20.00%
15.00%
10.00%
5.00%
0.00%
42%
0.07%
control (n=30)
laser ablation (n=55)

Figure 2.5 Laser ablation of the *shha*-expressing cells using *Tg(2.4shha:GFP-ABC)* transgenic fish induces the delay of fin ray branching morphogenesis during caudal fin regeneration (Adapted from Zhang *et al.*, 2012).

A: One control caudal fin regenerate at 21 dpa. Red lines above each number indicate the position of the first branching point for each individual fin ray. The black dotted line indicates the amputation plane. B: Percentage difference of the position of the origin of bifurcation (measured in number of segments) between the corresponding rays on the dorsal and ventral lobes observed in fin regenerates at 21 dpa. 30 fin rays are examined. 0.07% of the rays show a delay of greater than 2 segments from the origin of bifurcation; 36.70% of the rays show a delay of 1-2 segments from the origin of bifurcation; 63.30% of the rays show a delay of less than 1 segment from the origin of bifurcation. C: An example of the fin regenerate at 20 days post laser ablation (dpl), or at 23 dpa, of the *shha*-expressing cells on the *Tg(2.4shha:GFP-ABC).* Laser cell ablation is done on the *shha*-expressing cells by ablating GFP positive cells in the ventral No. 2, No. 3 and No. 4 fin rays at 3 dpa. The No. 2, No. 3 and No. 4 fin rays in the dorsal lobe are used as the internal control. Red lines indicate the origin of the bifurcation points. D: The percentage of rays presenting a delay of greater than 2 segments in the position of the origin of bifurcation between the experimental ventral lobe and the control dorsal lobe. Thirty fin rays are examined for control and 55 fin rays are examined for the experimental. 42% of the rays where ablation are performed show a branching delay of more than two segments compared to internal controls. Permission to reproduce obtained from publisher.

2.1.5.2 Conditional cell ablation using the Metronidazole / Nitroreductase (Mtz/NTR) system

To overcome the limitations of laser induced ablation and to induce a long-term cell ablation, another method of ablation was tested. This method is known as the Metronidazole / Nitroreductase (Mtz/NTR) system is used to genetically ablate target cells in a specific and inducible manner (Curado *et al.*, 2007; Pisharath *et al.*, 2007; Curado *et al.*, 2008)

Mtz is an antibiotic used in aquatic organisms for the treatment of infections caused by anaerobic bacteria and protozoan (Lanzky and Halting-Sørensen, 1997; Curado *et al.*, 2007). NTR is a bacterial enzyme coded by the *nfsB* gene of *Escherichia coli* (Bridgewater *et al.*, 1997). The Mtz/NTR ablation system is based on the ability of the NTR to convert the non-toxic pro-drug Mtz into a cytotoxic agent, causing cell death. In presence of NTR, Mtz is electrochemically reduced and converted into a potent DNA interstrand cross-linking agent, resulting in the death of the NTR-expressing cells (Knox *et al.*, 1988). By using the ectopic expression of a fluorescent protein (FP), such as enhanced green fluorescent protein (EGFP) or Cyan fluorescent protein (CFP), fused to NTR and a tissue-specific promoter, the targeted cell population can be ablated genetically when Mtz is exposed to the organism (Figure 2.6; Curado *et al.*, 2008; Pisharath and Parsons, 2009; Pisharath *et al.*, 2007).

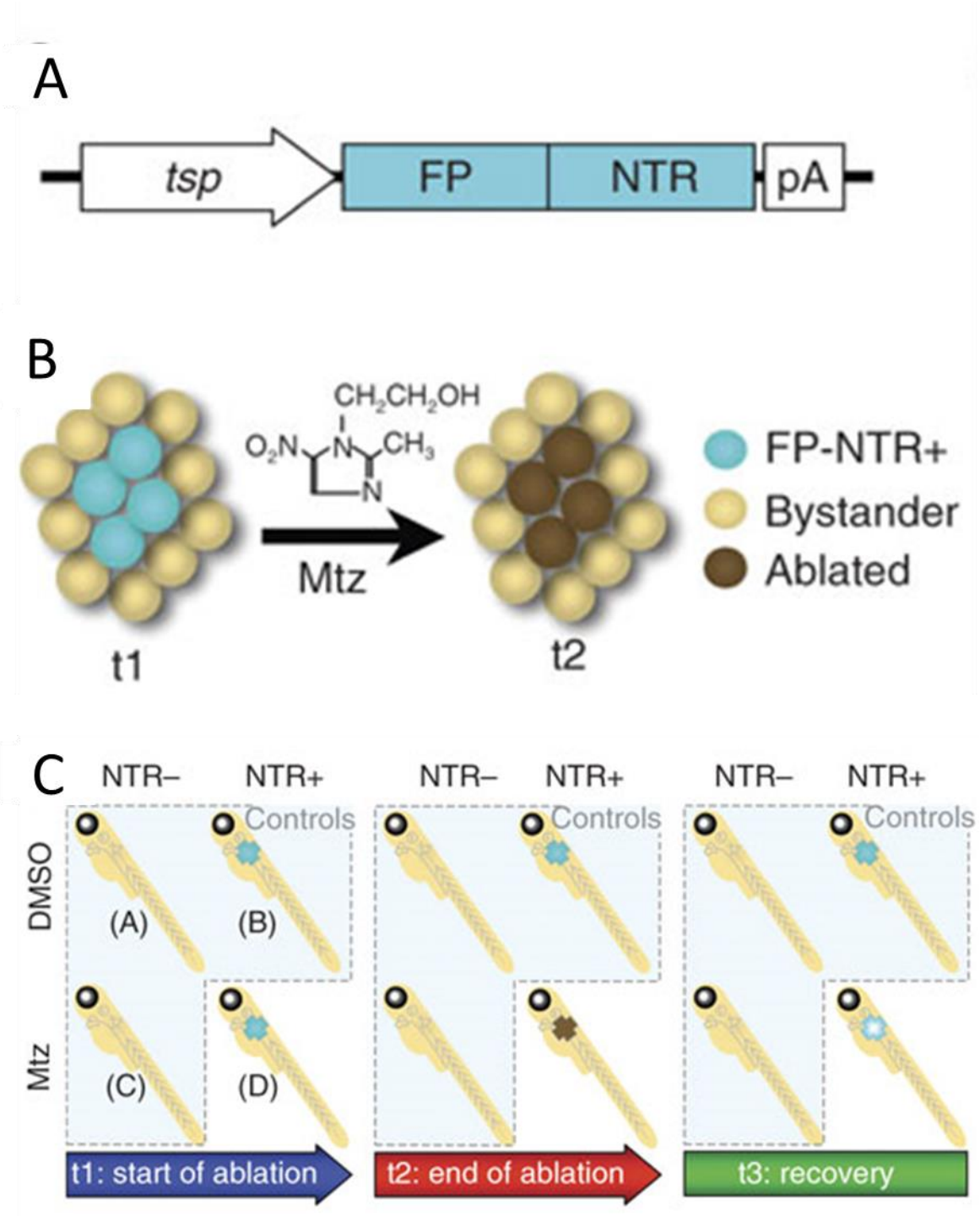
A
tsp
FP
NTR
pA
B
CH2CH2OH
O2N
N
CH3
N
Mtz
t1
t2
FP-NTR+
Bystander
Ablated
C
NTR–
NTR+
Controls
DMSO
Mtz
(A)
(B)
(C)
(D)
t1: start of ablation
t2: end of ablation
t3: recovery

Figure 2.6 Application of the Mtz/NTR system for cell-specific ablation (Adapted from Curado *et al.*, 2008).

A: A defined tissue-specific promoter (*tsp*) is cloned upstream of a cassette comprised of a fluorescent protein (FP), such as GFP, CFP, fused to NTR in a transgenesis vector. B: Mechanism of the ablation system. FP-NTR fusion protein is expressed in a defined population of cells (blue) at the start of ablation (t1). Addition of Mtz to the organisms causes programmed cell death (apoptosis) of the FP-NTR^+ cells (brown), but not neighboring cells (tan; t2). C: Four groups of samples are needed for the ablation experiment: DMSO treatment of (A) NTR^- and (B) NTR^+ embryos/larvae and Mtz treatment of (C) NTR^- embryos/larvae to control for nonspecific effects of Mtz or the transgene, and Mtz treatment of (D) NTR^+ embryos for tissue ablation. Different transgenic lines require variable optimization of conditions such as the concentration of Mtz and the time of exposure to Mtz. At t1 (start of ablation), the FP-NTR is visible in the tissue to be ablated (blue); at t2 (end of ablation), FP-NTR^+ cells will be depleted or absent (brown); and at t3 (during recovery after Mtz washout), new FP-NTR^+ cells may be produced by regeneration if the ablated tissues have the regenerative ability. Permission to reproduce obtained from publisher.

This system has a few advantages over other cell ablation methods. For example, long-term cell ablation effect can be studied because NTR-expressing cells can be ablated as long as Mtz is present, and treatment with Mtz can easily be conducted by addition of the drug in the water tank or by injection (Curado *et al.*, 2007; Pisharath *et al.*, 2007; Moss *et al.*, 2009); the ablation is cell specific because the toxic form of Mtz is restricted to the NTR-expressing cells, so that no "bystander effect" that damages the neighboring cells along with the targeted cells can be detected (Bridgewater *et al.*, 1997; Curado *et al.*, 2008); the application of the fluorescent protein tagged with NTR allows the tracing of the dynamics of the NTR-expressing cells during the course of cell ablation *in vivo* (Curado *et al.*, 2008); it offers spatially and temporally controllable ablation that can be used for regeneration studies, because after cell ablation or upon removal of the Mtz, cells regeneration or tissues recovery can be observed in the tissues that have the regenerative ability (Curado *et al.*, 2008).

2.1.5.3 Use of Mtz/NTR system in different zebrafish tissues or organs

Since the initial description of the use of the Mtz/NTR cell ablation system (Pisharath *et al.*, 2007; Curado *et al.*, 2007), this system has successfully been used to ablate different cell types (White and Mumm, 2013) including cardiomyocytes, hepatocytes and pancreatic beta-cells in zebrafish embryos (Pisharath *et al.*, 2007; Curado *et al.*, 2007), pancreatic beta-cells in adult zebrafish (Moss *et al.*, 2009), skin cells in both embryos and adult zebrafish (Chen *et al.*, 2011), retinal bipolar cells in zebrafish embryos (Ariga *et al.*, 2010; Zhao *et al.*, 2009), pineal photoreceptors in zebrafish larvae (Fernandes *et al.*, 2012) and retinal rod cells in adult zebrafish (Montgomery *et al.*, 2010), kidney podocytes in zebrafish embryos (Huang *et al.*, 2013), male testis cells in zebrafish embryos (Hsu *et al.* 2010), female oocytes in adult zebrafish (White *et al.*, 2011), as well as osteoblast in adult zebrafish (Singh *et al.*, 2012).

2.2 Objectives

1. To establish the *Tg(2.4shha:CFP-NTR-ABC)* to conditionally and durably ablate the *shha*-expressing cells via Mtz/ NTR system in the regenerating caudal fin

2. To analyze the effects of the ablation of the *shha*-expressing cells in the regenerating caudal fin

2.3 Materials and Methods

2.3.1 Zebrafish husbandry

Wild type (WT) zebrafish and the transgenic line *Tg(2.4shha:GFP-ABC)* (from Dr. Uwe Strähle laboratory, Karlsruhe Institute of Technology), were raised and maintained in the zebrafish facility at the University of Ottawa. The fish were kept in the fishroom at 28.5 °C with 14 hours light and 10 hours dark period. Zebrafish were fed regularly (Westerfield, 2000), including twice adult zebrafish food and once brine shrimp per day. Adult zebrafish ranging from 3 to 18 months were used for experiments. Zebrafish were maintained and manipulated according to the principles and guidelines of the Animal Care Committee at the University of Ottawa and the Canadian Council on Animal Care (CCAC).

2.3.2 Fin injury

Zebrafish were anesthetized in the fishroom system water that contains 0.17 g/mL tricaine as previously described (Westerfield, 2000). Fin amputation was performed one to two segments proximal to the first branching point among all the fin rays using a scalpel blade (Figure 3.4). Fish were kept individually or in groups after injury in the fishroom at 28.5°C.

2.3.3 Microscopy

Zebrafish were anesthetized as described above and placed on a 1.5% agarose plate for imaging. Images were taken using a dissection microscope (Leica MZ FLIII) integrated with the FLUOIII filter system or a Zeiss Axioskop compound microscope equipped with a digital camera (Zeiss AxioCam HRm) and AxioVision AC software.

2.3.4 Transposase mRNA synthesis

The pCS-TP plasmid that contains the *transposase* cDNA was linearized with *Not*I restriction enzyme. The RNA synthesis was performed using the Ambion SP6 mMessage mMachine kit, according to the manufacturer instructions (Invitrogen). The reaction was stopped and the RNA was precipitated by adding 30μL of nuclease-free water and 30μL of LiCl precipitation solution (available with the kit). The mixture was kept at -20°C for one hour, followed by centrifugation for 15 minutes at 13000 revolutions per minute (rpm) of the microcentrifuge at 4°C. The supernatant was carefully removed and the pellet (that contains RNA) was washed with 70% ethanol in Diethylpyrocarbonate (DEPC)-treated water. Finally, RNA was re-suspended in DEPC-treated water, and stored in aliquots at -80°C.

2.3.5 Microinjection in zebrafish embryos

The injection mix consists of the DNA and Tol2 transposase mRNA. The DNA construct was made by the former graduate student Shirine Jeradi. The injection mix was freshly prepared prior to the injection with various DNA and mRNA concentrations along with 0.5% phenol red, a monitoring dye for injection. DNA concentrations ranging from 50 ng/μL to 200 ng/μL and mRNA concentrations ranging from 30 ng/μL to 200 ng/μL were tested. Several trial injections with different concentrations of DNA and mRNA indicated that the final DNA concentration of 100 ng/μL and the final mRNA concentration of 50 ng/μL could produce the highest number of CFP-expressing cells in the injected embryos; therefore, this concentration was used for all the injection work. The injection was performed in one-cell stage embryos, which were collected and treated with a bleach solution (made by placing 0.1 mL of 5.25% sodium hypochlorite (bleach) and 170 mL of system water into a 250 mL beaker) for two minutes (Westerfield, 2000), before being aligned on an agarose injection plate. Microinjection was performed using a "Narishige IM-300" microinjector.

2.3.6 Screening of zebrafish embryos

Injected embryos were screened at 24 hours post fertilization (hpf) and 48 hpf for cyan fluorescence under fluorescent microscope. Fluorescent embryos were separated into two groups, the first group (+++) fish (regarded as a high number of the CFP-expressing cells) had a total number of more than 20 CFP-expressing cells in the floor plate cells of the neural tube, notochord, and eyes (Figure 2. 8), whereas the second group (+) fish (regarded as low number of the CFP-expressing cells) had a total number of less than 20 CFP-expressing cells in the floor plate cells of the neural tube, notochord, and eyes. Both groups of embryos were raised for three months and then bred; the progenies were screened at 24 hpf and 48 hpf for transmission of the transgene. For the screening of founder fish (F0), one founder fish was crossed with a wild type (WT) fish. If F1 offspring showed cyan fluorescence, the F0 fish was regarded as a transgenic fish because the construct was transmitted to the next generation. If fluorescence was not detected among 300 embryos, the injected fish was not considered as transgenic and not used for further research. Fluorescent embryos from the transgenic fish were raised in order to make a stable transgenic line.

2.3.7 Polymerase chain reaction (PCR) genotyping of embryos or fin regenerates

At least 300 embryos at 2-4 dpf from each potential founder fish and at least 5 fin regenerates from the 11 founder fish at 3-6 dpa were collected, labeled, and put in different 1.5 mL tubes. 500 µL genomic DNA extraction buffer (10 mM Tris buffer (pH=8), 100 mM EDTA (pH = 8.0), 0.5% SDS and 200 µg/mL proteinase K) was added to each tube and the tubes were incubated overnight at 65°C. The next day, tubes were removed from the incubator and 1 mL 100% ETOH was added to each tube before placing them on ice for 30 minutes. Each tube was centrifuged at 13000 rpm of the microcentrifuge for 10 minutes and the supernatants from each tube were discarded. Finally, 20-30 µL nuclease-free water was added to each tube and DNA was resuspended by vigorously vortex in the water. After that, DNA was used to

run the PCR reaction with CFP primers or CFP-NTR primers and PCR products were shown by gel electrophoresis. Sequences of primers are listed in the Appendix I. PCR reactions were carried out for 30 cycles with the following cycling parameters: denaturing at 95°C for 1 minute, primer annealing at 55°C for 1 minute, elongation at 72°C for 2 minutes.

2.3.8 Mtz treatment on the *Tg(2.4shha:CFP-NTR-ABC)* embryos

F3 offspring of *Tg(2.4shha:CFP-NTR-ABC)* embryos were screened at 24 hpf under a fluorescent microscope. Chorions of embryos were removed and fluorescent embryos were imaged to record the expression pattern of CFP before Mtz treatment. Embryos were then separated into two groups: experimental and control groups. 0.1% 1-phenyl 2-thiourea (PTU), a tyrosinase inhibitor, was used to block pigmentation during zebrafish development (Karlsson *et al.*, 2001). 0.02% Dimethyl sulfoxide (DMSO) was used to help solubilize Mtz (Curado *et al.*, 2008). Transgenic embryos in the experimental group were transferred to the embryo medium containing 0.2% DMSO, 0.003% PTU and 10 mM Mtz (Metronidazole) for three days. Transgenic embryos in the control group were transferred to the embryo medium containing 0.2% DMSO and 0.003% PTU at the same time with the experimental group. The two groups of embryos were kept in the dark at 28.5 °C. All the embryos were observed and imaged every 24 hours for fluorescence signal strength/ fluorescent cells. The treatment solution for each group was freshly prepared and changed every day until embryos reached 4 days post fertilization (dpf).

2.3.9 Mtz treatment on the *Tg(2.4shha:CFP-NTR-ABC)* adult fish

Caudal fin amputation of the *Tg(2.4shha:CFP-NTR-ABC)* adult zebrafish was performed one to two segments proximal to the first branching point among all the fin rays using a scalpel blade . Fish were treated with 10 mM Mtz solution, which was prepared by dissolving the

Mtz (Sigma, M1547) in the system water as described (Singh *et al.*, 2012). All the fish that underwent Mtz treatment had their tanks covered by aluminum foil to avoid pro-drug Mtz exposure to the light. Fish were maintained in the fishroom at 28.5°C. After 1 day of Mtz treatment, fish were washed three times in system water and then put back to the circulating system water in the fishroom. Fish were fed twice a day with adult zebrafish food. WT adult zebrafish were used as the control for the Mtz treatment. WT adult zebrafish were treated the same way as *Tg(2.4shha:CFP-NTR-ABC)* adult zebrafish (Singh *et al.*, 2012; Curado *et al.*, 2007). The Mtz treated fish were observed by light microscopy and fluorescent microscopy, and control fish were observed only by light microscopy on a daily basis for seven days since the day of amputation, and also at 14 dpa or 21 dpa. In order to better observe the bifurcating point of the fin regenerate, all the fish were stained by immersion in water containing alizarin red, which can *in vivo* stain the bone matrix (Tu and Johnson, 2011). Alizarin red staining was conducted for all the fish at 7 dpa and 14 dpa. Bright field pictures and alizarin red staining pictures were merged by Adobe Photoshop CS4. The dorsal and ventral fin rays No.2, No.3, and No.4 were used for the analysis of fin rays branching delay. The branching delay of one fin ray was counted by using the number of bone segments from the amputation plane to the first branching point of one regenerating fin ray, minus the number of bone segments from the amputation plane to the first branching point of the same fin ray in the intact fin. The total number of the branching delay was calculated by adding the branching delay of each fin ray (No.2, No.3 and No.4 rays). The mean of the branching delay for each fin ray was calculated by using the total number of the bifurcation delay divided by the total number of measured fin rays.

2.4 Results

2.4.1 Generation of the *Tg(2.4shha:CFP-NTR-ABC)* line

To study the long-term ablation effect on the *shha*-expressing cells, the Mtz/NTR ablation system was used so that *shha*-expressing cells would continually undergo cell death and be ablated in the presence of Mtz in the transgenic line *Tg(2.4shha:CFP-NTR-ABC).* The *Tg(2.4shha:CFP-NTR-ABC)* would be generated to observe and to analyze the long-term effect of ablation of the *shha*-expressing cells. This 2.4shha:CFP-NTR-ABC construct is very similar to the construct for the established *Tg(2.4shha:GFP-ABC).* 2.4*shha* is a 2.4kb genomic fragment containing thepromoter of *shha*; CFP-NTR is the cDNA for the *cyan fluorescent protein* (CFP) fused to the nitroreductase (NTR) cDNA to make the fusion protein CFP-NTR (kindly provided by Dr. Didier Stainier lab, University of Califonia in San Francisco); the ArA, ArB and ArC (ABC) are enhancers of the *shha* gene (Muller *et al.*, 1999). The (2.4shha:CFP-NTR-ABC) construct also contains Tol2 elements. This plasmid construct was made by the former graduate student Shirine Jeradi (Figure 2.7). *Tol2* mRNA is used because it can translate into a functional transposase that is capable of catalyzing transposition. The functional transposase can excise Tol2 construct from the plasmid and integrate the excised construct into the chromosomal DNA, increasing the efficiency of the transgenesis (Kawakami *et al.*, 2000). Therefore, Tol2 transposon elements are used to enhance the germ-line transmission rate of my construct.


Tol2
2.4shh
CFP-NTR
ArA
ArB
ArC
Tol2

Figure 2.7 DNA construct for establishing *Tg(2.4shha:CFP-NTR-ABC)* (this construct was made by a former graduate student, Shirine Jeradi).

2.4*shha* is a 2.4kb genomic fragment containing the promoter of *shha*; CFP-NTR is the cDNA for the *cyan fluorescent protein* fused to the nitroreductase (NTR) cDNA to make the fusion protein CFP-NTR; the ArA, ArB and ArC (ABC) are enhancers of *shha* gene (Muller *et al.*, 1999); *Tol2* mRNA can translate into a functional transposase that is capable of catalyzing transposition, increasing the efficiency of the transgenesis (Kawakami *et al.*, 2000).

2.4.1.1 Transient activity of the 2.4shha:CFP-NTR-ABC construct after microinjection in zebrafish embryos

About 5,000 one-cell stage embryos were micro-injected with the injection mix and screened for transient expression of CFP under fluorescent microscopy from August 2011 to February 2012. All the injected embryos were screened at 1 dpf and 2 dpf for mosaic CFP expression when *shha* was strongly expressed. The expression pattern was mosaic and varied in the injected embryos because the injected embryos do not contain stable germ-line inserts of the foreign DNA (Stuart *et al.*, 1998). The transient or mosaic CFP expression could be detected in the floor plate cells of the neural tube, notochord, and eyes in the represented injected embryos at both 1 dpf and 2 dpf (Figure 2.8). Based on the level of the mosaic CFP expression, fluorescent embryos were separated into two groups at 2 dpf, the first group (+++) (considered as high number of CFP-expressing cells) had a total number of more than 20 CFP-expressing cells in the entire embryo (Figure 2.8 A and C), whereas the second group (+) fish (considered as low number of CFP-expressing cells) had a total number of less than 20 CFP-expressing cells in the entire embryo (Figure 2.8 B and D).

Both group (+++) and group (+) fish were raised to adulthood (approximately three months) and bred for screening of the adult for transmission of the transgene. Ninety three fish survived and were able to breed after three months from the group (+++) and 87 fish from the group (+). Therefore, a total number of 180 fish were screened for transmission of the transgene (Table 1).

High number of CFP –expressing cells (+++)

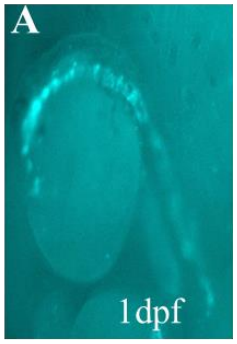

Low number of CFP –expressing cells (+)

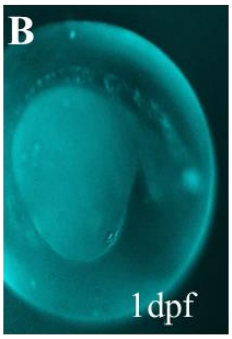

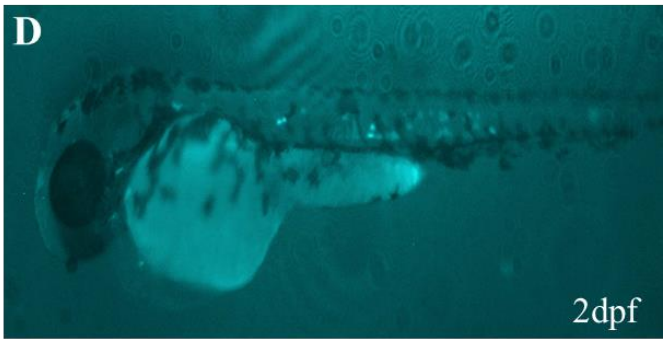

Figure 2.8 Screen for the micro-injected zebrafish embryos.

Injected embryos were screened for mosaic CFP expression and separated into two categories. The first category was for embryos that had the high number of CFP-expressing cells (+++) (embryos had more than 20 CFP-expressing cells) (A, C) and the second category was for embryos that had the low number of CFP-expressing cells (+) (embryos had less than 20 CFP-expressing cells) (B, D). A and B show (+++) and (+) embryos at 1 dpf, respectively; C and D show (+++) and (+) embryos at 2 dpf, respectively.

Table 1. Summary of injection results

Injection at the one-cell stage	Adult fish that survived from the group of injected embryos with:	
	high number of *CFP*-expressing cells (+++)	low number of *CFP*-expressing cells (+)
Aug. - Nov. 2011	55	60
Feb.- Mar. 2012	38	27
Total	93	87

2.4.1.2 Generation of 11 founder fish and analysis of CFP expression in the caudal fin regenerates of the F1 from those founder fish

Founder fish are the fish that transmit the transgene to the next generation. For the screening of founder fish (F0), one injected fish was crossed with a wild type (WT) fish. If F1 offspring showed cyan fluorescence in the domains corresponding to the endogenous expression of *shha*, the F0 fish was considered as a founder fish because the construct had been transmitted to the next generation. If not detected amongs 300 F1 embryos, the injected fish would not be considered as a founder fish and would not be used for further research. Fluorescent embryos from the founder fish were raised in order to make a stable transgenic line.

In total, I have generated 11 founder fish and F1 transgenic embryos from each founder fish showed various levels of cyan fluorescence. CFP expression in the transgenic embryos was observed in the eyes, brain, notochord, the floor plate cells of the neural tube, and the urogenital region (Figure 2.9). This expression pattern is not the same as the expression pattern of the endogenous *shha* gene, since it misses the expression in the pectoral fin buds. However, it is identical to the expression pattern observed in embryos of the *Tg(2.4shha:GFP-ABC)* transgenic line (Krauss *et al.*, 1993; Ekker *et al.*, 1995; Currie and Ingham, 1996; Ingham and McMahon, 2001; Hadzhiev *et al.*, 2007). This CFP expression pattern indicated that the transgene was inserted into the germ-line but the level of CFP expression varied among transgenic lines. Particularly, line #2 (F1 transgenic embryos from founder fish number 2) showed strong CFP expression, compared to other lines, in the floor plate cells of the neural tube, notochord, brain, and eyes, which mimicked the endogenous *shha* expression pattern. In order to examine CFP expression in the adult zebrafish fin regenerates, I raised at least 50 F1 transgenic embryos from each founder fish for two months before their caudal fins were amputated. CFP expression in the fin regenerates were observed

at 4 dpa under fluorescent microscope. However, only fin regenerates from F1 of the founder fish #2 showed CFP expression in the caudal fin regenerates. Moreover, the CFP expression pattern varied from fish to fish of the line #2. Three types of expression patterns were characterized: a) no CFP expression was detected in any of the regenerating fin rays; b) partial expression pattern in which CFP expression was detected in some regenerating fin rays but not all the fin rays; or c) complete expression pattern which means that CFP expression was detected in all the regenerating fin rays (Figure 2.10). However, even in the case of the complete expression pattern, CFP expression was mosaic. This mosaic expression pattern did not recapitulate or resemble the expression pattern seen in the *Tg(2.4shha:GFP-ABC)* (Figure 2.10, 2.12).

Tg (2.4shha:CFP-NTR:ABC)

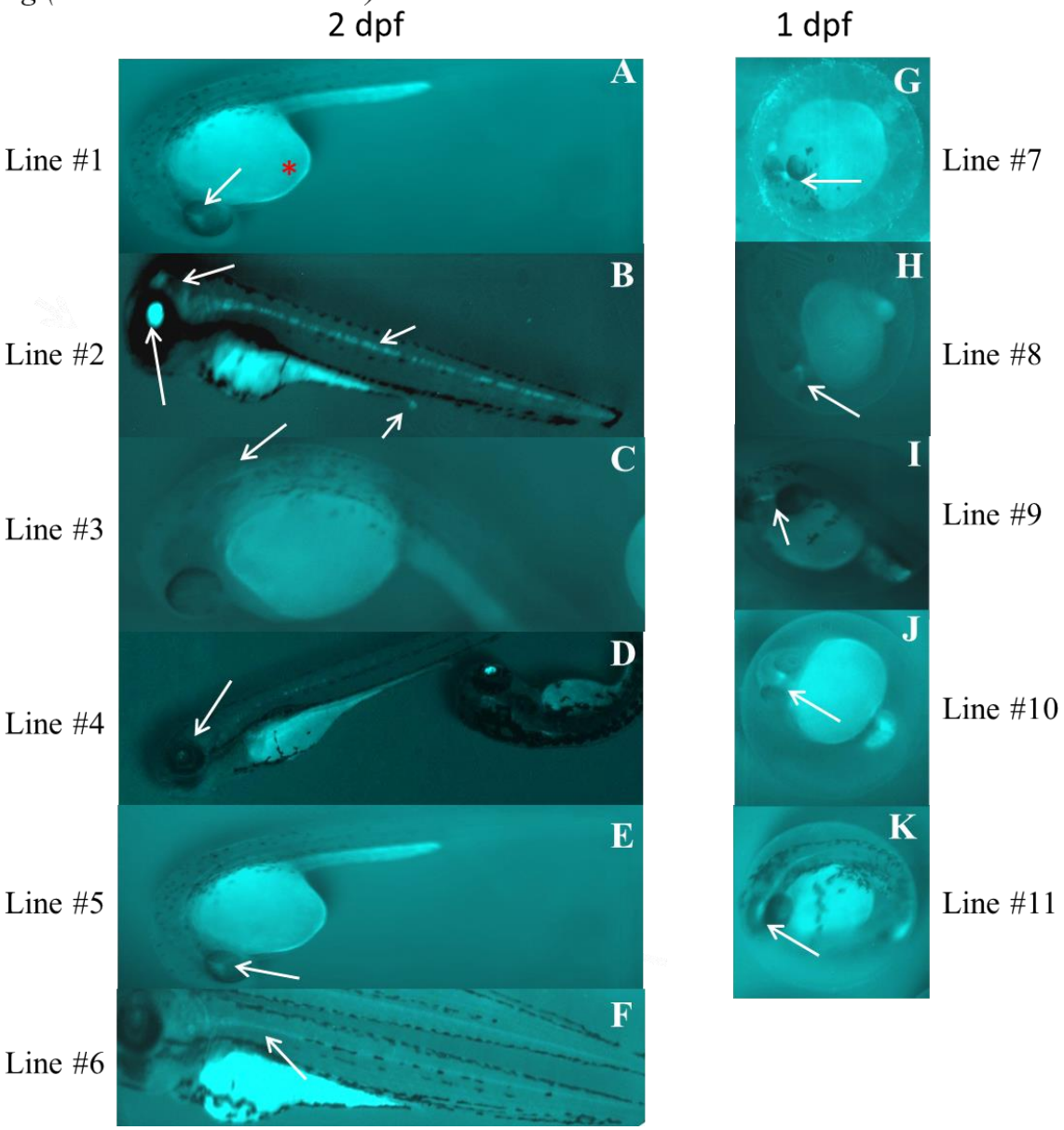

Figure 2.9 Eleven transgenic lines (#1-#11) were generated.

A-F show one of the representative embryo of the first six lines at 2 dpf, G-K show one representative embryo of the other five lines at 1 dpf. CFP expression is observed in the eyes, brain, floor plate cells of the neural tube, the urogenital region, and notochord, indicated by white arrows. The asterisk indicates the auto fluorescence of the yolk sac.

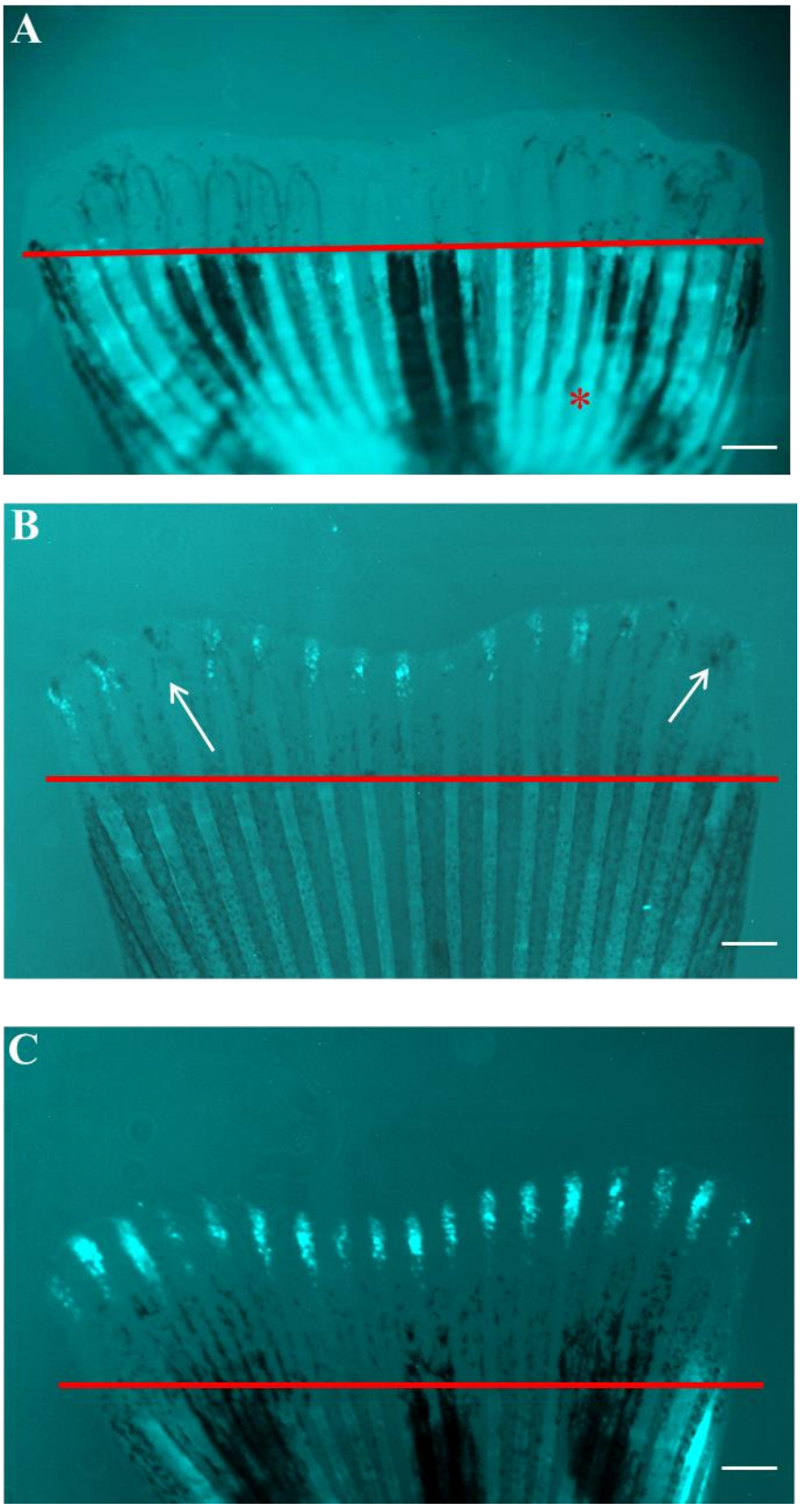
A
B
C

Figure 2.10 Three types of CFP expression in the 4 dpa fin regenerates of F1 fish of the *Tg(2.4shha:CFP-NTR-ABC)* #2.

A) No CFP expression was detectable. B) CFP expression was seen in some fin rays but not all the rays. C) CFP expression was seen in all the rays, though the number of the CFP-expressing cells was different among rays. White arrows in B indicate the missing CFP expression in two fin rays. The amputation plane in (A-C) is indicated by a red line. The asterisk indicates the auto fluorescence of the intact bone segments. Scale bars: 500 μm.

Table 2. Summary of three types of CFP expression in the fin regenerates of F1 fish of the *Tg(2.4shha:CFP-NTR-ABC) #2*

Expression pattern	Number of fins
No expression	233
Partial expression	98
Complete expression	55
Total	386

2.4.1.3 Improved CFP expression following selection of one transgenic line

Since some F1 fish from the founder fish #2 had a complete CFP expression pattern, it was hypothesized that the number of the CFP-expressing cells or the level of the CFP expression per cell could be increased through generations. It has been shown that sib-pair matings can generate zebrafish strains with homogeneous expression of the transgene (Shinya and Sakai, 2011), suggesting that more copy numbers of the transgene can be inserted into the germ-line of the next generation through inbreeding. Therefore, more F1 fish from the founder fish #2 were raised and their fin regenerates at 3-4 dpa were scored for CFP expression pattern (Table 2). 233/386 fin regenerates showed no CFP expression, 98/386 fin regenerates showed partial CFP expression pattern, and 55/386 fin regenerates showed complete expression pattern. Next, F1 fish showing complete expression patterns were inbred to generate F2 transgenic embryos. As a result, CFP expression in the F2 larva was stronger than CFP expression in the F1 larvae, indicating that the level of CFP expression per cell had increased (Figure 2.11). CFP was strongly expressed in the brain, eyes, notochord and floor plate cells of the neural tube, and recapitulated the expression pattern of the *Tg(2.4shha:GFP-ABC).* Furthermore, in the caudal fin regenerates of the F2 fish, CFP expression mimicked the expression pattern of the GFP-expressing cells in the *Tg(2.4shha:GFP-ABC)* (Figure 2.12). In conclusion, the *Tg(2.4shha:CFP-NTR-ABC)* was established from the founder fish #2, and F3 offspring were used for further analysis.

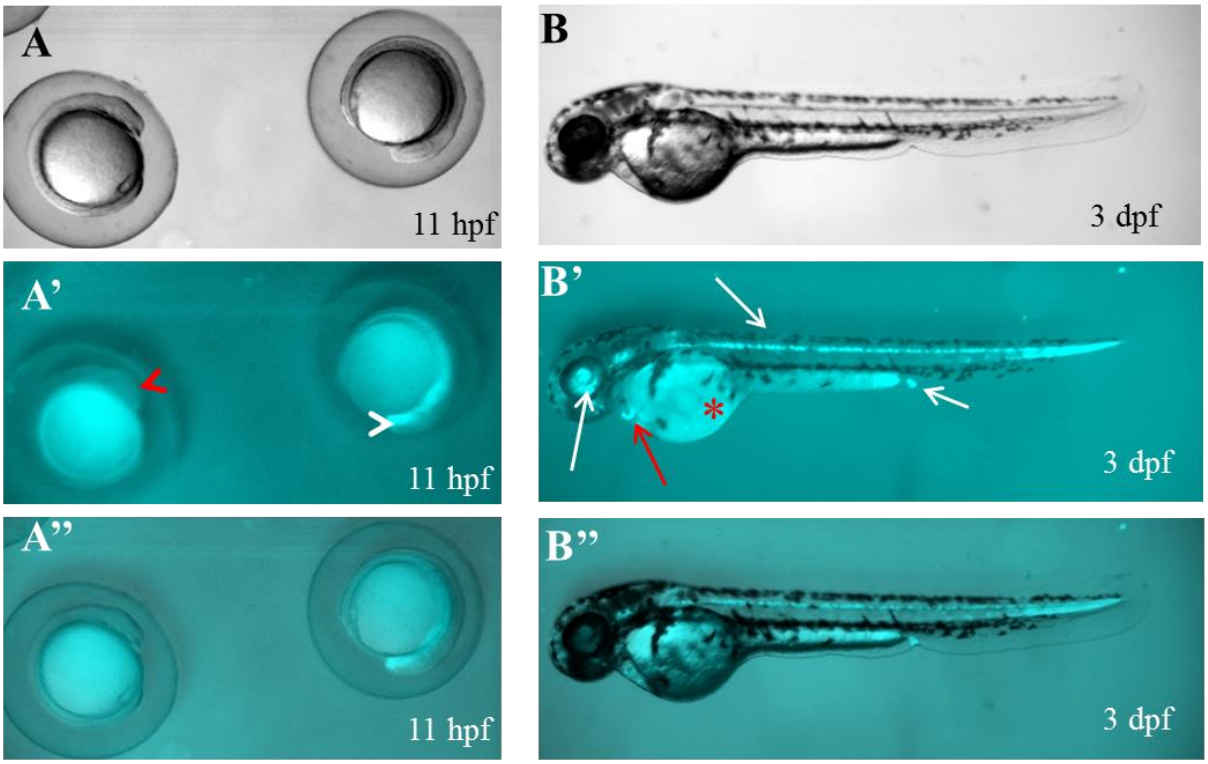
A
11 hpf
B
3 dpf
A'
11 hpf
B'
3 dpf
A''
11 hpf
B''
3 dpf

Figure 2.11 F2 *Tg(2.4shha:CFP-NTR-ABC)* #2 embryos.

A and A’ are the bright field and fluorescent images, respectively, of a 11 hpf embryos. B and B’ are the bright field and fluorescent images, respectively, of a 3 dpf larva. A’’ and B’’ are the merged images from A, A’ and B, B’ respectively. The red arrowhead in A’ indicates a CFP negative embryo and the white arrowhead in A’ indicates a CFP positive embryo, suggesting that this embryo is transgenic. White arrows in B’ indicate CFP expression in the eyes, brain, the urogenital region, and floor plate cells of the neural tube of the transgenic larva. The red arrow in B’ indicates the ectopic expression in the heart region. The asterisk indicates the auto fluorescence of the yolk sac.

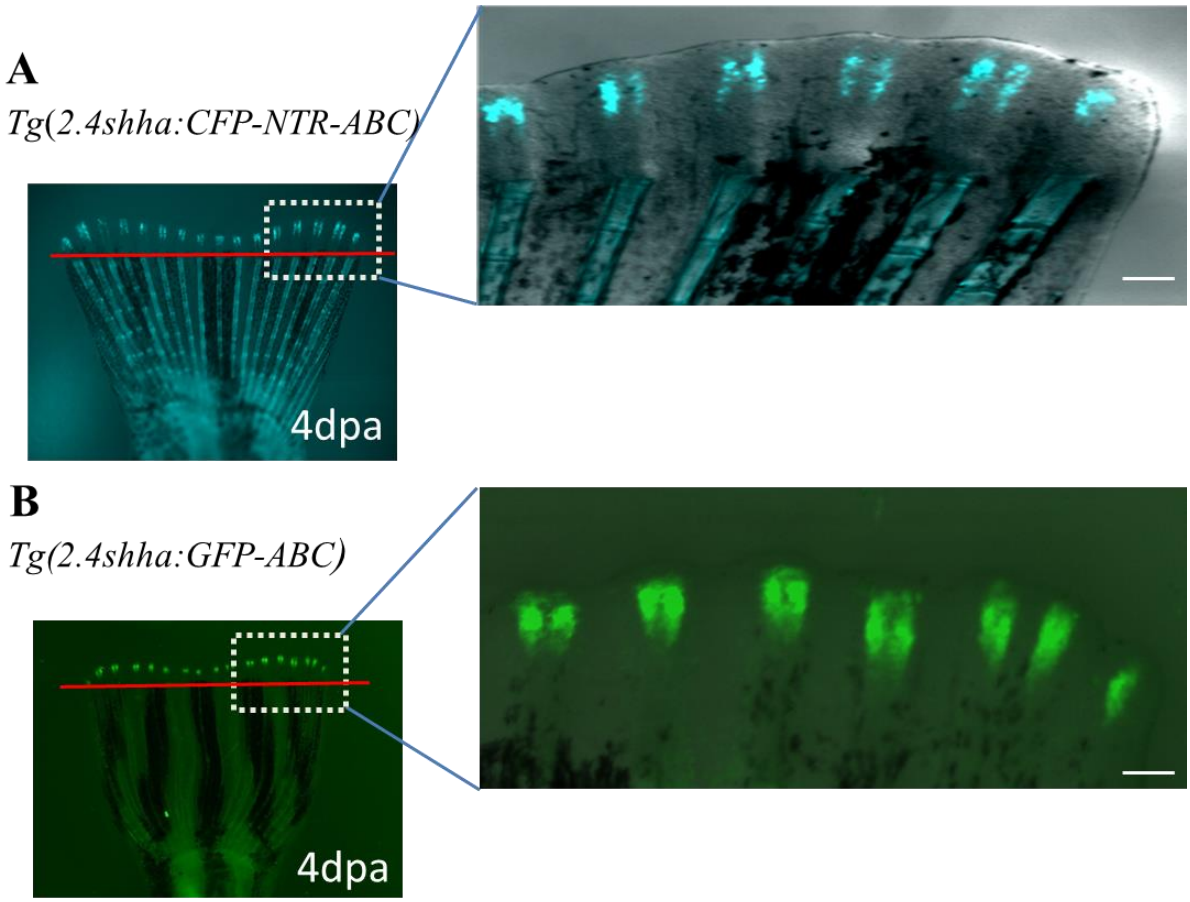
A
Tg(2.4shha:CFP-NTR-ABC)
4dpa
B
Tg(2.4shha:GFP-ABC)
4dpa

Figure 2.12 Comparison of CFP and of GFP expression in the 4 dpa regenerating fins of a F2 fish of the *Tg(2.4shha:CFP-NTR-ABC)* #2 and of a *Tg(2.4shha:GFP-ABC)* transgenic zebrafish.

Although the number of the CFP-expressing cells or the level of CFP expression (A) is low compared to the *GFP*-expressing cells or the level of GFP expression (B), the expression pattern of the CFP-expressing cells in the *Tg(2.4shha:CFP-NTR-ABC)* (A) mimicks the expression pattern of the GFP-expressing cells in the *Tg(2.4shha:GFP-ABC)* (B). The right panels show the close-view of a few fin rays in the white dotted box on the left panels. The amputation plane is indicated by a red line. Scale bars: 200 μm.

2.4.2 Mtz treatment to ablate *shha*-expressing cells

2.4.2.1 Mtz treatment on F3 *Tg(2.4shha:CFP-NTR-ABC)* embryos

In order to test the Mtz/NTR cell ablation system, I conducted Mtz treatment on F3 *Tg(2.4shha:CFP-NTR-ABC)* embryos (Figure 2.13). Ten mM Mtz was used for a period of one day or a period of three days, because this concentration and exposure time has been successfully used in other research studies, such as ablation of hepatocytes, ablation of cardiomyocytes, ablation of pancreatic beta-cells in embryonic/larval zebrafish (Pisharath *et al.*, 2007; Curado *et al.*, 2007; Curado *et al.*, 2008). 1-Phenyl 2-thiourea (PTU), a tyrosinase inhibitor, was used to block pigmentation during zebrafish development (Karlsson *et al.*, 2001). Dimethyl sulfoxide (DMSO) was used to help solubilize Mtz (Curado *et al.*, 2008). Based on the protocols to ablate hepatocytes in zebrafish embryos (Curado *et al.*, 2008), experimental group embryos (n=17) of the F3 *Tg(2.4shha:CFP-NTR-ABC)* were treated with 10 mM Mtz with 0.2% DMSO and 0.1% PTU in embryo medium for three days starting from 1 dpf; Control group embryos (n=16) of the F3 *Tg(2.4shha:CFP-NTR-ABC)* were treated with 0.2% DMSO and 0.1% PTU in embryo medium without Mtz for three days starting from 1 dpf. The fresh solutions for both groups of embryos were changed daily, and pictures of embryos were taken daily.

Before treatment (at 1 dpf), embryos in both the experimental and control group, showed CFP expression in the floor plate cells of the neural tube, notochord, brain, and eyes, mimicking the endogenous expression pattern of *shha*. At 1 day of treatment (dot) (2 dpf), no CFP loss was observed in both the experimental embryos and control embryos. At 2 dot (3 dpf), loss of CFP expression was shown in the floor plate cells of the neural tube and in the ventral forebrain in the Mtz-treated embryos compared to the control embryos. At 4 dpf, all of the

young larvae in the experimental group showed a dramatic decrease of the CFP-expressing cells, but no CFP expression loss was observed in all of the young larvae in the control group (Figure 2.13). This work was repeated two more times and the same results were observed (n=35 for experimental embryos and n=33 for control embryos). Furthermore, experimental embryos showed craniofacial defects, a growth delay, a curved body shape and those embryos did not respond to touch phenotype that resembled the phenotype observed in the *shh*$^{-/-}$ mutant fish (Figure 2.13; Schauerte *et al.*, 1998). Similar results were observed under the same conditions except 1 dpf embryos were treated with 10 mM Mtz for a period of one day instead of a period of three days (n=25 for experimental embryos and n=15 for control embryos) (data not shown). The loss of CFP expression and these phenotypes of malformation in the young larvae after Mtz treatment suggested that the CFP-expressing cells are ablated and Mtz/NTR ablation system was functioning in the *Tg(2.4shha:CFP-NTR-ABC)* larval fish. Next, I examined the effects of Mtz/NTR ablation during fin regeneration of the *Tg(2.4shha:CFP-NTR-ABC)* adult fish.

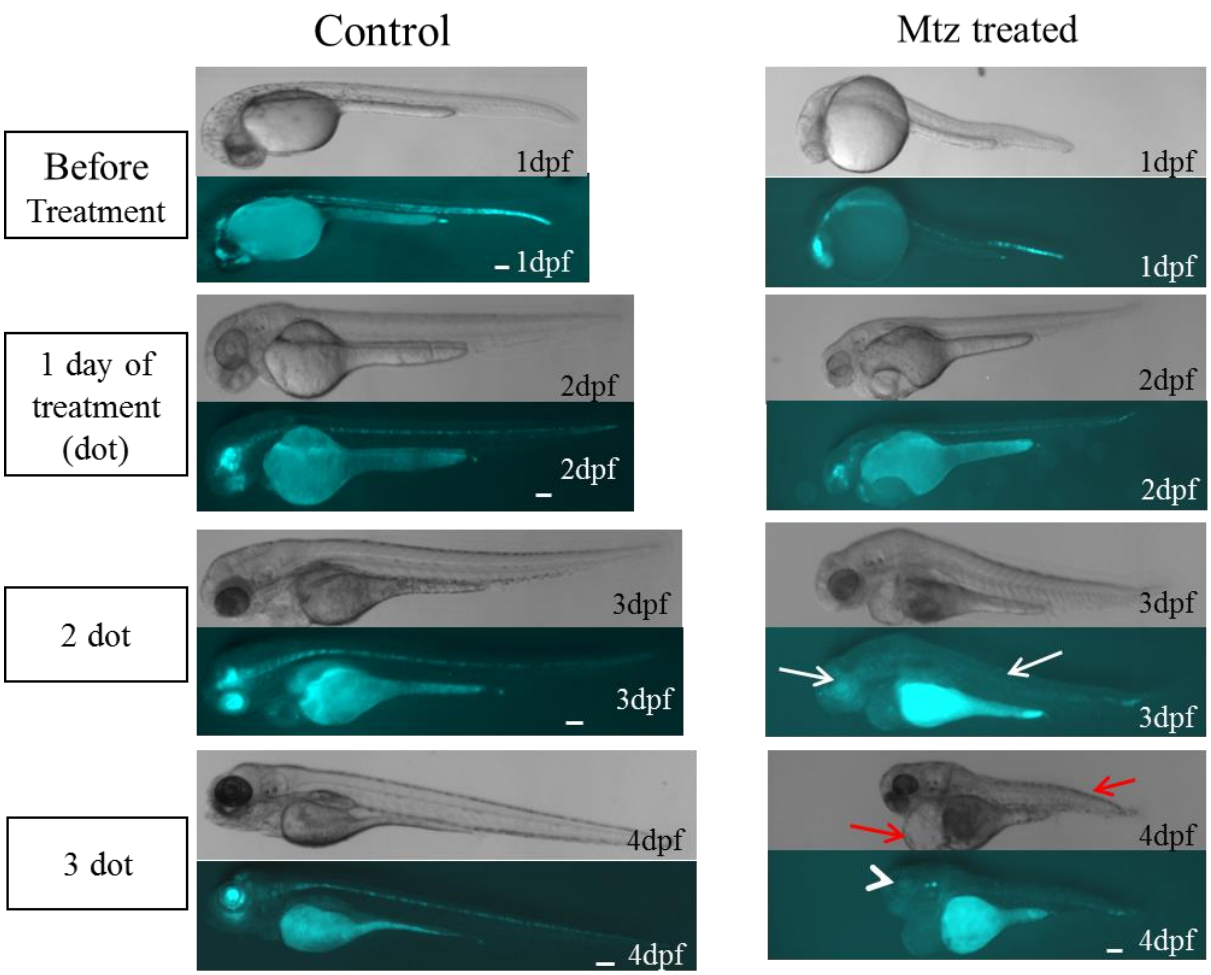
Control
Mtz treated
Before Treatment
1 day of treatment (dot)
2 dot
3 dot
1dpf
1dpf
1dpf
1dpf
2dpf
2dpf
2dpf
2dpf
3dpf
3dpf
3dpf
3dpf
4dpf
4dpf
4dpf
4dpf

Figure 2.13 Treatment of the *Tg(2.4shha:CFP-NTR-ABC)* embryos with 10 mM Metronidazole (Mtz) starting at 1 day post fertilization (dpf).

The control embryo is shown in the left panel, and the experimental embryo is shown in the right panel between 1-4 dpf. Experimental embryos were treated with 10 mM Mtz at 1 dpf for three consecutive days, while control embryos were not treated with Mtz. At 1 day of treatment (dot) (2 dpf), no CFP loss was observed in either the experimental embryos or control embryos. At 2 dot (3 dpf), loss of CFP expression was observed in the neural tube and in the ventral forebrain (white arrows) in the Mtz-treated embryos compared to the control embryos. At 3 dot (4 dpf), loss of CFP expression was also observed in the eyes (the white arrowhead). In addition, treated embryos had a heart edema (the red arrow), a curved body shape (the red arrow), craniofacial defects, and a growth delay and did not respond to touch. N=35 for Mtz-treated embryos, n=33 for control embryos. Scale bars: 200 μm.

2.4.2.2 Experimental design for Mtz treatment on adult *Tg(2.4shha:CFP-NTR-ABC)*

Due to the low number of available F3 adult fish of the *Tg(2.4shha:CFP-NTR-ABC)*, preliminary data were obtained from a test, which was performed on a small sample size of F2 adult fish of the *Tg(2.4shha:CFP-NTR-ABC)* that showed partial CFP expression pattern.

Using the Mtz/NTR system, a complete osteoblasts ablation has been obtained 4 days post treatment (dpt) following 1 day of treatment with 10 mM Mtz in the adult *Tg(osx:NTR/osc:EGFP)* zebrafish caudal fin (Singh *et al.*, 2012). This result suggests that Mtz needs several days to be present to fully ablate the targeted cells. Since 10 mM Mtz concentration can successfully ablate target cells in adult zebrafish, and Mtz concentration higher than 10 mM can cause nonspecific background and lethality of fish (Singh *et al.*, 2012; Li *et al.*, 2012; Curado *et al.*, 2008), I decided to use the concentration of 10 mM for my test. Furthermore, the exposure time of fish to Mtz is crucial because Mtz can be toxic after prolonged exposure (Curado *et al.*, 2008). Since 1 day exposure has been shown to be successful in ablating osteoblasts in the adult zebrafish caudal fin, I decided to use one day Mtz treatment for my test. Hence, I designed an experimental scheme to perform a one day treatment with 10 mM Mtz starting at three different time points following amputation: 0, 1 and 2 dpa based on the consideration that the *shha*-expressing cells are observed as early as 1.5 dpa (Zhang *et al.*, 2012) (Figure 2.14). WT fish treated with Mtz were used as control.

Three F2 adult fish of the *Tg(2.4shha:CFP-NTR-ABC)*, and three WT control fish were used for each experimental design (Figure 2.14). Caudal fins of both the experimental and control zebrafish were amputated one to two segments below the first bifurcation point of all fin rays, then fin regeneration was observed by light microscopy on a daily basis for seven days, and also at 14 dpa or later time points. Following one day of treatment with 10 mM Mtz between

0-1 dpa or 1-2 dpa, no CFP expression loss was observed by 4 dot (6 dpa) (data not shown). However, following one day of treatment with 10 mM Mtz between 2-3 dpa, the number of CFP-expressing cells was decreased at 4 dot (6 dpa) (Figure 2.15), but there were still some CFP-expressing cells in the regenerating fin rays, indicating that the treatment with 10 mM Mtz for one day was not sufficient to ablate all the CFP-expressing cells.

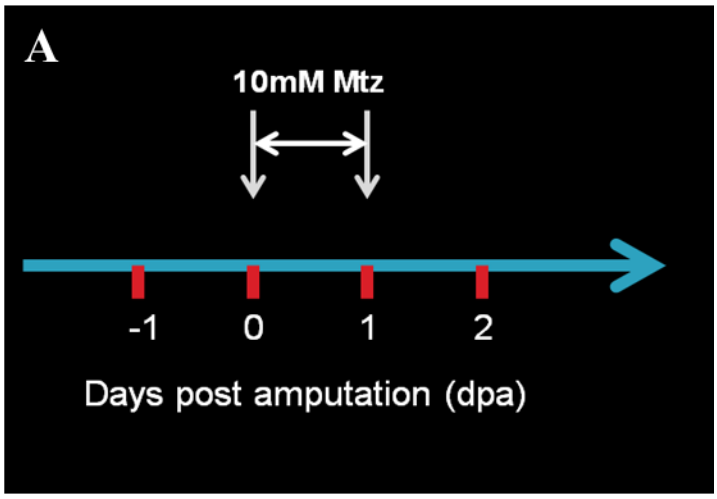
A
10mM Mtz
-1
0
1
2
Days post amputation (dpa)

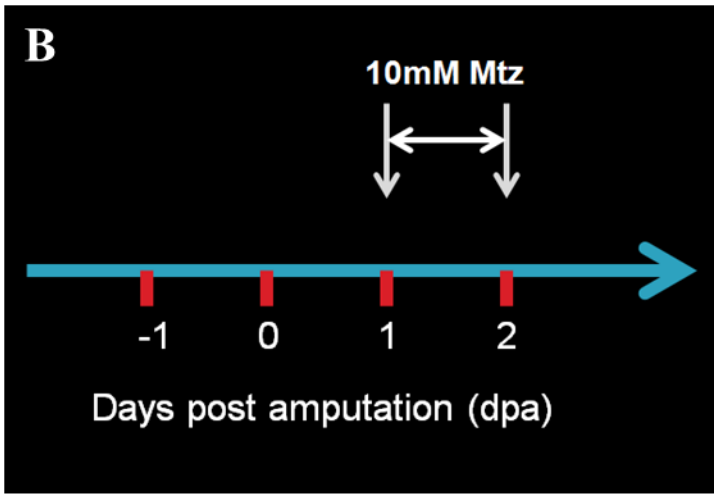
B
10mM Mtz
-1
0
1
2
Days post amputation (dpa)

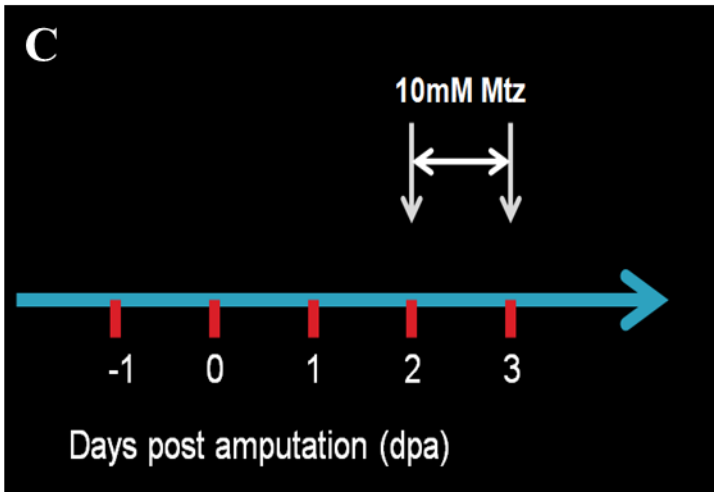
C
10mM Mtz
-1
0
1
2
3
Days post amputation (dpa)

Figure 2.14 Experimental designs for the Mtz treatment on the regenerating caudal fin of F2 fish of the *Tg(2.4shha:CFP-NTR-ABC)*.

Experimental fish are F2 fish of the *Tg(2.4shha:CFP-NTR-ABC)* that show partial CFP expression pattern. WT control fish are used and treated the same way as experimental fish. The caudal fins are amputated one to two segments below the first branching point of all fin rays. A) Experimental design A. Transgenic fish are treated with 10 mM Mtz immediately after caudal fin amputation at 0 dpa for a period of one day. B) Experimental design B. Transgenic fish are treated with 10 mM Mtz starting at 1 dpa for a period of one day. C) Experimental design C. Transgenic fish are treated with 10 mM Mtz starting at 2 dpa for a period of one day (n=3 for each group).

2.4.2.3 Branching delay after Mtz treatment on adult *Tg(2.4shha:CFP-NTR-ABC)* zebrafish fin regenerates

The observation of the partial loss of CFP expression in the experimental design C (10 mM Mtz treatment for one day between 2-3 dpa) indicated a partial ablation of the *shha*-expressing cells. Since transient ablation of the *shha*-expressing cells using a laser beam induced a delay of the branching morphogenesis during fin regeneration (Zhang *et al.*, 2012), I then investigated the effects on branching formation in fish showing a partial loss of CFP-expressing cells using the Mtz/NTR system.

To calculate the branching delay, 6 fin rays of each fish were sampled, namely the dorsal and the ventral fin rays No. 2, No. 3, and No. 4. The numbers of bone segments were counted from the amputation plane to the first branching point in each fin ray of the piece of fin removed just after amputation (denoted as "x") (Figure 2.15B2) and at 14-15 dpa, in the regenerated part of the same fin (denoted as "y") (Figure 2.15B3). The branching delay of each fin ray ($y - x = z$) was calculated. All branching delays were added: ($z_1+z_2 + ...+z_n$) and divided by the total number of measured fin rays (n).

Both the experimental fish and control fish were analyzed for the branching delay. In each fish, bone segments of six fin rays (the dorsal and ventral fin rays No. 2, No. 3 and No. 4) were counted. For fish treated from the experimental design A (a period of one day 10 mM Mtz treatment in the fin regenerates between 0-1 dpa), 1.89 and 0.42 segments of the bifurcation delay were calculated in the experimental fish and control fish, respectively (Table 3). For fish treated from the experimental design B (a period of one day 10 mM Mtz treatment in the fin regenerates between 1-2 dpa), 0.17 and -0.58 segments of the bifurcation delay were calculated in the experimental fish and control fish, respectively (Table 3). For

fish treated from the experimental design C (a period of one day 10 mM Mtz treatment in the fin regenerates between 2-3 dpa), 1.5 and -0.25 segments of the bifurcation delay were calculated in the experimental fish and control fish, respectively (Table 3). These results indicated that the loss of CFP expression in the fin regenerates after Mtz treatment may lead to the delay of the branching morphogenesis. However, no statistical analysis could be performed because our treatment was not sufficient to ablate all the *shha*-expressing cells and more defects may be observed after a complete ablation of the *shha*-expressing cells. However, these preliminary data suggest that Mtz/NTR ablation system is working in the *Tg(2.4shha:CFP-NTR-ABC)* embryos, and this system needs to be developed for the use in the adult zebrafish fins during regeneration (See Discussions).

A

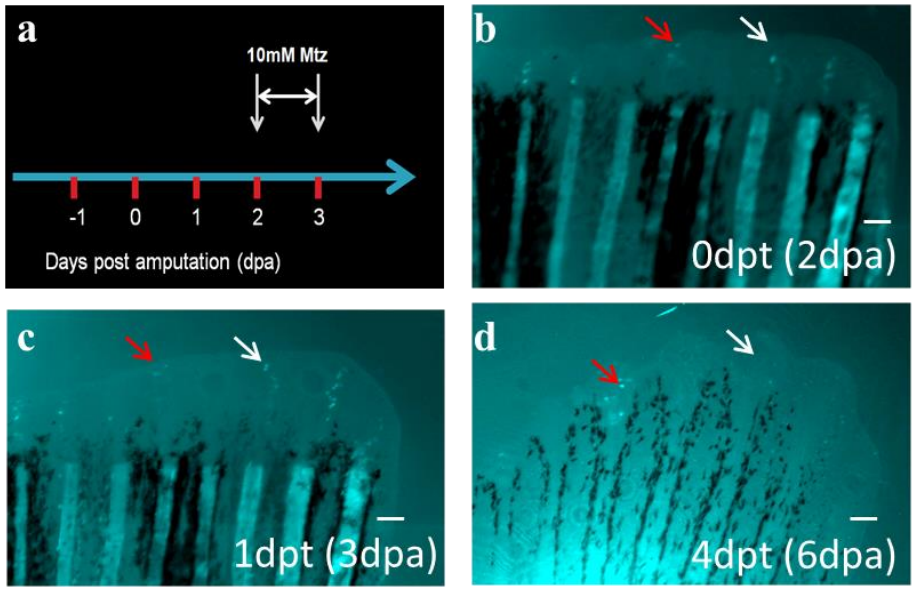
a
10mM Mtz
-1
0
1
2
3
Days post amputation (dpa)
b
0dpt (2dpa)
c
1dpt (3dpa)
d
4dpt (6dpa)

B

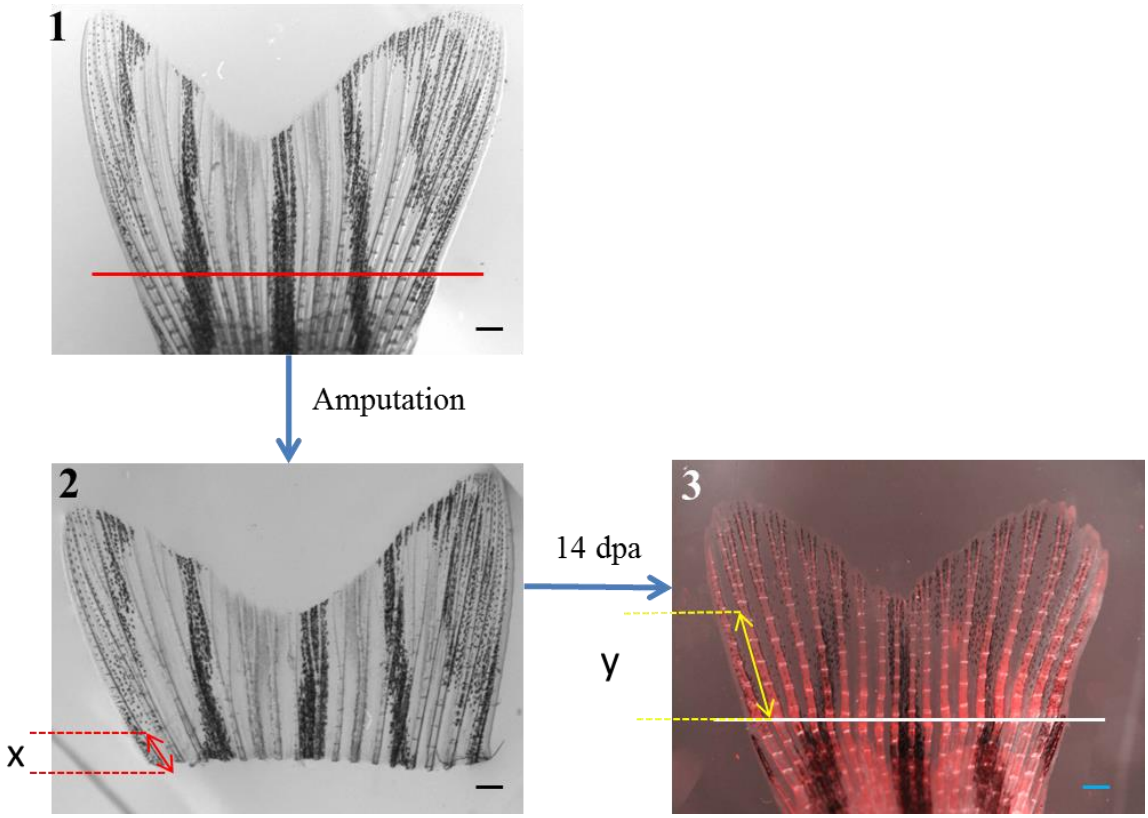
1
Amputation
2
x
14 dpa
3
y

Figure 2.15 Reseults of treatment of the F2 fish of the *Tg(2.4shha:CFP-NTR-ABC)* #2 with 10 mM Mtz for 1 day starting at 2 dpa.

A and B show the same fish with the partial CFP expression pattern (the CFP-expressing cells can be observed in a few fin rays but not all fin rays).

A: Partial CFP expression pattern in the caudal fin of the *Tg(2.4shha:CFP-NTR-ABC)* #2 treated with 10 mM Mtz for one day at 2 dpa. a) Experimental design C shows that treatment of the F2 fish of the *Tg(2.4shha:CFP-NTR-ABC)* #2 with 10 mM Mtz for 1 day starting at 2 dpa. b) The CFP-expressing cells were observed in several fin rays of the regenerating caudal fin at 2 dpa (0 days post treatment (0 dpt)). c) CFP expression in the same fin rays of the regenerating caudal fin at 3 dpa (1 dpt). d) Some CFP-expressing cells were ablated, but there were still CFP-expressing cells in the regenerating fin rays at 6 dpa (4 dpt). White arrows in (b, c, d) show the CFP-expressing cells are ablated in one fin ray after Mtz treatment. Red arrows in (b, c, d) show the CFP-expressing cells are still present in one fin ray after Mtz treatment. Scale bars: 200 μm.

B: An example of one fin ray measurement for the branching delay analysis. 1) The intact caudal fin before amputation. The red line indicates the amputation plane. 2) The F2 fish of the *Tg(2.4shha:CFP-NTR-ABC)* #2 was amputated two segments below the first branching point of all fin rays (despite the fact that most of the rays were cut more than 2 segments proximal to their first bifurcation points). The red double arrow indicates the ray that was cut two segments proximal to the first bifurcation point. 3) Fish were treated with 10 mM Mtz for one day between 2-3 dpa. At 14 dpa, the caudal fin was stained with alizarin red to visualize the bone segments. The white line indicates the amputation plane that was also shown in A. The yellow double arrow indicates an example of the measurement of one fin ray for the

branching delay analysis. The number of bone segments was counted from the amputation plane to the first branching point in the regenerating dorsal fin ray No.2 (in this ray, 5 segments were observed). The branching delay of one fin ray was calculated by using the number of segments in the yellow double arrow (“y”, 5 segments) minus the number of segments in the red double arrow (“x”, 2 segments). Detailed measurements and calculations for the branching delay analysis are described in Materials and Methods. Scale bars: 500 μm.

Table 3. Summary of the bifurcation delay

Experimental design	Average bifurcation delay-Experimental fish	Average bifurcation delay-Control fish
Group A	1.89 segments	0.42 segments
Group B	0.17 segments	-0.58 segments
Group C	1.5 segments	-0.25 segments

2.5 Discussion

Branch formation is observed extensively in both animal and plant kingdom. In vertebrates, such as mammals, many organs including lungs, kidneys, mammary glands, the prostate and salivary glands, have a branched morphology (Figure 2.16; Davies, 2002). It has been proposed that the branched morphology has been favored in evolution because of the advantages of maximizing surface area in a given volume and minimizing transport distances in the most efficient manner (Ochoa-Espinosa and Affolter, 2012).

The adult zebrafish caudal fin is used in our lab for the study of branching morphogenesis of fin rays during regeneration. Previous work in our lab has shown that ectopic expression of Shha results in bone fusion (Quint *et al.*, 2002), and temporal ablation of the *shha*-expressing cells by laser results in a delay of branch formation in the regenerating fin rays of the caudal fin, suggesting that the *shha*-expressing cells play a role in fin ray patterning (Zhang *et al.*, 2012). Since laser ablation can only cause a transient ablation of the *shha*-expressing cells, we proposed to use the Metronidazole/Nitroreductase (Mtz/NTR) system to study the long-term effect of ablating the *shha*-expressing cells during zebrafish caudal fin regeneration. Therefore, the objective of this study was to establish a new *Tg(2.4shha:CFP-NTR-ABC)* line to allow me to use the Mtz/NTR cell ablation system and analyze the long-term effects of ablating the *shha*-expressing cells in the regenerating caudal fin.

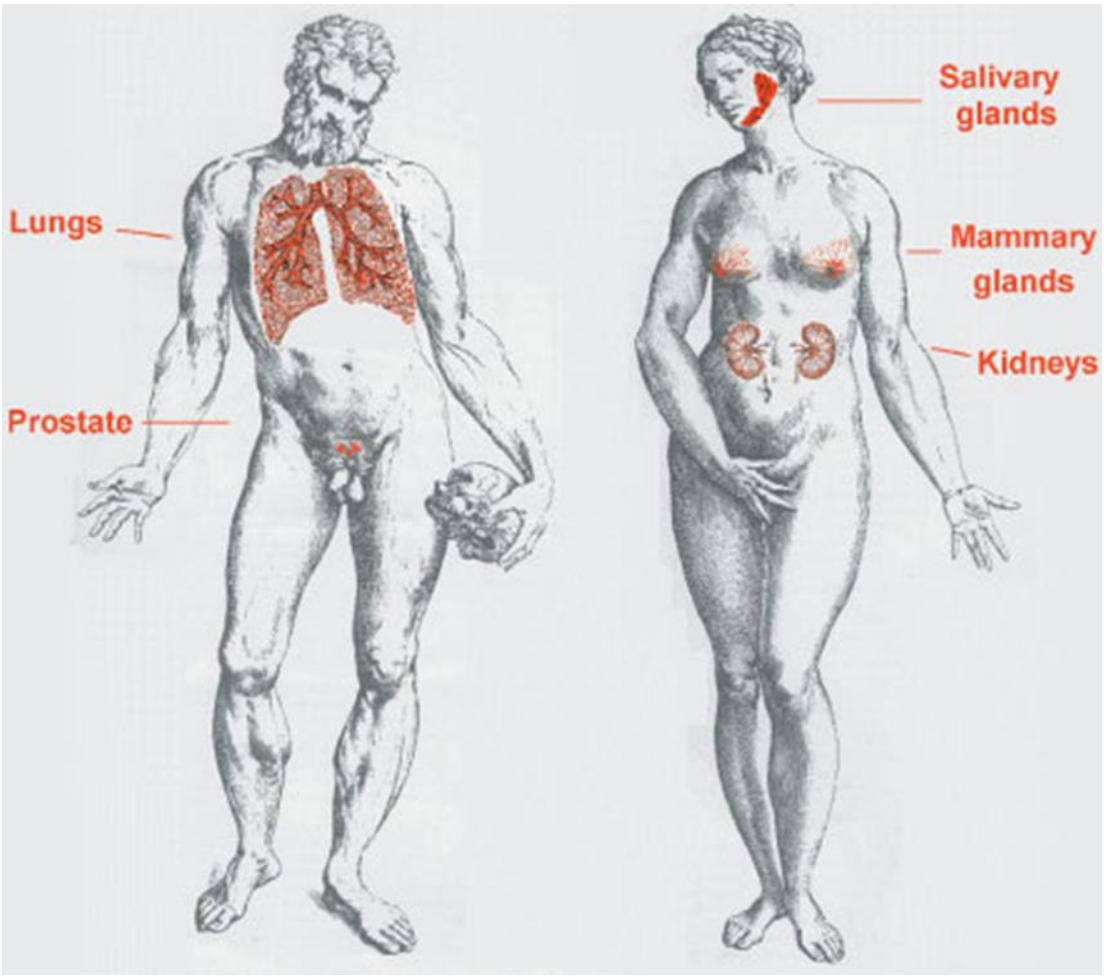
Lungs
Prostate
Salivary glands
Mammary glands
Kidneys

Figure 2.16 Illustration of organs forming branches in humans (the drawings on which the organs have been superimposed are by the anatomist Versalius, and were first published in 1543) (Adapted from Davies, 2002).

In the man, the lungs and the prostate are indicated; in the woman, the salivary glands, mammary glands and kidneys are indicated. Permission to reproduce obtained from publisher.

2.5.1 Successful generation of the *Tg(2.4shha:CFP-NTR-ABC)*

After microinjection into the one-cell stage embryo and screening of the adult for transmission of the transgene, I generated 11 founder fish of the *Tg(2.4shha:CFP-NTR-ABC)*. CFP expression in the transgenic embryos is observed in the eyes, brain, notochord, the floor plate cells of the neural tube, and the urogenital region. This expression pattern is not the same to the expression pattern of the endogenous *shha* gene since it misses the expression in the pectoral fin buds, but it is identical to the expression observed in embryos of the *Tg(2.4shha:GFP-ABC)* transgenic line (Krauss *et al.*, 1993; Ekker *et al.*, 1995; Currie and Ingham, 1996; Ingham and McMahon, 2001; Hadzhiev *et al.*, 2007). However, compared to GFP expression observed in the *Tg(2.4shha:GFP-ABC),* CFP expression is weak and mosaic in the transgenic embryos from the 11 founder fish. The mosaicism (expression in a subset of cells in a given organ or domain of expression) is difficult to explain as all cells possess the transgene. One possibility is that CFP may be expressed in every *shha*-expressing cell but the expression is hardly visualized, due to the nature of the weak fluorescence level of the cyan fluorescent protein (Heim and Tsien, 1996). Compared to the green fluorescent protein, the fluorescence quantum yield for CFP is only 0.36 (Heim and Tsien, 1996), whereas the fluorescence quantum yield for GFP is 0.79 (Phillips, 2001).

To test if the CFP-NTR gene was present in the fin regenerates that showed no clear CFP expression, polymerase chain reaction (PCR) genotyping with CFP-NTR primers was performed on the fin regenerates of the line #2 at 4 dpa. PCR genotyping showed positive result for the presence of CFP-NTR in the caudal fin regenerates (Figure 2.17), indicating that the lack of CFP expression in some fin regenerates might be due to the low number of the CFP-expressing cells, or the low level of CFP expression per cell, making it undetectable.

Among the 11 founder fish, only F1 transgenic fish from the founder fish #2 showed CFP expression in the adult fin regenerates. However, F1 fish from other founder fish showed no CFP expression in the adult fin regenerates, but showed the presence of CFP-NTR transgene by PCR genotyping (Figure 2.17). It was hypothesized that the level of CFP expression per cell could be increased through generations, because sib-pair mating can generate homogeneous zebrafish strains (Shinya and Sakai, 2011), as more copy numbers of the transgene can be transmitted to the next generation through inbreeding. Inbreeding of F1 from line #2 generated F2 that showed stronger CFP expression compared to F1 in the adult fin regenerates, and a similar expression pattern was observed from the *Tg(2.4shha:GFP-ABC)* which recapitulates the endogenous *shha* expression during fin regeneration (Zhang *et al.*, 2012). From then, the *Tg(2.4shha:CFP-NTR-ABC)* was established from the founder fish #2. However, one of the pitfalls of this transgenic line was that transgenic embryos from line #2 showed an ectopic expression in the heart region, which was not observed in the endogenous *shha* expression by *in situ* hybridization (ISH) and was not found in the *Tg(2.4shha:GFP-ABC)* embryos. This ectopic expression might be caused by the random insertion of the transgene close to an enhancer needed for heart expression.

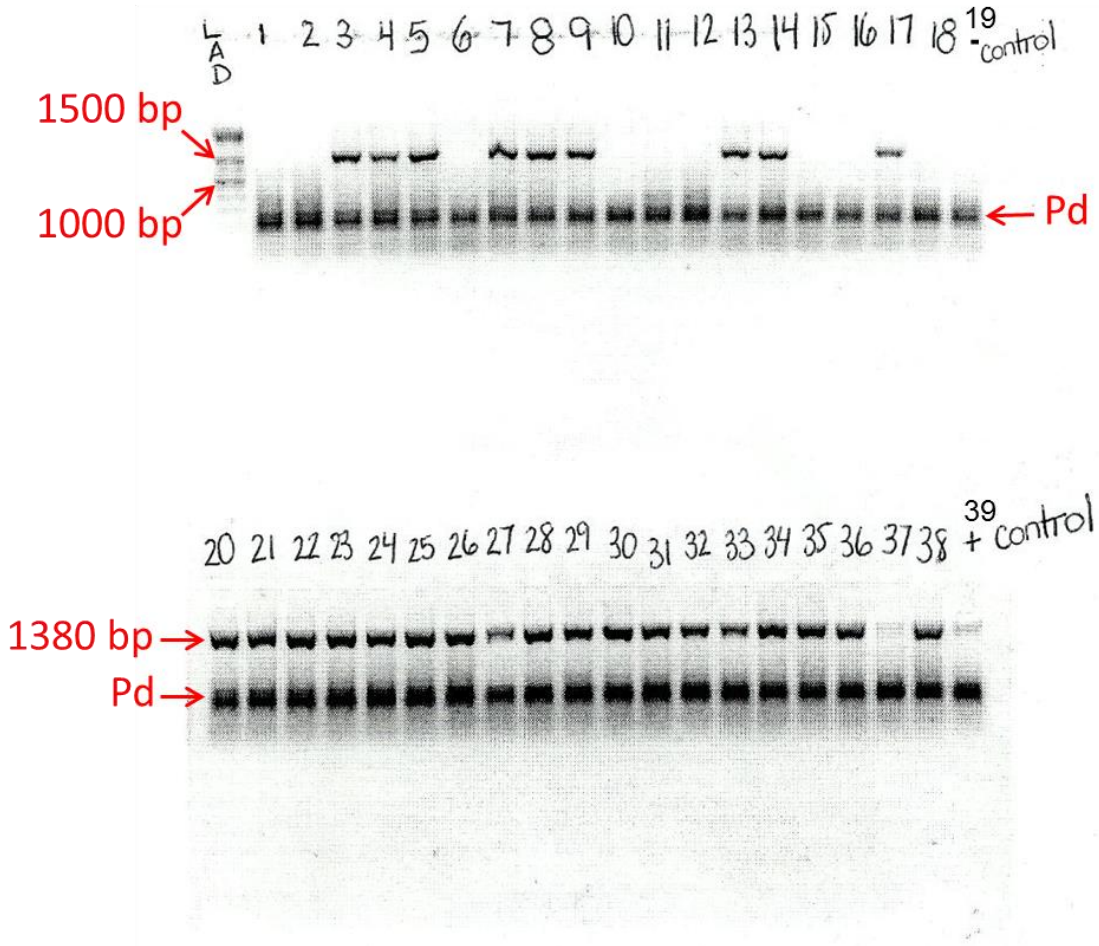
L
A
D
1 2 3 4 5 6 7 8 9 10 11 12 13 14 15 16 17 18 19 - control
1500 bp
1000 bp
Pd
20 21 22 23 24 25 26 27 28 29 30 31 32 33 34 35 36 37 38 39 + control
1380 bp
Pd

Figure 2.17 Genotyping of F1 *Tg(2.4shha:CFP-NTR-ABC)* adult zebrafish fin regenerates at 4 dpa from different founder fish.

Of the 37 samples, no visible CFP expression was detected under the fluorescent microscope. However, genotyping those fins by PCR shows that 27 out of 37 fins have the CFP-NTR transgene as indicated by the 1380 base pairs (bp) DNA fragments in the fin regenerates, whereas the other 11 fins are negative for the transgene. The positive control contained the plasmid DNA of 2.4shha:CFP-NTR-ABC, labeled No. 39 (far right of the lower panel). The negative control was No. 19 (far right of the upper panel). Pd indicates the primer dimers.

2.5.2 Pitfalls and solutions for the Mtz treatment of *Tg(2.4shha:CFP-NTR-ABC)* adult fish

The Mtz/NTR system was first tested on the *Tg(2.4shha:CFP-NTR-ABC)* larvae to ablate the *shha*-expressing cells. Optimal Mtz concentration and exposure is dependent on the promoter used to drive NTR expression and it depends of each particular transgenic line (Curado *et al.*, 2008). A Mtz concentration of 10 mM was used for a period of one day or a period of three days, because this concentration and exposure time have been successfully used in other research studies, such as ablation of hepatocytes, ablation of cardiomyocytes, ablation of pancreatic beta-cells in larval transgenic zebrafish expressing NTR in the respective organs (Pisharath *et al.*, 2007; Curado *et al.*, 2007; Curado *et al.*, 2008). After one-day Mtz or three-day Mtz treatment, the loss of CFP expression was observed in the ventral forebrain, eyes, and the floor plate cells of the neural tube in the Mtz-treated F3 larvae of the *Tg(2.4shha:CFP-NTR-ABC)*, compared to the control (F3 larvae without Mtz treatment). Furthermore, Mtz treated larvae displayed craniofacial defects, growth delay, no response to touch as well as a curled body shape, which resembled the phenotype that is observed in the $shh^{-/-}$ mutant fish (Schauerte *et al.*, 1998). This result indicates that there are enough NTR-expressing cells in the transgenic line and enough NTR produced to ablate the *shha*-expressing cells although CFP expression level is low.

Based on these results, I performed a series of preliminary experiments to determine the most efficient treatment to ablate the NTR-expressing cells in the fin regenerate of adult fish. In the adult zebrafish, a concentration of 10 mM Mtz and exposure for one day has been successfully used for ablation of targeted cells, the osteoblasts in the fin regenerates of the transgenic line *Tg(osx:NTR/osc:EGFP)* (Singh *et al.*, 2012). Using a similar treatment (10

mM Mtz for one day), starting at the time of *shha* activation in the fin regenerate (2 dpa), I observed a delay in branching formation. This result is similar to what has previously been observed following laser ablation of the *shha*-expressing cells (Zhang *et al.*, 2012) and indicates that the method of ablation was successful. As expected, Mtz treatment between 1-2 dpa had no effect as there are no *shha*-expressing cells during this time frame. However, a delay of branch formation was observed when Mtz treatment was performed between 0-1 dpa. I cannot explain this observation based on previous reports (Laforest *et al.*, 1998; Zhang *et al.*, 2012), since there is no *shha* expression before 2 dpa. One potential explanation that will need further investigation is that, when applied just after amputation, the drug may have a better access to the tissue because of the wound and may persist for a longer period of time in the tissues than when it is applied after wound healing. It is however important to note that these experiments have been performed on a very small number of fish (n=3) and will need to be repeated on larger sample groups.

It has been reported that, after a 10 mM Mtz treatment of adult zebrafish for one day, it takes 3-4 days after the treatment to observe a complete ablation of the NTR-expressing cells (Singh *et al.*, 2012). Despite the fact that a branching delay was observed following a one-day treatment between 2-3 dpa, many CFP-expressing cells were still present in the fin regenerates 4 days after the treatment. This observation indicates that our treatment was not sufficient to ablate all the NTR-expressing cells. It also suggests that we may potentially have seen more defects if all the cells would have been ablated.

It has been reported that Mtz may be toxic at high concentrations (>10 mM) or after prolonged exposure (more than one day treatment) (Curado *et al.*, 2008; Singh *et al.*,

2012). In order to ablate more *shha*-expressing cells, we increased the exposure time to 10 mM Mtz but a prolonged Mtz treatment (two days or three days) led to the death of the fish. To overcome the toxic effect due to a prolonged exposure to Mtz, Li and colleagues (2012) successfully used a scheme of treatment that can increase the prolonged exposure to 10 mM Mtz to ablate pineal photoreceptor cells in eyes of adult transgenic zebrafish *Tg(Gnat2:gal4-VP16/UAS:nfsB-mCherry)* without causing lethality (Li *et al.*, 2012). This scheme of treatment consists in treating fish with 10 mM Mtz for 4 times (with 2-day intervals in the system water to remove Mtz) (Figure 2.18). In the future, it would be worth trying this scheme of Mtz treatment to completely ablate the targeted cells and to study the effects of the complete and long-term absence of the *shha*-expressing cells during fin regeneration.

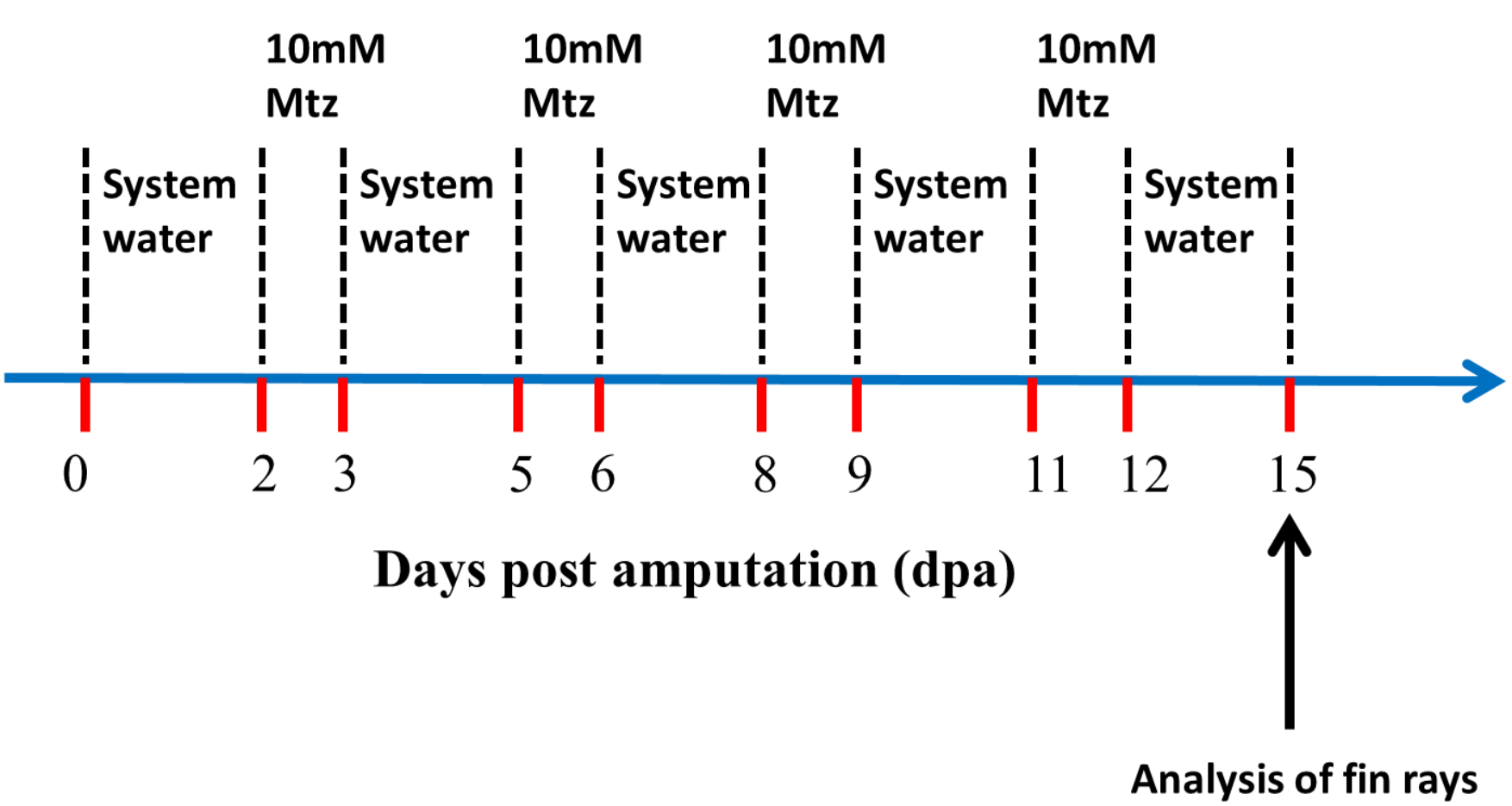
10mM Mtz
10mM Mtz
10mM Mtz
10mM Mtz
System water
System water
System water
System water
System water
0
2
3
5
6
8
9
11
12
15
Days post amputation (dpa)
Analysis of fin rays

Figure 2.18 Proposed intermittent treatment with Mtz of *Tg(2.4shha:CFP-NTR-ABC)* to observe the long-term effect of the ablation of the *shha*-expressing cells during fin regeneration.

Following fin amputation, fish are treated with 10mM Mtz four times for one day with 2-day intervals during which fish are transferred in the regular system water to wash-off Mtz. Analysis of the fins is performed at 15 dpa.

An alternative way to perform the Mtz treatment is to directly inject Mtz into the fin rays in the caudal fin regenerates. Injection of Mtz in the abdominal cavity has previously been done to ablate pancreatic beta cells in the adult zebrafish transgenic line *Tg(T2Kins:nfsB-mCherry)* (Moss *et al.*, 2009). Three days after Mtz injection, pancreatic beta cells were ablated and zebrafish had elevated blood glucose levels (Moss *et al.*, 2009). Therefore, it is worth testing if injection of Mtz into the fin rays of the blastema of the caudal fin regenerates (possibly at 2-3 dpa) can locally ablate the NTR-expressing cells (Figure 2.19). If this approach is efficient in ablating the desired cells and does not impair the survival of the fish, repeated injections of Mtz at several time intervals could be done to observe the long-term effects of the ablation of the *shha*-expressing cells.

Furthermore, it is possible that the transgene may not only be expressed in the adult fin regenerates, but also in other tissues or organs in the adult zebrafish either because the regulatory elements used in the construct are necessary for *shha* expression in various tissues of the adult zebrafish, or because of the ectopic expression of the transgene due to its random insertion in the genome close to an enhancer. If the lethality of fish after prolonged 10 mM Mtz treatment was not caused by Mtz toxicity, but by the ablation of cells in essential organs in adult zebrafish, the approach of local injection of Mtz in the caudal fin regenerates would be preferable for the ablation of the *shha*-expressing cells of the fin rays without impairing the survival of the fish.


10 mM Mtz
Fin
Amputation
==>

Figure 2.19 The cartoon shows the injection of 10 mM Mtz in the *Tg(2.4shha:CFP-NTR-ABC)* fin regenerates.

Injection can be done in the blastema of the caudal fin regenerate at various time points following fin amputation.

2.5.3 Roles of the *shha*-expressing cells and other factors involved in branching morphogenesis

After optimization of the Mtz treatment to successfully ablate the *shha*-expressing cells during fin regeneration, it would be interesting to investigate the effects of this ablation on the expression of factors involved in branching formation in the rays and more particularly to analyze the effects on the potential target cells, such as osteoblasts. Previous results from our laboratory suggest that Shha may direct the positioning of the proliferating osteoblasts in the regenerating fin ray through cross talks with factors expressed in osteoblasts (Zhang *et al.*, 2012).

For example, Ptch1 (the Shha receptor) is normally expressed in both newly differentiated osteoblasts and the basal layer of the epidermis during fin regeneration (Laforest *et al.*, 1998). Since Shh binding to Ptch1 receptor can activate Gli1 transcription factor and *ptch1* is among the genes that are activated by Gli (Buttitta *et al.*, 2003), expression of *ptch1* is hypothesized to decrease after ablation of the *shha*-expressing cells. Analysis of the effects on Ptch1 expression will be facilitated by the use of the reporter transgenic line *Tg(Ptch1:EGFP)* expressing EGFP under the control of the Ptch1 regulatory region (gift of Dr. Phil Ingham, Institute of Molecular and Cellular Biology, Singapore). *In vivo* analysis of the effects of NTR ablation on Ptch1 expression could be studied in the double transgenic line *Tg(Ptch1:EGFP/2.4shha:CFP-NTR-ABC).* We also expect that, since *ptch1* is expressed in both basal epidermal layer and osteoblasts, ablation of the *shha*-expressing cells that are in the basal layer of epidermis, will also result in the ablation of some *ptch1*-expressing cells that overlap with the *shha*-expressing cells.

BMP2 is known to be important for the osteoblast proliferation and differentiation (Choi *et al.*, 2005). Previous studies have shown that *bmp2b* is expressed in both the differentiating osteoblasts and basal epidermal cells during zebrafish fin regeneration (Quint *et al.*, 2002; Smith *et al.*, 2006). Functional analysis has shown that ectopic expression of Shha in the fin regenerate induces *bmp2b* expression, suggesting that Bmp signaling is acting downstream of Shha signaling in the regenerating fin (Quint *et al.*, 2002). It will be interesting to investigate the dynamic spatial-temporal expression of *bmp2b* after ablating the *shha*-expressing cells. During fin regeneration, *Col10a1* is strongly expressed in osteoblasts and in the basal epidermal layer (Avaron *et al.*, 2006; Smith *et al.*, 2006). After laser ablation of the *shha*-expressing cells, it has been shown that separation of *col10a1* expression domain in osteoblasts is delayed and thus branching formation of fin rays is delayed (Zhang *et al.*, 2012). Col10a1 is an excellent marker to analyze the presence and function of osteoblasts and it can be used to examine the direct effects on osteoblast function of the ablation of the *shha*-expressing cells. Previous studies have also shown that inhibition of Hh signaling using cyclopamine results in the arrest of fin regeneration due to an inhibition of cell proliferation (Quint *et al.*, 2002). Furthermore, the separation of the *shha*-expressing cells into two domains prior to branching formation is immediately followed by the separation of the proliferating population of osteoblasts, suggesting that *Shha* signaling regulates branching formation by directing the proliferation of osteoblasts (Zhang *et al.*, 2012). Therefore, it will be interesting to examine the proliferation pattern of the osteoblasts and other cells of the blastema in the absence of the *shha*-expressing cells.

Chapter III: Characterization of the Organ-Wide Response to Local Injury in Zebrafish Caudal Fin

3.1 Introduction

3.1.1 Inflammatory response to injury in zebrafish

Following zebrafish caudal fin injury, acute inflammation is activated and the inflammatory response plays an essential role in protecting the organisms from bacteria infection, in removing dead cells and in maintaining tissue homeostasis (Medzhitov, 2007; Li *et al.*, 2012). Recent studies have shown that infiltrating immune cells are positive regulators of neuronal regeneration in the zebrafish central nervous system and they are required for adult zebrafish fin regeneration as well as adult salamander limb regeneration (Kyritsis *et al.*, 2012; Godwin *et al.*, 2013).

Recently, the *in vivo* behavior and function of the neutrophils during larval zebrafish tail fin regeneration has been characterized (Li *et al.*, 2012). Upon amputation of the larval zebrafish tail fin, neutrophils are the first immune cells that respond to the injury and migrate to the site of the wound (Martin and Leibovich, 2005; Serhan *et al.*, 2007; Li *et al.*, 2012). Neutrophils are recruited to the wound site in 6 hours post amputation (6 hpa), where they can fight against the invasion of microorganisms and act as scavengers to remove apoptotic bodies and small cell debris. After the neutrophil early response to injury, neutrophils are removed by either apoptosis followed by phagocytosis by macrophages, or reverse migration to enter the vascular lumen in the host. The removal of the neutrophils is essential for successful

inflammation resolution (Henry *et al.*, 2013; Li *et al.*, 2012; Starnes and Huttenlocher, 2012). In addition, after injury, bleeding has to be stopped. Hemostasis is a self defense mechanism that is initiated to protect the organism from bleeding (Mann, 1999). In zebrafish, thrombocytes are the functional equivalent of the mammalian platelets, which serve as the coagulation regulator in hemostasis (Jagadeeswaran *et al.*, 1999).

One of the advantages of using the zebrafish as an animal model is that zebrafish has an excellent regenerative ability in the caudal fin and the organism is genetically tractable. By using different transgenic lines of zebrafish, specific cells can be labeled with fluorescent reporters *in vivo* to understand the functions of various cells following injury and during regeneration process (Henry *et al.*, 2013). *Tg(mpx:GFP)* is an established zebrafish transgenic line that can be used for the study of neutrophils infiltration. *mpx* is the myeloid-specific peroxidase gene that is very often used as a marker for neutrophils (Renshaw *et al.*, 2006). This line expresses the green fluorescent protein (GFP) under the regulatory elements of the myeloperoxidase (*mpx*) gene and allows *in vivo* tracking of the dynamics of neutrophils in both larval and adult zebrafish (Renshaw *et al.*, 2006; Richardson *et al.*, 2013). Another zebrafish transgenic line, *Tg(CD41:GFP),* allows *in vivo* tracking of the dynamics of thrombocytes in zebrafish larvae (Kim *et al.*, 2012). CD41 is the α subunit of the platelet integrin CD41/CD61 (α_{IIb}/β_3, glycoprotein IIb [GPIIb]/GPIIIa) complex and the marker for thrombocytes and prothrombocyte precursors (Ferkowicz *et al.*, 2003; Mikkola *et al.*, 2002; Khandekar *et al.*, 2012). In *Tg(CD41:GFP)* line, the regulatory region of the *CD41* gene drives the expression of the fluorescent reporter GFP (Lin *et al.*, 2005).

3.1.2 Organ-wide response to local injury in the zebrafish heart

As with the fins, the zebrafish heart displays extraordinary regenerative capacity after injury and is used as an excellent model for studies of heart development and regeneration (Poss *et al.*, 2002; Nemtsas *et al.*, 2010; Major and Poss, 2007; Nachtrab and Poss, 2012).

The adult zebrafish heart is composed of three layers of tissues: the epicardium, myocardium and endocardium. Adult zebrafish hearts can regenerate after amputation of up to 20% of the ventricle (Poss *et al.*, 2002). Immediately after injury, the ventricle is sealed at the wound site by the formation of a large clot of erythrocytes, preventing the heart from excessive bleeding. After 2-3 days post amputation (dpa), the blood clot of erythrocytes matures into a fibrin clot, which reaches maximum levels at 7-9 dpa. Between 9-30 dpa, cardiac myofibers surround, penetrate and eventually replace the clot. Between 30-60 dpa, the fibrin clot has completely disappeared, indicating the end of the regeneration. The amputated region is regenerated with the newly formed cardiac muscles and the coronary vasculature, resulting in a functional and normal heart (Poss *et al.*, 2002; Raya *et al.*, 2003; Kikuchi *et al.*, 2010). Recent studies have shown that the majority of the regenerated cardiac muscles are derived from cells expressing the gene *cardiac myosin light chain 2 (cmlc2),* which is required for the contractile function of cardiac cells (Kikuchi *et al.*, 2010). Most newly regenerated cardiomyocytes are derived from existing cardiomyocytes, suggesting that dedifferentiation of existing cardiomyocytes is the dominant source mechanism for heart regeneration in zebrafish (Kikuchi *et al.*, 2010; Choi and Poss, 2012)

Additionally, after the 20% ventricular resection as a partial amputation in the adult zebrafish heart, an organ-wide injury response takes place by the activation of gene expression in the entire heart that is not limited to the site of injury during the regeneration (Raya *et al.*, 2003; Lepilina *et al.*, 2006). The organ-wide response is defined by the presence of an injury

response occurring not only near the wound but also in the entire organ (Kikuchi and Poss; 2012). This organ-wide response involves all three layers of tissues: epicardial tissues, endocardial tissues and myocardial tissues (Kikuchi *et al.*, 2010, 2011; Lepilina *et al.*, 2006). For example, at 1 hpa, endocardial cells all over the heart show detachment from the myofibers. By 3 hpa, endocardial and epicardial cells induce the expression of *raldh2*, a developmental gene marker coding for an enzyme involved in the synthesis of retinoic acid (RA), in an organ-wide manner (Figure 3.1; Kikuchi *et al.*, 2011). Between 1-3 dpa, two embryonic epicardial markers, *tbx18* and *raldh2* are induced in adult epicardial cells and are expressed in the periphery of the entire heart (Figure 3.1; Lepilina *et al.*, 2006). By 7 dpa, *gata4,* a gene coding for a transcription factor and the marker for myocardial activation, is induced in ventricular cardiomyocytes that are located in the subepicardial compact layer of the entire ventricle (Figure 3.1; Kikuchi *et al.*, 2010). Finally, between 7-30 dpa, the organ-wide activated gene expression signatures localize to the site of injury, depending on the cell type (Figure 3.1; Will *et al.*, 2008; Kikuchi and Poss, 2012). Provoked by local injury signals, the activation of injury response throughout the heart is suggested to be an essential property for the regenerative success and homeostasis, however, the organ-wide response to local injury in the adult zebrafish heart has not specifically been analyzed and little is known about the mechanisms behind this phenomenon (Will *et al.*, 2008; Kikuchi and Poss, 2012).

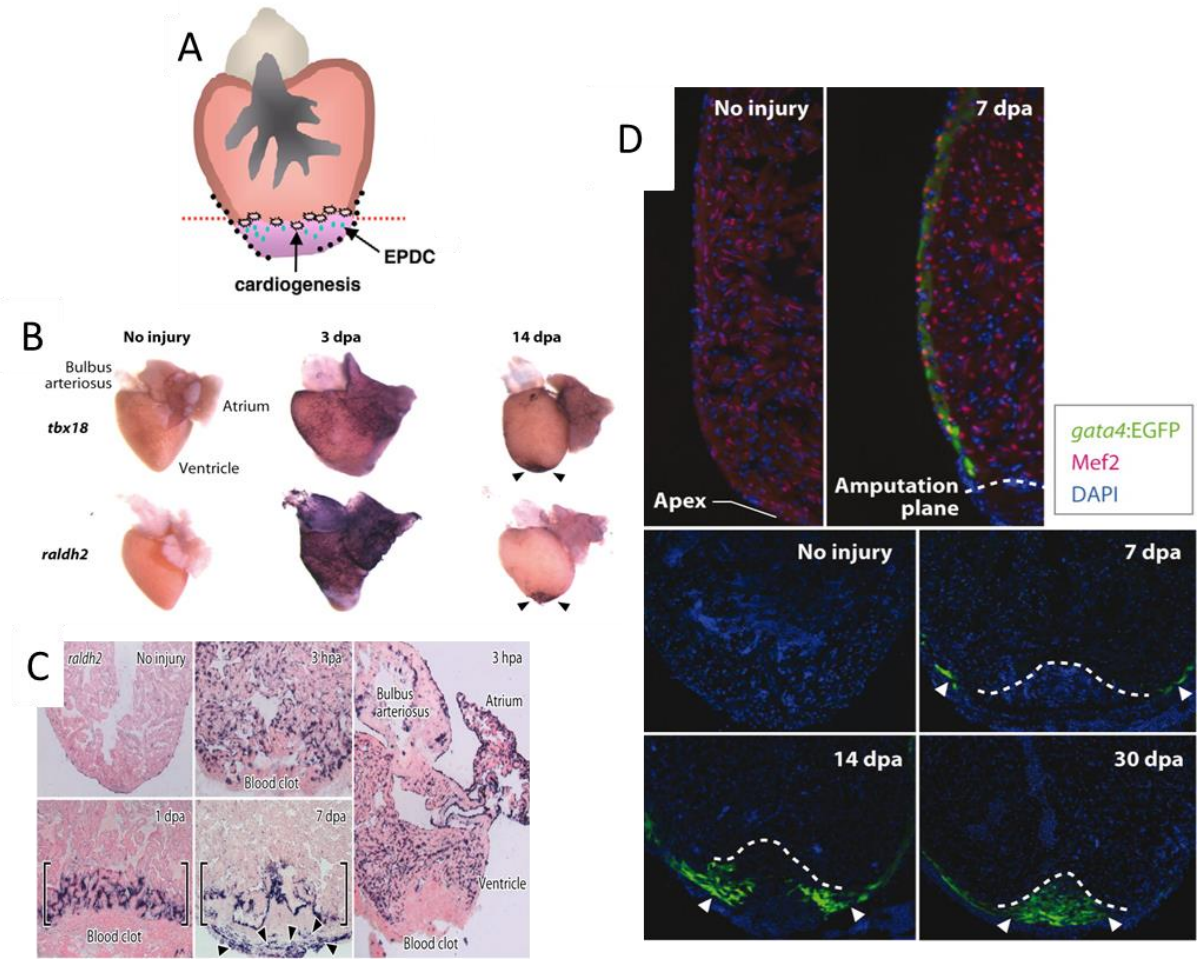
A
EPDC
cardiogenesis
B
No injury
3 dpa
14 dpa
Bulbus arteriosus
Atrium
tbx18
Ventricle
raldh2
C
raldh2
No injury
3 hpa
Blood clot
1 dpa
7 dpa
Bulbus arteriosus
Atrium
Ventricle
D
No injury
7 dpa
Apex
Amputation plane
gata4:EGFP
Mef2
DAPI
14 dpa
30 dpa

Figure 3.1 Organ-wide response to local injury in the adult zebrafish heart (Modified from Kikuchi and Poss, 2012; Kikuchi *et al.* 2010, 2011; Lepilina *et al.* 2006).

A: A cartoon of the ventricle at 7 dpa showing epicardial response has localized to the injury site. Regeneration involves developmental activation of the epicardium (black dots) and local recruitment of epicardial-derived cells (EPDCs) to a focus of new cardiomyocytes (CM) production (pink explosions) at the wound (red dotted line) (Modified from Will *et al.*, 2008). B: Injury responses of the developmental genes such as *tbx18 and raldh2* within several days following injury. *tbx18 and raldh2* expression is activated in the entire epicardium by 3 dpa, but gene expression localizes to the wound area by 14 dpa (arrowheads). C: Cryosection image of the upregulation of *raldh2* in the endocardial cells of the entire heart in 3 hpa, and the expression progressively localizes to the site of injury (brackets). D: Induction of a gata4:EGFP reporter indicates myocardial activation. Mef2 indicates the cardiomyocyte nuclei. DAPI (4, 6-diamidino-2-phenylindole) is used to label cells nuclei. Note that gata4:EGFP is first detected in the entire compact layer of the myocardium by 7 dpa and becomes localized to the regenerating myocardium by 14–30 dpa (arrowheads). Dotted lines indicate approximate amputation planes. Permission to reproduce obtained from publisher.

3.1.3 Organ-wide response to local injury in the zebrafish brain

Zebrafish brain has a life-long ability to generate new neurons for the persistent growth of the brain, a process known as constitutive neurogenesis. When an injury is induced in the zebrafish brain, regenerative neurogenesis is activated and can produce sufficient neurons to help the recovery of function of the central nervous system (Kroehne *et al.*, 2011; Antos and Brand, 2010). A novel traumatic stab lesion model in the adult zebrafish brain has been developed and used as a standard traumatic injury method to induce damage on one lobe of the telencephalon, leaving the non-lesioned hemisphere as control (Figure 3.2; Kroehne *et al.*, 2011). After the stab lesion, the initial cellular responses are characterized by widespread traumatic degeneration of neuronal cells and processes (Kizil *et al.*, 2011), followed by injury-induced proliferation of the radial glial cells and regenerative neurogenesis (Kizil *et al.*, 2012).

No one has previously addressed the organ-wide response after local stab lesion in the adult zebrafish brain. However, I noticed in the publication (see Figure 2D in Kishimoto *et al.*, 2012) that there seemed to be an increased number of proliferating cells in the telencephalon not only at the lesion site but also at the non-lesion site (Kishimoto *et al.*, 2012). Moreover, S100B, a marker of neural stem cells in the ventricle (Lam *et al.*, 2009; Marz *et al.*, 2010a), is upregulated at 3 days post lesion (dpl) in both the lesion and non-lesion regions (Marz *et al.*, 2011). Kizil and colleagues have found that *gata3*, a specific injury-induced pro-regenerative factor, is upregulated in the non-lesion region of the regenerating adult zebrafish brain, suggesting that the regenerative program in the non-lesion region has been activated (Figure 3.2; Kizil *et al.*, 2012). However, the mechanisms for the organ-wide response to the locally stab lesion in the adult zebrafish brain are not fully characterized and largely unknown.

AA

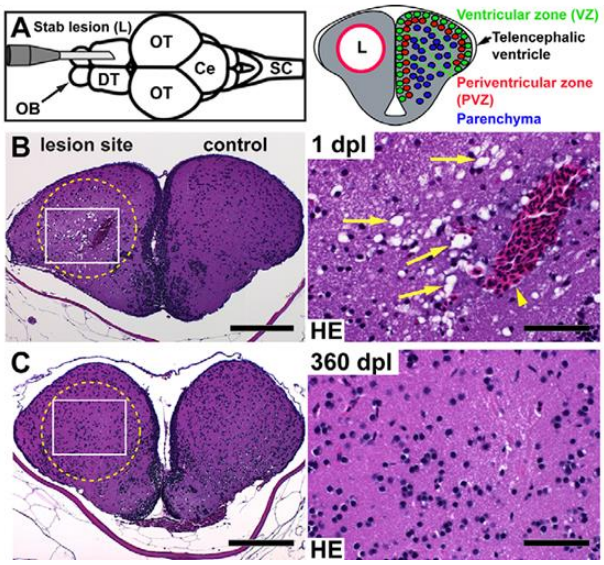
A Stab lesion (L)
OT
Ce
SC
DT
OT
OB
L
Ventricular zone (VZ)
Telencephalic ventricle
Periventricular zone (PVZ)
Parenchyma
B lesion site
control
1 dpl
HE
C
360 dpl
HE

BB

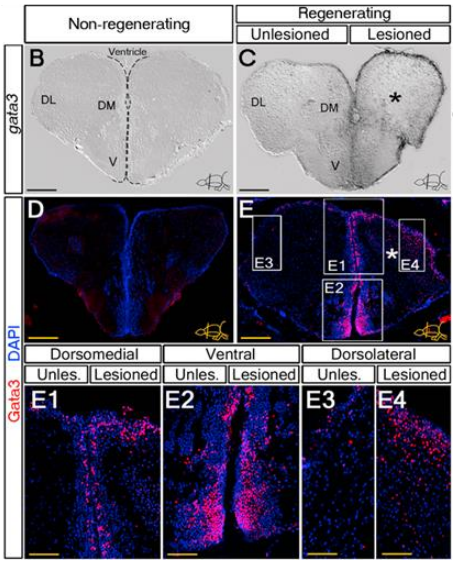
Non-regenerating
Regenerating
Unlesioned
Lesioned
gata3
B
Ventricle
DL
DM
V
C
DL
DM
V
*
DAPI
D
E
E3
E1
E2
*
E4
Dorsomedial
Ventral
Dorsolateral
Unles.
Lesioned
Unles.
Lesioned
Unles.
Lesioned
Gata3
E1
E2
E3
E4

Figure 3.2 Stab lesion in the adult zebrafish brain.

AA: The newly developed stab lesion assay and tissue regeneration in the adult zebrafish telencephalon (Adapted from Kroehne *et al.*, 2011). (A) Stab lesion in the adult zebrafish telencephalon is induced by the insertion of a canula (dorsal view; OB, olfactory bulb; DT, dorsal telencephalon; OT, optic tectum: Ce, cerebellum; SC, spinal cord). The cross-section image (right) shows the injured telencephalon indicated by L and the ventricular zone (VZ, green) that contains neural progenitor cells. During constitutive neurogenesis, all newborn neurons integrate into the periventricular zone (PVZ, red, one or two cell diameters adjacent to the VZ). The uninjured central parenchyma (blue) does not receive new neurons. (B) Haematoxylin/Eosin (HE) stained sections show that 1 day post lesion (dpl), vacuolated tissues (arrows) and a prominent blood clot (arrowhead) are observed in the lesion site. (C) By 360 dpl, restoration of the tissue architecture is complete. Scale bars: 200 μm in B,C overviews; 50 μmm in B,C insets. Circles indicate the lesion canal. Permission to reproduce obtained from publisher.

BB: *gata3* gene expression and Gata3 protein expression before and after the stab lesion (Kizil *et al.*, 2012). (B) *gata3* is not expressed in the uninjured adult telencephalon, shown by *in situ* hybridization (ISH). DM, dorsomedial; DL, dorsolateral; V, ventral. (C) *gata3* expression (shown by ISH) is induced in the lesioned hemisphere and part of the unlesioned hemisphere at 3 dpl. The stab lesion is indicated as (*). (D) Gata3 is not expressed in the uninjured adult telencephalon, shown by immunohistochemistry (IHC). (E) Gata3 expression (shown by IHC) is induced in the lesioned hemisphere and part of the unlesioned hemisphere at 3 dpl. (E1–E4) High-magnification images from different regions. Scale bars: 100 μm (B–E); 50 μm (E1–E4); n = 8 fish for (B–E4). Permission to reproduce obtained from publisher.

3.1.4 Organ-wide response to local injury in other animal models

Organ-wide responses to local injury have been previously mentioned but not fully characterized or described. Newt and axolotl are used as excellent animal models for studies of limb regeneration (Poss, 2010). In the experimental designs for studies of limb regeneration, one limb of the animal is often used as a control, whereas another limb of the same animal receives the experimental treatment, because it was shown that the removal of multiple limbs from adult vermilion-spotted newt *(Diemyctylus uiridescens)* did not alter the rate of regeneration compared with the removal of only one limb (Mogan, 1906). However, in 1971, Tweedle reported that, in both the newt and axolotl, the regeneration rate was slower after the simultaneous removal of the contralateral to the first limb that was removed (Tweedle, 1971). However, simultaneous removal of a second limb that was not contralateral to the first one had no significant effect on the rate of regeneration. This latter result suggested that a general systemic effect was not involved in the delay of the regeneration rate. Furthermore, it indicated that the amount of tissue removed was not the cause for the slower regeneration rate. In addition, removal of the denervated contralateral double limbs had no effect on the regeneration rate, suggesting that the brachial nerves in the contralateral double limbs were responsible for the slower regeneration rate.

Therefore, after local injury (here one limb removal), it has been postulated that the delay of the regeneration process was due to the damage of the nerves or a delay of the axonal flow which delivers neural factors to the regenerating limbs (Tweedle, 1971). This effect has been named “transneural effect” (tweedle, 1971).

More importantly, a number of case studies have shown an organ-wide response to local injury in human patients (Suzuki *et al.*, 1993; Knecht *et al.*, 1996; Eltzschig and Collard, 2004; Wu *et al.*, 2008). For example, one case study of Suzuki *et al.*, (1993) reported the

long-term effect of amputation of one upper arm in the patient. The loss of axons induced retrograde degeneration of anterior horn and spinal ganglion cells in the spinal cord on the amputated side. This loss of axons also influenced the contralateral side and led to neuronal degeneration. As a result, the number of neurons in the anterior horn on both the amputated side and the contralateral side was significantly decreased (Suzuki *et al.,* 1993). This result indicated that amputation of one arm could provokes an injury response in both the amputated side and the contralateral (spared) side. Furthermore, Knecht and colleagues (1996) have shown that patients with arm amputation have referred phantom sensations, which evoked from painful stimuli. These referred sensations are from sites on the face and the trunk not only ipsilaterally but also contralaterally to the amputation. This result indicates that there is an injury response of the painful stimuli to arm amputation in both the amputated and the contralateral side in humans (Knecht *et al.*, 1996).

3.2 Objectives

For fin regeneration experiments in adult zebrafish, researchers often use one of the lobes of the caudal fin for experimental purposes and the other lobe as an internal control. For example, for functional analysis of gene(s) during caudal fin regeneration, morpholino-based technique)to knock down gene functionare often performed in the regenerating fin rays of one lobe of the caudal fin, while the fin rays of the other lobe are used as an internal control (Thummel *et al.*, 2006; Hyde *et al.*, 2012; Münch *et al.*, 2013). In another study, a few fin rays in one lobe of the caudal fin were injured by bone crush and a few fin rays were amputated in the other lobe. This experiment was designed to compare the two types of injury response, bone crush versus amputation (Sousa *et al.,* 2012). However, no one has previously examined whether partial or local injury of the zebrafish caudal fin induces an organ-wide response. In a larger perspective, we want to test whether the zebrafish caudal fin can be used

as a model to study organ-wide responses to local injury. This study may provide new insights into the field of regenerative medicine, in which stimulating regeneration locally may trigger responses in unintended locations.

The purpose of this study is to

1. To characterize the morphological changes due to local injury of the caudal fin
2. To characterize the dynamics of *shha*-expressing cells in response to local injury of the caudal fin of the *Tg(2.4shha:GFP-ABC)*
3. To characterize the dynamics of blood vessels in response to local injury of the caudal fin of the *Tg(fli1:EGFP)*
4. To characterize the dynamics of neutrophils in response to local injury of the caudal fin of the *Tg(mpx:GFP)*
5. To characterize the dynamics of thrombocytes in response to local injury of the caudal fin of the *Tg(CD41:GFP)*
6. To characterize the nerve fibers response to local injury of the caudal fin of the *Tg(fli1:EGFP)*

3.3 Materials and Methods

3.3.1 Zebrafish husbandry

Wild type (WT) zebrafish and transgenic lines, including *Tg(fli1:EGFP)* (from Dr. Brant Weinstein laboratory, National Institutes of Health), *Tg(mpx:GFP)* and *Tg(CD41:GFP)* (from Dr. Tom Moon laboratory, University of Ottawa) and *Tg(2.4shha:GFP-ABC)* (from Dr. Uwe Strähle laboratory, Karlsruhe Institute of Technology), were raised and maintained in the zebrafish facility at the University of Ottawa. The fish were kept in the fishroom at 28.5 °C with 14 hours light and 10 hours dark period. Zebrafish were fed regularly (Westerfield, 2000), including twice adult zebrafish food and once brine shrimp per day. Adult zebrafish ranging from 3 to 18 months were used for experiments. Zebrafish were maintained and manipulated according to the principles and guidelines of the Animal Care Committee at the University of Ottawa and the Canadian Council on Animal Care (CCAC).

3.3.2 Fin injury

Zebrafish were anesthetized in the fishroom system water that contains 0.17 g/mL tricaine as previously described (Westerfield, 2000). One bone segment amputation was performed on the dorsal or ventral fin ray No. 3 or No. 5 of the caudal fin using a blade or the needle of an insulin syringe (28 gauge); six bone segments of the dorsal or ventral fin ray No. 3 or No. 5 of the caudal fin were amputated using the needle of an insulin syringe (28 gauge); Half-fin amputation was performed by amputating 7 or 8 fin rays of the dorsal lobe for fish that had 16-17 fin rays, or 18 fin rays, respectively, in the caudal fin. Among these 7 or 8 fin rays, amputation was conducted one to two segments proximal to the first branching point of the fin rays or at approximately half length of these fin rays using a scalpel blade (Figure 3.4). Fish were kept individually or in groups after injury in the fishroom at 28.5°C.

3.3.3 Microscopy and image processing

Zebrafish were anesthetized as described above and placed on a 1.5% agarose plate for imaging. Images were taken using a dissection microscope (Leica MZ FLIII) integrated with the FLUOIII filter system or a Zeiss Axioskop compound microscope equipped with a digital camera (Zeiss AxioCam HRm) and AxioVision AC software. Confocal microscopy was performed under either a confocal scanning system (Zeiss LSM META510, Thornwood, NY, USA) or a confocal laser scanning spectral microscope FV1000 with BX61 (Olympus) equipped with argon (Ar) and helium–neon (He–Ne) lasers with peak outputs of 488 nm and 543 nm, respectively. Pictures were processed with Image J and Photoshop for adjustments.

3.3.4 Alcian blue, alizarin red and calcein staining

Alcian blue stains acidic polysaccharides in cartilages, and mucopolysaccharides in tissues through electrostatic interactions (Scott, 1996). Alizarin red binds to free ionic calcium and stains calcified bone matrix (Puchtler, 1969). After the half-fin amputation, the caudal fins at various regenerating time points, such as 1 hpa and 8 hpa, were collected and fixed in 4% paraformaldehyde (PFA) overnight. Fins were washed three times for 5 mins each in phosphate buffered saline (PBS) before staining. 0.1% Alcian blue staining solution was freshly prepared by dissolving 0.01 g of alcian blue powder (Sigma, A5268) in 10 mL 70% ethanol in acetic acid (70% EtOH:30% AcOH). Fins were stained in alcian blue solution for 6 h at room temperature. Following staining, the fins were dehydrated in a series of 1 h washes through a gradient of ethanol in PBS (25% EtOH: 75% PBS, 50% EtOH: 50% PBS, 75% EtOH: 25% PBS) and fins were placed in fresh 100% EtOH overnight at 4°C. On the next day, fins were rehydrated in a series of 1 h washes in dilutions of ethanol and PBS (80% EtOH: 20% PBS, 50% EtOH: 50% PBS, 30% EtOH: 70% PBS). 0.1% Alizarin red staining solution was freshly prepared by dissolving 1.8 mg of alizarin red powder (Sigma, A5533) in

18 ml of freshly prepared 0.5% potassium hydroxide (KOH). Fins were stained in alizarin red solution for 5 h at room temperature. Following alizarin red staining, fins were rinsed twice in system water and placed on a 2% agarose gel plate for imaging (Yan Li, unpublished data).

Calcein staining allows tracking the dynamics of ionic calcium in zebrafish. The main difference between alizarin red and calcein is that alizarin red forms an insoluble precipitate with calcium and is fixed to one position, whereas calcein forms a soluble complex with calcium (Hale *et al.*, 2000). Calcein is a fluorescent chromophore that also binds to ionic calcium and stains the bone in green that can be observed under the fluorescence microscope (Du *et al.,* 2001). *In vivo* calcein staining in adult zebrafish were carried out according to the authors' instructions (Du *et al.,* 2001). The final concentration of 0.2% calcein staining solution with pH 7 was freshly prepared by dissolving 2 g of calcein powder (Sigma) in 1 L of system water. pH value was adjusted by addition of NaOH (0.5N) into the staining solution because calcein has strong acidifying effect. WT adult zebrafish were allowed to swim in the staining solution for 1 h. After staining, fish were rinsed several times in system water and fish were allowed to swim in fresh system water overnight to wash off the excess, unbound calcein on the tissues. After that, half-fin amputation was performed according to the above description. Finally, fish were placed on a 2% agarose gel plate for imaging under fluorescent microscope. Observations were carried out at various time points, including 0 dpa, 2 dpa, and 5 dpa. Images were taken under a dissection microscope (Leica MZ FLIII) with a green fluorescence filter set (Excitation 480/40mm, transmission 510) (Yan Li, unpublished data).

3.3.5 Immunohistochemistry

The distribution of neuronal axons in the caudal fin was determined using the zn-12 antibody, the neuronal cell surface marker (University of Oregon, USA) (Metcalfe *et al.*, 1990; Trevarrow *et al.*, 1990; Andreasen *et al.*, 2007). The zn-12 antibody staining was carried out based on the modifications of previous documents (Metcalfe *et al.*, 1990; Andreasen *et al.*, 2007). After half-fin amputation of the caudal fin of the *Tg(fli1:EGFP)* adult fish, the caudal fin regenerates were collected at various time points and fixed overnight in 4% PFA. They were then washed three times for 5 mins each in PBST (1x PBS, 0.1% Tween-20) and 1 h in double-distilled water. Fins were then permeabilized with acetone at − 20°C for 20 mins, followed by a quick rinse in double-distilled water for 5 mins. Next, fins were digested with collagenase (1 mg/ml) for 90 mins. Fins were then blocked in 10% normal calf serum in PBST and incubated with the primary antibody, mouse monoclonal anti-zn-12 antibody (1:100) (Zebrafish International Resource Center (ZIRC), USA) for 14 h at 4°C. Fins were washed three times for 10 mins per wash in PBST. Fins were incubated with a secondary antibody, Alexa Fluor® 594 Goat anti-mouse antibody (Invitrogen, A-11005) for 5 h at 22°C. Tissues were then washed three times for 10 mins each in PBST, mounted in the slides and imaged using confocal microscopy.

3.3.6 Various types of injuries tested on the adult zebrafish

Stab lesion in the adult zebrafish brain was conducted according to Kroehne *et al.*, (2011). Briefly, adult zebrafish were anaesthetized as described above. A canula (30 gauge, outer diameter 300 μm) was pushed through a nostril to approximately 6-8 mm deep along the rostrocaudal body axis, which injured the telencephalon in seven adult zebrafish brains. Intraperitoneal injection in the abdominal region of adult zebrafish was done in five fish, based on the modifications from Stewart *et al.*, (2011). Briefly, adult zebrafish were held by a sponge and injected with about 3 mL the system fish water using an insulin needle. Repeated

injections were performed for three times in three different spots in the abdominal region. Removal of scales was carefully performed under a microscope according to (the instruction from) Vrieze *et al.*, (2011). At least 3 scales were removed from different part of the five zebrafish. The dorsal fin and paired pelvic fins were amputated based on the instructions for the caudal fin amputation, which were performed using a scalpel blade (Zhang *et al.*, 2012). Fins were amputated at ~50% of their original length. However, paired pectoral fins amputation was performed according to (the instruction from) Nachtrab *et al.*, (2011). An iridectomy scissor was used to cut off ~50% of the original length of the pectoral fins. 14 fish were tested for the amputation of pelvic and pectoral fins; 6 fish were tested for the amputation of the dorsal fin. Incision wounding was performed according to (the instruction from) Lévesque *et al.*, (2011). A puncture was made through the skin and muscle using an insulin needle and this was repeated for three different spots on nine adult zebrafish, in order to induce a larger wound response.

3.3.7 Antibiotic treatment

Erythromycin stock solution at the concentration of 1 mg/L was prepared by dissolving 10 mg erythromycin powder (Sigma, E5389) in 100 mL double-distilled water, which was stored in the dark at 4°C as the stock solution. Before treatment with erythromycin, two erythromycin solutions at the final concentrations of 0.25 and 0.5 mg/L were freshly prepared from the stock solution through dilution in system water. Two groups of the *Tg(fli1:EGFP)* adult zebrafish were pretreated in two different concentrated erythromycin solutions for six days, with daily changes of fresh solutions. After the six-day pre-treatment with the erythromycin solutions, the *Tg(fli1:EGFP)* adult zebrafish were "half-fin" amputated, maintained in the erythromycin solutions, and examined for GFP disappearance at: 2 hpa and

48 hpa. During the course of the experiment (including six-day pre-treatment), fish were maintained in the fishroom facility at 28.5°C (Yan Li, unpublished data).

3.4 Results

3.4.1 Small local injury induces gene shut down in the caudal fin

3.4.1.1 Interesting findings after a small injury of one fin ray of the *Tg(2.4shha:GFP-ABC)* adult zebrafish

In February 2012, I performed a small injury (less than one bone segment) of one fin ray through the GFP expression domain corresponding to the domain of expression of *shha* in the caudal fin of a fish of the transgenic line (*Tg) (2.4shha:GFP-ABC)* (Figure 3.3 A, B). To my surprise, in the following hours, I observed the disappearance of the rest of GFP expression in the fin ray that had been cut, and also the disappearance of GFP expression in the neighbouring fin rays as well as in the corresponding fin ray on the other lobe of the caudal fin (Figure 3.3). Later, the loss of GFP expression seemed to progress from the lateral fin rays towards the fin rays in the middle of the caudal fin (Figure 3.3 C, D). Fin rays with GFP disappearance were not injured, indicating that this disappearance was due to some internal mechanisms of the organism rather than to an external damage. This phenomenon has not been described in previous reports on fin regeneration and the mechanisms for it were unknown. To rule out the possibility that the manipulation of fish might be responsible for the loss of GFP expression by damaging the tissues at the distal tip of the caudal fin, I repeated the local injury on ventral or dorsal fin ray No. 3 by amputation of less than one segment with extra caution, and I used control fish in which no injury was induced at all. Control fish were manipulated the same way as the experimental fish: control fish were anesthetized at the same time as the experimental group of fish and for the same amount of time. Control fish were returned to the fish tank with the experimental group of fish, but I did not induce any external injury to fins in the control group of fish. One hour later, 10/12 *Tg(2.4shha:GFP-ABC)* fish that were locally injured showed a loss of GFP in the non-amputated fin rays,

similar to what was shown in Figure 3.3, whereas 6/6 control fish showed intact GFP expression in all the fin rays. This result suggested that the loss of GFP expression in the non-amputated fin rays was not due to the manipulation of the fish.

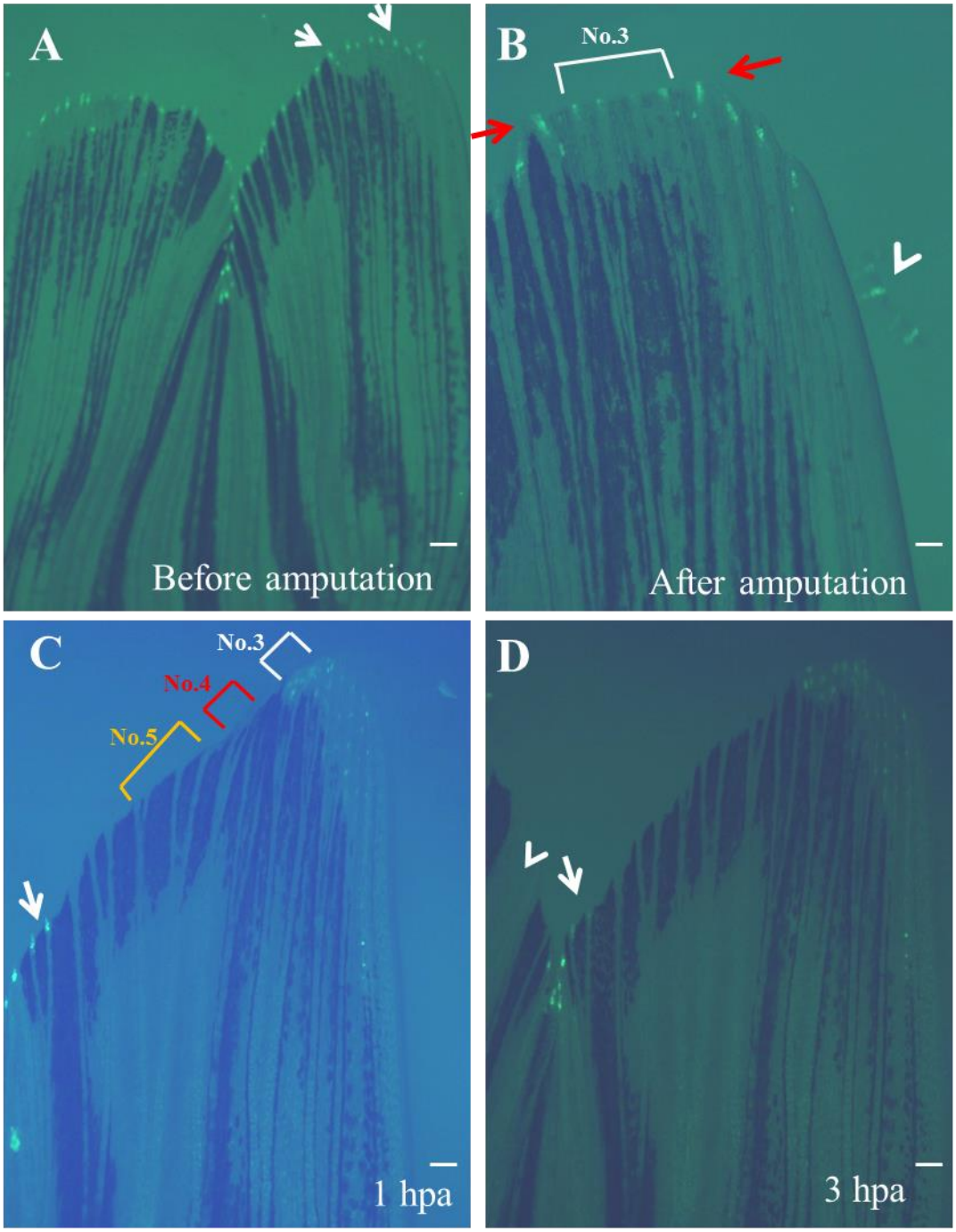
A
Before amputation
B
No.3
After amputation
C
No.3
No.4
No.5
1 hpa
D
3 hpa

Figure 3.3 Loss of GFP expression in the non-amputated fin rays after the local injury of less than one bone segment on one fin ray of the caudal fin of the *Tg(2.4shha:GFP-ABC)*.

A) Before amputation, *shha*-expressing cells are shown by GFP expression in the distal ends of each fin ray. White arrows indicate GFP expression. B) Amputation of less than one bone segment was performed on the ventral fin ray No. 3. Red arrows indicate the amputation plane; the white arrowhead indicates the piece of amputated tissue; the bracket indicates the amputated ventral fin ray No. 3. C) Loss of GFP expression is observed in some non-amputated fin rays of the ventral lobe of the caudal fin at 1 hour post amputation (hpa). Close to the injured fin ray No. 3, neighbouring fin rays No. 4 and No. 5 are shown by the red and the yellow brackets, respectively. The white arrow indicates GFP expression in the fin ray No. 7 of the ventral lobe. D) Loss of GFP expression is seen in the neighbouring fin rays of the ventral lobe and fin rays of the dorsal lobe at 3 hpa. The white arrowhead indicates the loss of GFP expression in one fin ray of the dorsal lobe. The white arrow indicates the same ray as in C, but GFP expression is disappearing in D. It seems that GFP disappearance progresses from the lateral rays towards rays in the middle part of the caudal fin. The scale bar in (A): 400 μm. The scale bar in (B): 200 μm. Scale bars in (C, D): 266 μm.

3.4.1.2 Test of other types of injury in the caudal fin of the *Tg(2.4shha:GFP-ABC)* adult zebrafish

After the initial observation described above, I tested the effect of other types of fin injury on GFP expression in the *Tg(2.4shha:GFP-ABC).* Instead of only cutting the tip of the fin ray, I removed six bone segments of a long fin ray (No. 3) or of a short fin ray (No. 5) of the dorsal or ventral lobe of the caudal fin. As in the previous experiment, one hour after injury, I observed the loss of GFP expression in the non-amputated fin rays (neighbouring fin rays and fin rays in the opposite lobe), following injury of the dorsal or ventral long fin ray (No. 3) in 6/6 and 5/5 fish, respectively. Similarly, following injury of the dorsal or ventral long fin ray (No. 5) I observed a loss of GFP expression in the non-amputated fin rays (neighbouring fin rays and fin rays in the opposite lobe) one hour after injury in 4/6 and 4/5 fish, respectively.

Another type of injury, named half-fin amputation, was developed by Shahram Eisa-beygi (PhD student in Dr. Tom Moon lab, University of Ottawa) and Ali Al-Rewashdy (MSc student in Dr. Marie-Andrée Akimenko lab, University of Ottawa). This type of injury consisted in amputating the dorsal lobe of the caudal fin one or two segments proximal to the first branching points of the fin rays or at approximately half length of the fin rays (Figure 3.4). Next, I observed that in 7/9 *Tg(2.4shha:GFP-ABC)* fish, GFP expression disappeared in all fin rays of the ventral (intact) lobe by 8 hpa. I then performed a time course analysis of the reappearance of GFP expression on fin rays of both the injured and the intact lobe. GFP expression in the amputated fin rays re-appeared by 48 hpa, which corresponded to the timing of the normal regeneration process as previously described by Zhang *et al.*, (2012). However, to our surprise, GFP expression in the non-amputated fin rays re-appeared later, between 168-192 hpa, and the expression levels seemed to be higher than the level of GFP expression observed in an intact fin (Figure 3.5). This result suggested that the regeneration program that

regulates *shha* expression in the non-amputated fin rays was activated after the loss of GFP expression, but with a delay compared to the amputated fin rays. The delayed reactivation of GFP expression was observed in 7/9 fish.

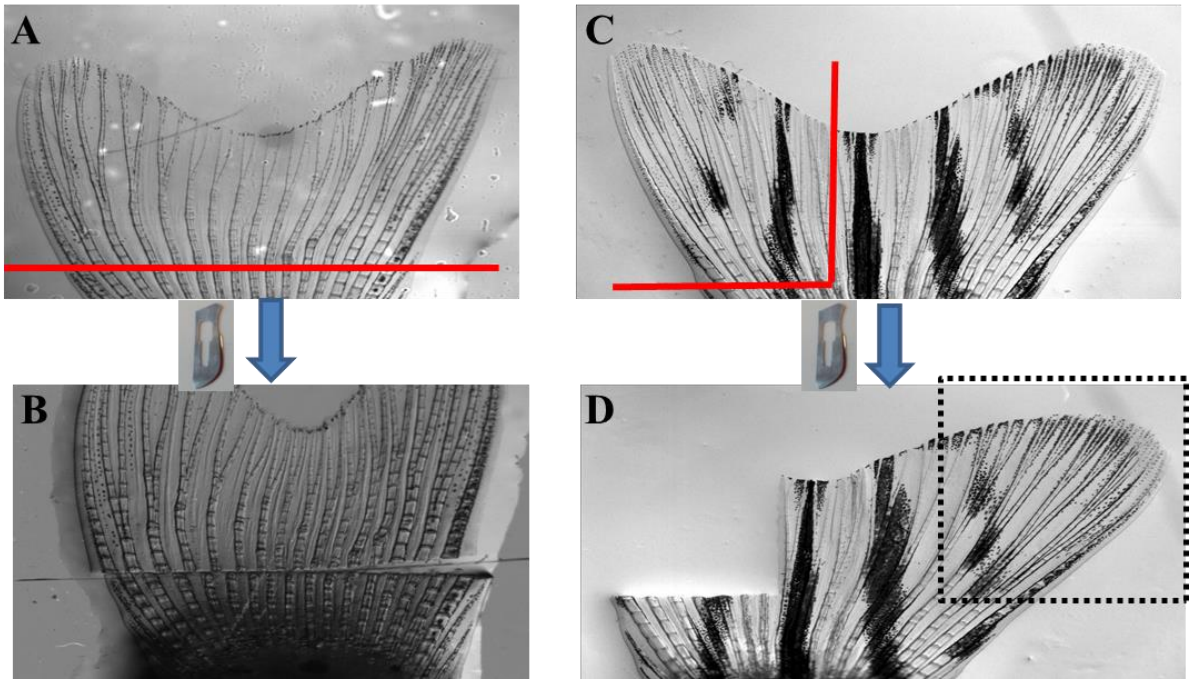
A
B
C
D

Figure 3.4 Fin amputations on the zebrafish caudal fin.

A) Amputation across the entire fin is performed one to two segments proximal to the first bifurcation points of the fin rays. The amputation plane is indicated by the red line. B) The caudal fin after amputation of all fin rays. C) Half-fin amputation of the dorsal lobe of the caudal fin one or two segments proximal to the first branching points of the fin rays or at approximately half length of these fin rays. The amputation plane is indicated by the red lines. D) The caudal fin after amputation as described in (C). The black dotted box shows the area of interest, where no injury is induced and therefore regarded as the intact (non-amputated) lobe.

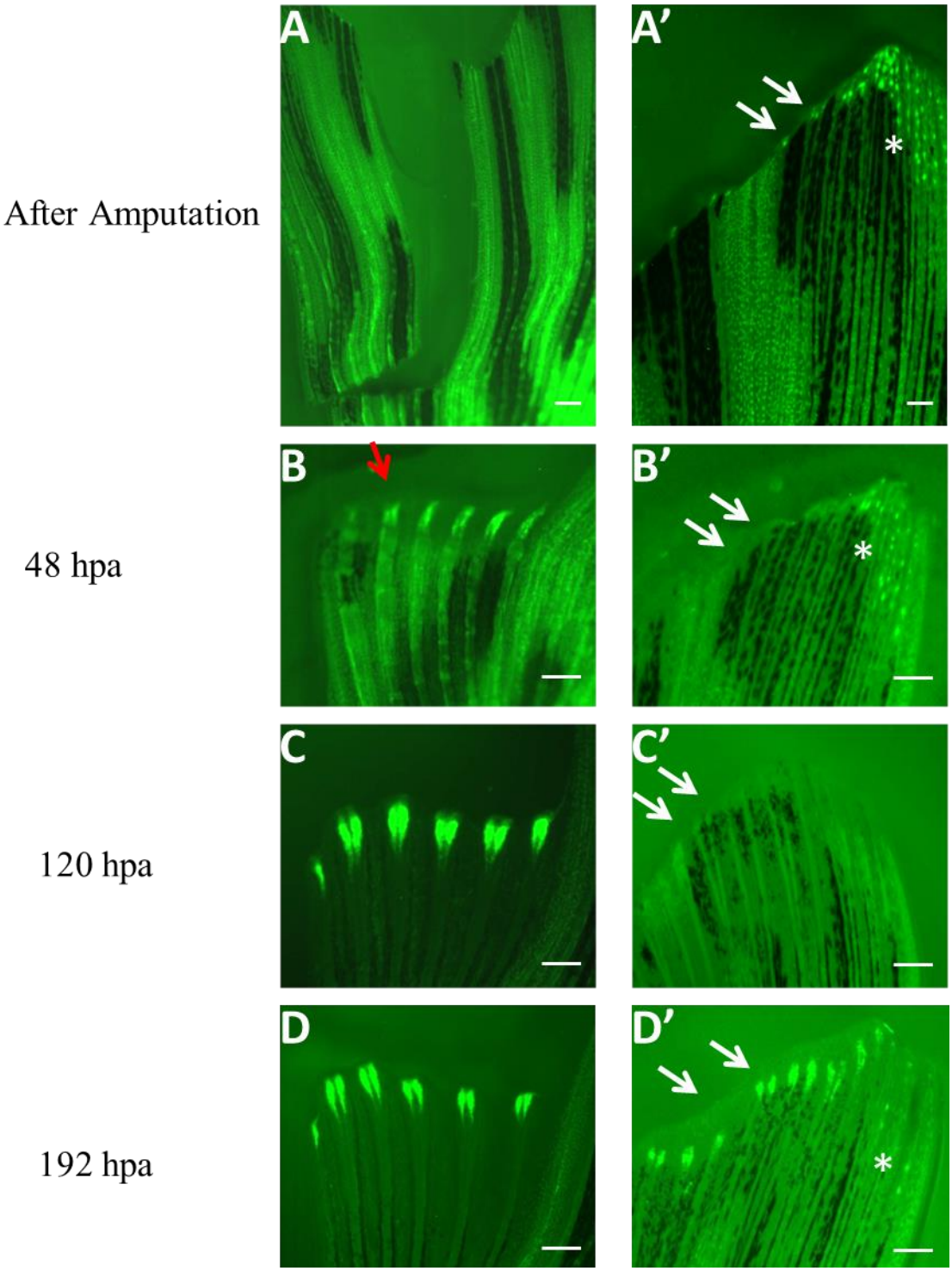
After Amputation
48 hpa
120 hpa
192 hpa
A
A'
B
B'
C
C'
D
D'

Figure 3.5 Time course analysis of GFP expression following half-fin amputation of the caudal fin of the *Tg(2.4shha:GFP-ABC)*.

A-D) GFP expression in the amputated lobe. A'-D') GFP expression in the non-amputated lobe. A) Dorsal fin rays No. 1-6 were amputated about half-fin length. B) GFP expression reappears at 48 hpa. The red arrowhead shows *shha* expression domain in the regenerating fin rays. C and D) The *shha* expression domain separates into two domains in each fin ray by 120 hpa. A') GFP expression in the non-amputated fin rays of the ventral lobe at 0 hpa. White arrows indicate *shha* expression; the asterisk indicates the auto fluorescence of pigment cells (white cells). B') GFP expression is diminished by 48 hpa, indicated by white arrows. C') At 120 hpa, no GFP expression can be observed. D') By 192 hpa, GFP expression is reactivated in the non-amputated fin rays. GFP expression levels are higher than the expression levels at 0 hpa. White arrows indicate the same fin rays during the time course (0 hpa to 192 hpa). The asterisk indicates the auto fluorescence of pigment cells (white cells). Scale bars: 200 μm.

3.4.1.3 Response to local injury of one fin ray of regenerating caudal fins of *Tg(2.4shha:GFP-ABC)* adult zebrafish

Next, I investigated the response to local injury on regenerating caudal fins, instead of analyzing this response on the intact caudal fins as described above. I first performed the amputation of all the fin rays of the caudal fin of eight *Tg(2.4shha:GFP-ABC)* fish. Fin amputation was done 1–2 segments proximal to the first branching point of the fin rays (Figure 3.4).

At 6.5 dpa, a secondary local injury was performed by amputation of one bone segment on the dorsal fin ray No. 3, including the two branches of this ray (Figure 3.6 A, B). After the one-segment amputation, the remaining GFP expression disappeared in 3/4 fish in 9 h (Figure 3.6 B', C'). Interestingly, GFP expression in the dorsal fin ray No. 2 adjacent to the injured ray, and the ventral fin rays (No. 2 and No. 3) that were not injured, showed various degrees of GFP loss (Figure 3.6 C', C''). GFP expression re-appeared in the amputated dorsal fin ray No. 3 and the non-amputated ventral fin rays No. 2 and No. 3 in 41 hours (Figure 3.6 D', D''). Similar results were observed when the secondary injury was performed in the fin ray No. 3 of the ventral lobe (instead of the dorsal lobe) of 4/4 regenerating fins (Figure 3.7).

Although we often observed in the experiments described above that injury of a given fin ray induced the loss or decrease of GFP expression in the corresponding fin ray on the opposite lobe, we still do not know whether there is a strict correlation between the locations of the injured fin ray and the intact ray that will respond to this injury. This global loss of GFP expression after a local injury on the intact caudal fin or the regenerating caudal fin, followed by the regeneration suggests the existence of mechanisms involved in the down-regulation of the *shha* expression, and mechanisms responsible for the activation of the regeneration

program that up-regulate *shha* expression. These unknown mechanisms are activated by internal cues rather than an external injury. To sum up, I have shown for the first time that there is an organ-wide response to local injury in the zebrafish caudal fin.

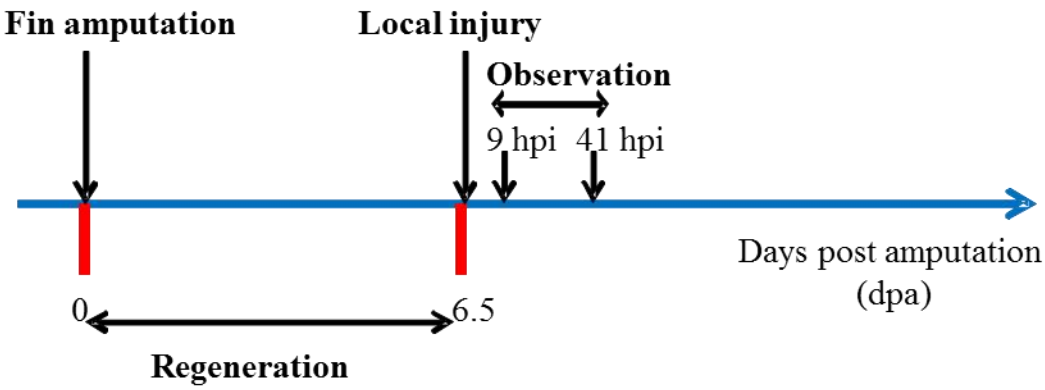
Fin amputation
Local injury
Observation
9 hpi
41 hpi
Days post amputation
(dpa)
0
6.5
Regeneration

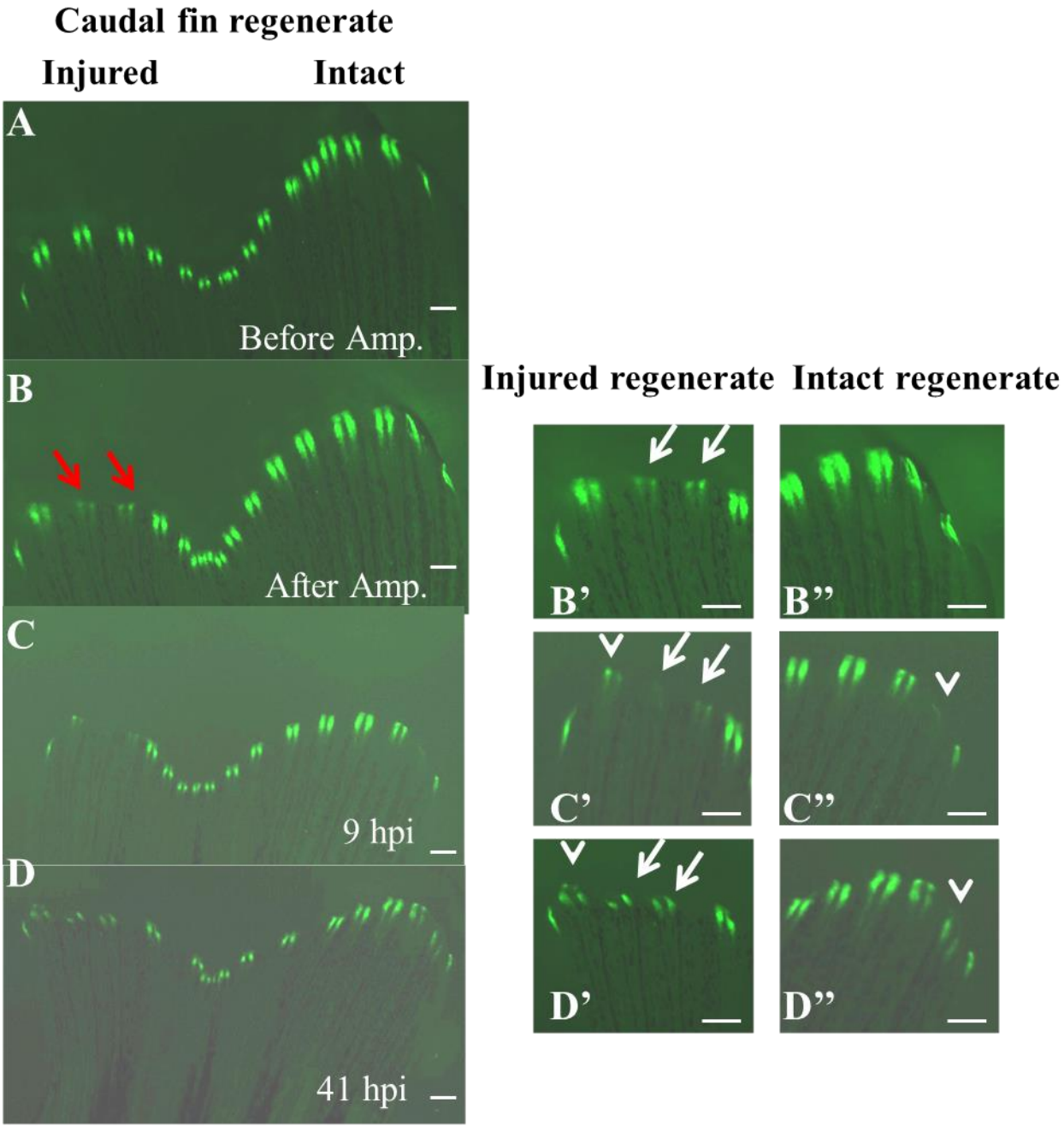
Caudal fin regenerate
Injured
Intact
A
Before Amp.
B
After Amp.
C
9 hpi
D
41 hpi
Injured regenerate
Intact regenerate
B'
B''
C'
C''
D'
D''

Figure 3.6 Time course analysis of GFP expression after a secondary local injury of dorsal fin ray of a regenerating caudal fin of the *Tg(2.4shha:GFP-ABC)* at 6.5 dpa.

GFP expression is observed before local injury (A), immediately after local injury (B, B' and B''), at 9 hours post injury (hpi) (C, C' and C''), and at 41 hpi (D, D' and D''). Observations are made on the entire fin (A-D). Higher magnification of the long fin rays in the injured regenerate and in the intact regenerate are shown in (B'-D') and (B''-D''), respectively. A) GFP expression on the regenerating caudal fin at 6.5 dpa, before the secondary local injury. B, B', and B'') Dorsal fin ray No. 3, which includes ray branches, was amputated of less than one bone segment within the GFP expression domain, leaving some GFP expression in the fin ray. Red arrows in B and white arrows in B' indicate the amputated dorsal fin ray No. 3 and the remaining GFP expression of that ray. No loss of GFP expression is observed in the corresponding rays of the opposite lobe to the injury (B''). C, C', and C'') Loss of GFP expression is seen in the neighbouring fin rays of the dorsal fin ray No. 3 and fin rays No. 2 and No. 3 of the ventral lobe in 9 hpi. The white arrowhead in C' indicates the decreased GFP expression of the dorsal fin ray No. 2, and white arrows show the amputated dorsal fin ray No. 3 have lost the remaining GFP expression. The white arrowhead in C'' indicates the loss of GFP expression in the ventral fin rays No. 2 and No. 3. D, D', and D'') Loss of GFP expression is followed by the GFP re-expression at 41 hpi. The white arrowhead in D' shows the GFP re-expression in the dorsal fin ray No. 2 where GFP expression was previously decreased, and white arrows indicate the GFP re-expression in the amputated dorsal fin ray No. 3. The white arrowhead in D'' indicates the GFP re-expression in the ventral fin rays No. 2 and No. 3. Scale bars: 200 μm.

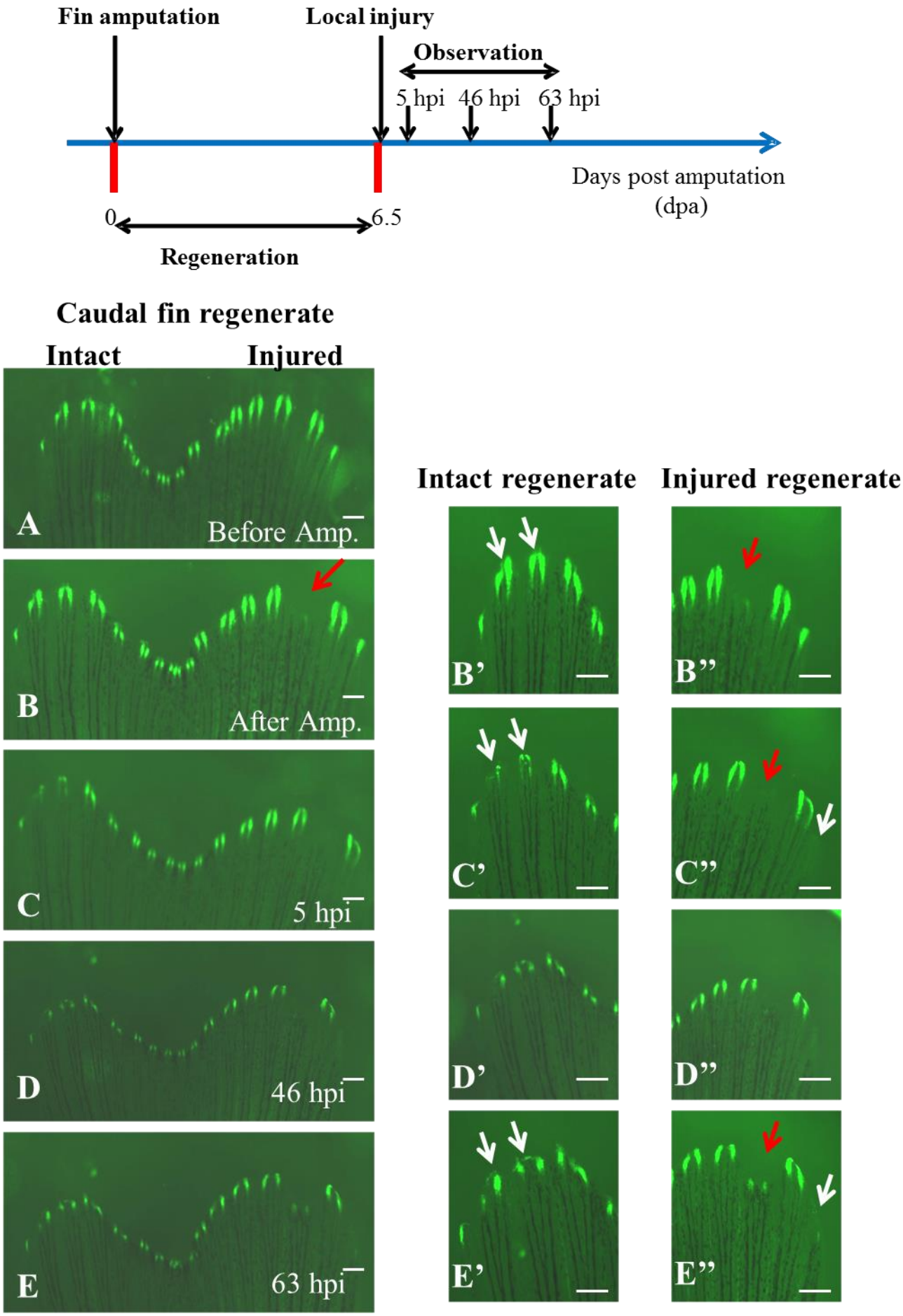
Fin amputation
Local injury
Observation
5 hpi
46 hpi
63 hpi
Days post amputation
(dpa)
0
6.5
Regeneration
Caudal fin regenerate
Intact
Injured
A
Before Amp.
B
After Amp.
C
5 hpi
D
46 hpi
E
63 hpi
Intact regenerate
Injured regenerate
B'
B''
C'
C''
D'
D''
E'
E''

Figure 3.7 Time course analysis of GFP expression after a secondary local injury of ventral fin ray of a regenerating caudal fin of the *Tg(2.4shha:GFP-ABC)* at 6.5 dpa.

GFP expression is observed before local injury (A), immediately after local injury (B, B' and B''), at 5 hpi (C, C' and C''), at 46 hpi (D, D' and D''), and at 63 hpi (E, E' and E''). Observations are made on the entire fin (A-E). Higher magnification of the long fin rays in the injured regenerate and in the intact regenerate are shown in (B''-E'') and (B'-E'), respectively. A) GFP expression on the regenerating caudal fin at 6.5 dpa, before the secondary local injury. B, B', and B'') Ventral fin ray No. 3, which includes ray branches, was amputated of less than one bone segment within the GFP expression domain, leaving some GFP expression in the fin ray. The red arrow in B and B'' indicate the amputated ventral fin ray No. 3 and the remaining GFP expression of one of the branched ray. No loss of GFP expression is observed in the corresponding rays of the opposite lobe to the injury (B'). C, C', and C'') Loss of GFP expression is seen in the neighbouring fin rays of the ventral fin ray No. 3 and fin rays No. 2 and No. 3 of the dorsal lobe in 9 hpi. White arrows in C' indicate the decreased GFP expression of the dorsal fin ray No. 2 and No. 3. The red arrow in C'' indicate the amputated ventral fin ray No. 3 have lost the remaining GFP expression and the white arrow in C'' indicates the loss of GFP expression in the ventral fin rays No. 1. D, D', and D'') GFP expression is not changed between 5-46 hpi. E, E', and E'') Loss of GFP expression is followed by the GFP re-expression at 63 hpi. White arrows in E' show the GFP re-expression in the dorsal fin ray No. 2 and No. 3 where GFP expression was previously decreased. The red arrow in E'' indicate the GFP re-expression in the amputated ventral fin ray No. 3 and the white arrow in E'' indicates the beginning of GFP re-expression in the ventral fin rays No. 1. Scale bars: 200 μm.

3.4.2 Observations of defects following standardized half-fin amputation

After these initial observations, the next experiments were performed in collaboration with Shahram Eisa-beygi (PhD student in Dr. Tom Moon laboratory, University of Ottawa), Ali Al-Rewashdy (MSc student in Dr. Marie-Andrée Akimenko laboratory, University of Ottawa), and Yan Li (Honours student in Dr. Marie-Andrée Akimenko laboratory, University of Ottawa). In the following experiments, I performed the morphological analysis, the analysis of the dynamics of GFP expression of blood vessels and nerve fibers after the half-fin amputation on fin rays of both the injured and the intact lobe, and the analysis of injury response in adult zebrafish. Shahram, Ali and I performed the analysis of the neutrophils response after the half-fin amputation. Shahram and Ali performed the analysis of the thrombocytes response. Yan performed the analysis of erythromycin treatment.

Since we noticed from the previous experiments that the most severe injury, the half-fin amputation of one lobe, was giving the strongest response in the intact lobe, we standardized the "local injury" protocol by doing half-fin amputation in the rest of the experiments (Figure 3.4). Furthermore, we focused the analysis of the response on fin rays No. 2 and No. 3 in the intact lobe that always gave the strongest response.

3.4.2.1 Loss of GFP expression in the blood vessels after local injury

After half-fin amputation, the damage observed in fin rays of the intact lobe was suggesting that various types of tissue, such as blood vessels, might be affected. Since our laboratory had the *Tg(fli1:EGFP)* fish, in which GFP is expressed in the endothelial cells of the blood vessels (see Figure 1.5), I examined the dynamics of GFP expression in the blood vessels after local injury on fin rays of both the injured and the intact lobe of the *Tg(fli1:EGFP)*.

3.4.2.2 Loss of GFP expression in the amputated fin rays after half-fin amputation of the *Tg(fli1:EGFP)* and reappearance of GFP expression

After half-fin amputation on the dorsal lobe of the caudal fin, a loss of GFP expression in the fin ray tissue just beneath (proximal) the amputation level was immediately observed at 10 minutes post amputation (mpa) of the *Tg(fli1:EGFP)* (341/341 fish) (Figure 3.8 A, A'). Such rapid loss of GFP expression immediately after a traumatic injury in the zebrafish caudal fin has not been documented previously. Between 1-24 hpa, GFP expression re-appeared in the region where GFP had previously disappeared, suggesting that injured blood vessels were healed and started to regenerate new vessels (Figure 3.8 B-D, B'-D'). By 48 hpa, plexuses were formed at the wound site (Figure 3.8 E, E'). New arteries and veins were formed from remodelling of the plexuses at 72 hpa (Figure 3.8 F, F'). As the regeneration continued, more plexuses were formed (Figure 3.9 G, G') and the newly formed arteries and veins showed the dense intervessel commissures by 120 hpa (Figure 3.8 H, H'), corresponding to normal blood vessels regeneration processes (angiogenesis) described after a traumatic amputation in the zebrafish caudal fin.

amputated rays
amputated rays
10 mpa
1 hpa
8 hpa
24 hpa
48 hpa
72hpa
96hpa
120hpa
A
B
C
D
E
F
G
H
A'
B'
C'
D'
E'
F'
G'
H'

Figure 3.8 Time course analysis of blood vessels regeneration processes in the amputated fin rays after half-fin amputation of the caudal fin of the *Tg(fli1:EGFP)*.

GFP expression is observed at 10 mpa (A, A'), at 1 hpa (B, B'), at 8 hpa (C, C'), at 24 hpa (D, D'), at 48 hpa (E, E'), at 72 hpa (F, F'), at 96 hpa (G, G') and at 120 hpa (H, H'). Observations are made on the amputated lobe of the same fin (A-H). Higher magnifications of one amputated fin ray are shown in (A'-H'). White arrows in (A'-H') indicate the blood vessels of the same fin ray. A, A') Amputation induces blood vessels injury at 10 mpa. Loss of GFP expression is seen at the distal tip of the amputated fin rays, indicated by the white arrow. B, B') Blood vessels regeneration is activated and injured vessels start to heal the ends at 1 hpa. The white arrow indicates the expression of GFP is reactivated. C, C', D, D') Injured vessels heals their ends in 24 hpa. The white arrow indicates the GFP re-expression at the tip of the fin ray. E, E') The connecting bridge between the artery and the vein is formed, indicated by the white arrow. F-H, F'-H') Plexuses are formed and remodelled to form the arteries and veins, and the newly formed arteries and veins show the dense intervessel commissures. The plexuses are indicated by the white arrowhead. Scale bars in (A-H): 200 μm. Scale bars in (A'-H'): 20 μm.

3.4.2.3 Loss of GFP expression in the non-amputated fin rays after local injury of the *Tg(fli1:EGFP)* and reappearance of GFP expression

Since the response to local injury of GFP expression had not been tested in the non-amputated fin rays of the *Tg(fli1:EGFP)*, I first used the previously described local injury methods and tested the response of GFP expression of the *Tg(fli1:EGFP)*. The injury methods included amputation of one bone segment in the dorsal or ventral fin ray (No. 3 or No. 5), amputation of six bone segments in the dorsal or ventral fin ray (No. 3 or No. 5), the half-fin amputation on the dorsal lobe of the caudal fin. I also analyzed the effects of removing one bone segment in one fin ray from the middle part of the caudal fin.

3.4.2.4 The response of GFP expression on the intact lobe following one ray injury

Similar results were observed when various local injury methods were tested on the *Tg(fli1:EGFP)*. By 8 hpa, a loss of GFP expression was observed in fin rays on the intact lobe of the caudal fin after amputation of one or six bone segments of the dorsal fin ray No. 3 or No. 5 (Table 4). Similarly, by 8 hpa, a loss of GFP expression was observed in fin rays on the intact lobe of the caudal fin after amputation of one or six bone segments of the ventral fin ray No. 3 or No. 5 (Table 4). Surprisingly, after removal of one bone segment in one fin ray of the middle part of the caudal fin, by 24 hpa, 3/3 fish showed a loss of GFP expression in the distal end of all fin rays of the caudal fin (Figure 3.9). Furthermore, in all cases when the loss of GFP expression was observed, GFP disappearance progressed from the most distal tips to a more proximal region of the caudal fin, suggesting that the distal ends of each fin ray were more sensitive or responsive to the local injury of the fin.

3.4.2.5 The response of GFP expression on the intact lobe following half-fin amputation

I performed a time course analysis of GFP expression of the *Tg(fli1:EGFP)* to observe the dynamics of GFP expression after half-fin amputation (Figure 3.10). 131/341 fish showed the loss of GFP expression in the non-amputated fin rays on the ventral lobe following half-fin amputation on the dorsal lobe (Figure 3.10, Table 5). I observed the loss of GFP expression at the distal tips of the ventral fin rays in the intact lobe as early as 10 mpa (Figure 3.10 B, B', and B''). The disappearance of GFP was first visualized by the loss of the bridge between the artery and the veins at 10 mpa, indicating that blood vessels at the distal ends were not functional (Figure 3.10 B''). Video time lapse analysis showed that the blood flow stopped in the tips of the non-amputated fin rays, further suggesting the dysfunction of the blood vessels in the distal region where GFP expression was lost (data not shown). Between 1-8 hpa, the loss of GFP expression seemed to progress from the distal ends to the more proximal region in the non-amputated fin rays, and this process of GFP disappearance reached a maximum by 8 hpa (Figure 3.6 C, D, C', D', C'', D'', C''' and D'''). Between 8-24 hpa, tissue damage was observed at the very distal tips of the non-amputated fin rays following the loss of GFP expression, but no further GFP loss was observed (Figure 3.10 E, E', and E''). The white pigment cells that are autofluorescent (see Figure 3.9), were noticeably lost by 24 hpa at the distal tips of the non-amputated fin rays following the loss of GFP expression (Figure 3.10 E''). Between 24-48 hpa, the ends of the injured blood vessels seemed to be healed, suggesting the initiation of blood vessels regeneration (Figure 3.11 A, A' and A''). Between 48-120 hpa, GFP reappearance was observed in the non-amputated fin rays. The anastomotic bridge reconnecting the artery and the vein was formed by 72 hpa (Figure 3.11 B, B', and B''). The blood flow resumed in all the anastomotic bridges (data not shown). In addition, sprouts at the newly formed bridge developed and extended distally by 120 hpa, suggesting an active blood vessel regeneration (Figure 3.11 C, C', D, D', D''). These results indicate that

following the loss of GFP expression and tissue damage in the non-amputated fin rays, there is an active regeneration process of the blood vessels as shown by GFP expression.

Table 4. Summary of the response of blood vessels in the non-amputated fin rays after various methods to induce a local injury on the caudal fin of the *Tg(fli1:EGFP)*

Injury types by amputation (of)	No. of fish show loss of GFP expression	No. of fish show no loss of GFP expression
One segment in the dorsal fin ray No.3	3	3
One segment in the dorsal fin ray No.5	2	3
One segment in the ventral fin ray No.3	3	2
One segment in the ventral fin ray No.5	4	2
Six segments in the dorsal fin ray No.3	5	3
Six segments in the dorsal fin ray No.5	5	3
Six segments in the ventral fin ray No.3	6	3
Six segments in the ventral fin ray No.5	3	6

Table 5. Summary of the response in the non-amputated fin rays of the ventral lobe after half-fin amputation of the dorsal lobe of the caudal fin

Fish type	Mild damage	Severe damage
Wild type	77	61
Tg(2.4shha:GFP-ABC)	7	36
Tg(fli1:EGFP)	210	131
Tg(mpx:GFP)	10	18
Tg(CD41:GFP)	6	14

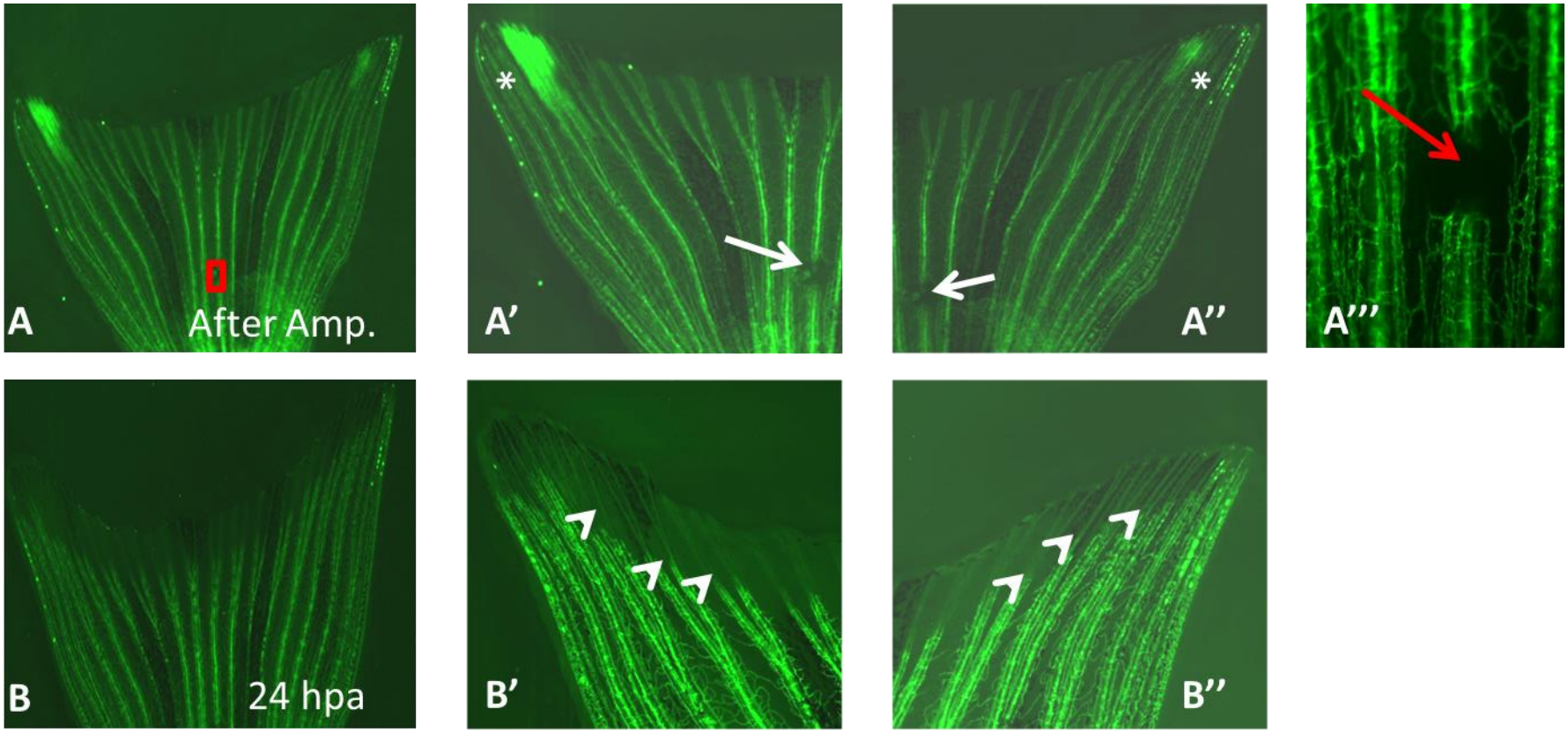
A
After Amp.
A'
A''
A'''
B
24 hpa
B'
B''

Figure 3.9 Loss of GFP expression at the distal tips of all fin rays after removal of one segment in the middle part of the caudal fin of the *Tg(fli1:EGFP)*.

GFP expression is observed immediately after local amputation (A, A', A'', and A'''), and at 24 hpa (B, B', and B''). Observations are made on the entire fin (A, B). Higher magnification of the dorsal lobe and the ventral lobe are shown in (A', B') and (A'', B''), respectively. A, A', A'') At 0 hpa, GFP expression remains intact at the distal tips of fin rays after removal of one segment in the middle part of the caudal fin. White arrows in (A', A'') indicate the amputated tissues. The red box in (A) indicates the removal of the one bone segment. A close-view image of the red box is shown in A''', and the red arrow indicates the amputated (removed) tissues, including the bone segment. B, B', B'') At 24 hpa, loss of GFP expression is seen in all fin rays. White arrowheads indicate the loss of GFP expression in fin rays of the dorsal lobe and the ventral lobe. The asterisk indicates the auto fluorescence of pigment cells (white cells).

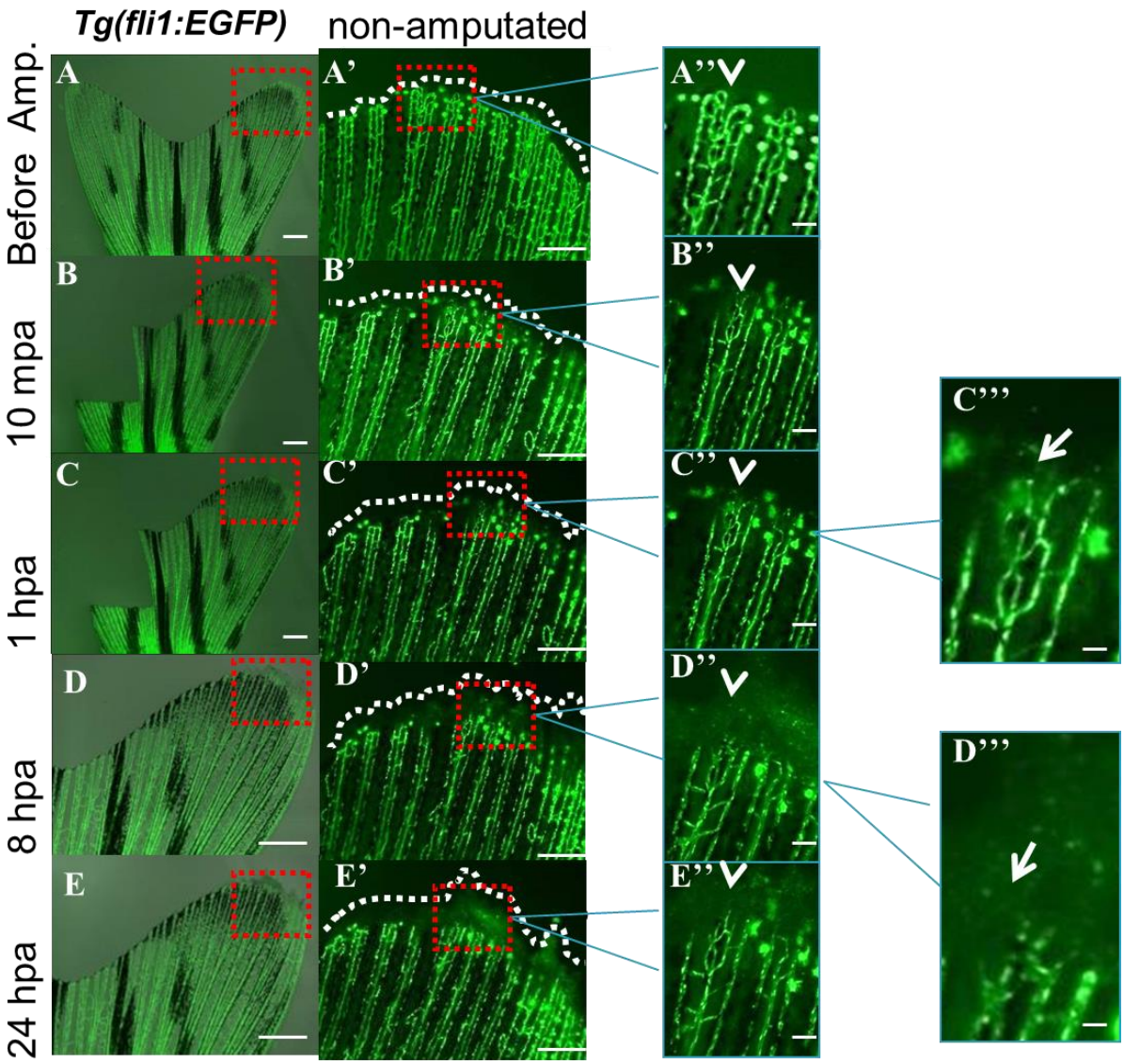
Tg(fli1:EGFP)
non-amputated
Before Amp.
10 mpa
1 hpa
8 hpa
24 hpa
A
A'
A''
B
B'
B''
C
C'
C''
C'''
D
D'
D''
D'''
E
E'
E''

Figure 3.10 Time course analysis of the loss of GFP expression at the distal tips of the non-amputated fin rays after half-fin amputation of the caudal fin of the *Tg(fli1:EGFP)*. GFP expression is observed before amputation (A, A', and A''), at 10 mpa (B, B', and B''), at 1 hpa (C, C', C'', and C'''), at 8 hpa (D, D', D'', and D'''), and at 24 hpa (E, E', and E''). Observations are made on the non-amputated lobe of the same fin (A'-E'). Higher magnification of the long fin rays (red boxes in A-E) and ventral fin ray No. 3 (red boxes in A'-E') are shown in (A'-E'), (A''-E''), respectively. C''' and D''' show a single ray of the branched ventral fin ray No. 3, respectively. White arrowheads in (A''-E'') and (C''', D''') indicate the blood vessels of one single ray of the branched ventral fin ray No. 3. White dotted lines indicate the distal epidermis. A, A', and A'') Before amputation, blood vessels are intact in fin rays of the caudal fin. B, B', and B'') At 10 mpa, the loss of GFP expression is observed at distal tips of fin rays of the non-amputated lobe. C, C', C'', and C''') At 1 hpa, the loss of GFP expression continues in the non-amputated fin rays. The white arrow in C''' indicates the disappearing GFP expression of a blood vessel and of a white pigment cell. D, D', D'', and D''') At 8 hpa, GFP disappearance is followed by tissue damage at the tip of the non-amputated fin rays. The white arrow in D''' indicates the disappeared GFP expression of a blood vessel and of a white pigment cell. E, E', and E'') At 24 hpa, more epidermal tissue damage is observed. Scale bars in (A-C): 1 mm. Scale bars in (D-E): 500 μm. Scale bars in (A'-E'): 200 μm. Scale bars in (A''-E''): 50 μm. Scale bars in (C'''-D'''): 16 μm.

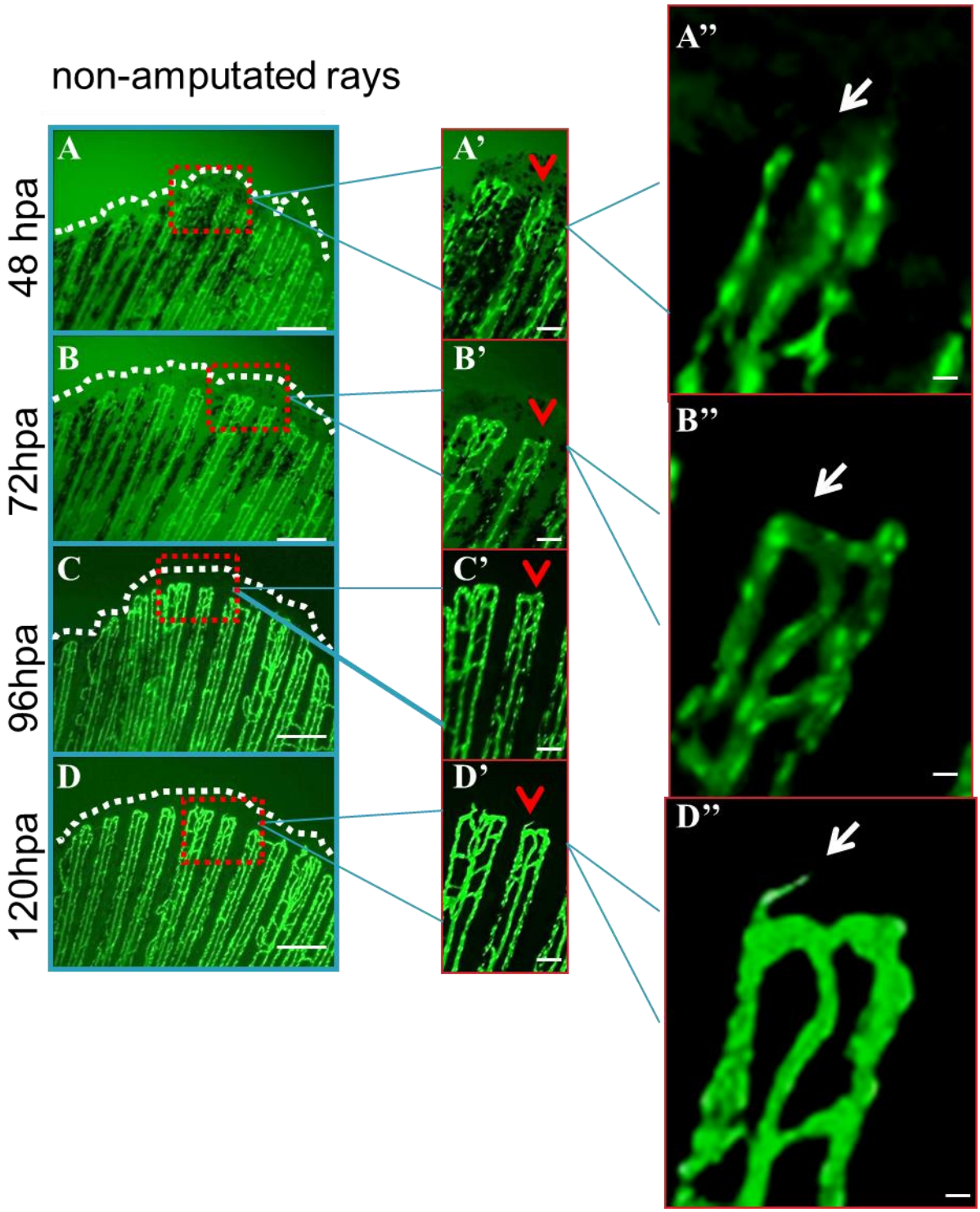
non-amputated rays
48 hpa
72hpa
96hpa
120hpa
A
B
C
D
A'
B'
C'
D'
A"
B"
D"

Figure 3.11 Time course analysis of the GFP re-expression at the distal tips of the non-amputated fin rays after GFP disappearance in the *Tg(fli1:EGFP)*.

Half-fin amputation was performed on the dorsal lobe of the caudal fin. GFP expression is observed at 48 hpa (A, A', and A''), at 72 hpa (B, B', and B''), at 96 hpa (C, C', and C''), and at 120 hpa (D, D', and D''). Observations are made on the non-amputated lobe of the same fin (A-D). Higher magnification images of the ventral fin ray No. 3 (red boxes in A-D) are shown in (A'-D'). A'', B'' and D'' show a single ray of the branched ventral fin ray No. 3, respectively. Red arrowheads in (A'-D') and (A'', B'' and D'') indicate the blood vessels of one single ray of the branched ventral fin ray No. 3. White dotted lines (in A-D) indicate the distal epidermis. A, A', and A'') At 48 hpa, blood vessels start regeneration by healing the ends of the vessels in the non-amputated fin rays. The white arrow in A'' indicates the loss of GFP expression stops. B, B', and B'') At 72 hpa, blood vessels regeneration continues and the connecting bridge between the artery and the vein is formed, indicated by the white arrow in B''. C, C', D, D', and D'') By 120 hpa, regenerating blood vessels form a sprout that grows distally, indicated by the white arrow in D''. Scale bars in (A-D): 200 μm. Scale bars in (A'-E'): 50 μm. Scale bars in (B''-D''): 12.5 μm.

3.4.2.6 Morphological changes

After half-fin amputation of the dorsal lobe of the caudal fin, the damages of the non-amputated fin rays of the ventral lobe were classified into two groups according to the severity of the damage: mild damage was defined as loss of pigment cells (melanocytes) without any other tissue damage, induced by 24 hpa (Figure 3.8 A); severe damage was defined as loss of pigment cells and tissue damage at the tip of the fin ray, induced by 24 hpa (Figure 3.12 B).

To test whether the severity of damage was dependent on some environmental or physiological factors, we performed the half-fin amputation of the *Tg(fli1:EGFP)* fish and then compared the ratio of fish showing severe damage and mild damage, in distinct groups of fish (at least 15 fish per group), including a) old fish (more than 1.5 year old) or young fish (3-6 months), b) male fish or female fish, c) fish kept in groups or individually during regeneration, and d) fish kept at 23 °C or 28.5 °C. However, we did not find any evidence suggesting those factors were related to the severity of damage or loss of GFP expression in the non-amputated fin rays (data not shown).

B
severe damage
A
mild damage
Before Amp.
1 hpa
8 hpa
24 hpa

Figure 3.12 Mild damage (A) and severe damage (B) observed in the intact lobe after half-fin amputation of the caudal fin.

Fins are shown before half-fin amputation and at 1 hpa, 8 hpa, and 24 hpa. Left panels in A and B are showing the entire fins. Right panels in A and B are higher magnification of the long fin rays of the non-amputated lobe. A) Mild damage is defined as loss of pigment cells (melanocytes) without any other tissue damage, induced by 24 hpa in the non-amputated lobe. B) Severe damage is defined as loss of pigment cells (melanocytes) and tissue damage at the tip of the fin ray, induced by 24 hpa in the non-amputated lobe. The close-view images are the area of the black dotted boxes. Red arrows indicate the loss of melanocytes (a type of pigment cells) (A) and loss of epidermal tissues (B).

3.4.2.7 Loss of GFP expression in the dorsal fin and the anal fin, but not in the pectoral fin and pelvic fin after half-fin amputation of the caudal fin

While we were observing the defects (e.g. GFP loss) after half-fin amputation of the dorsal lobe of the caudal fin of the *Tg(fli1:EGFP)*, we observed the loss of GFP expression not only in the non-amputated fin rays in the ventral lobe of the caudal fin, but also, in some occasions (4/17 fish), at the tips of the fin rays in the anal fin and the dorsal fin by 1 hpa (Figure 3.13). However, the loss of GFP expression was never observed in the paired pectoral fins and the paired pelvic fins by 1 hpa (0/17 fish) (data not shown).

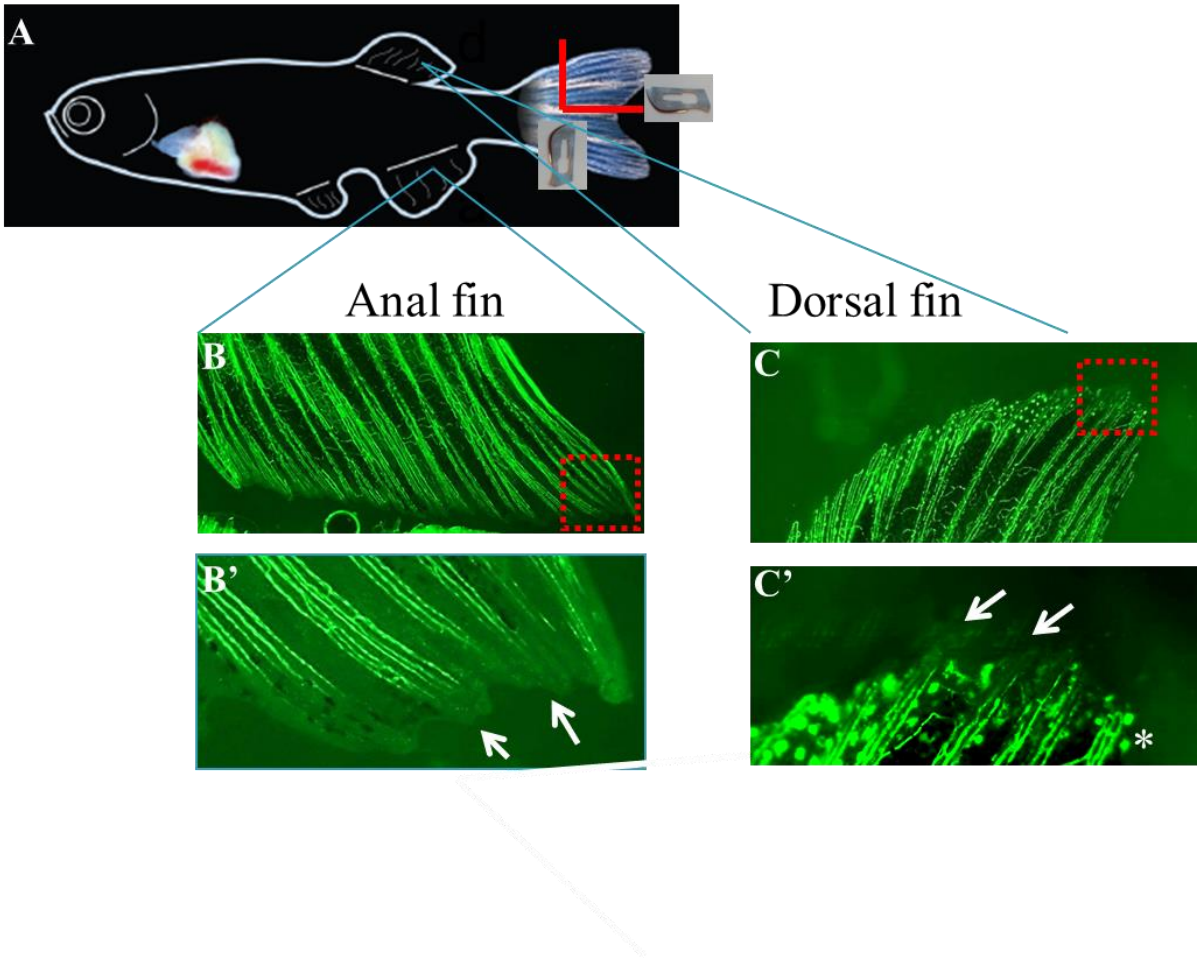
A
Anal fin
Dorsal fin
B
B'
C
C'
*

Figure 3.13 GFP disappearance in the fin rays of the anal fin and the dorsal fin after half-fin amputation of the caudal fin of *Tg(fli1:EGFP)*.

A) A schematic image shows the half-fin amputation of the dorsal lobe of the caudal fin (indicated by the red lines and the scalpel blade) (Modified from "International Innovation" 43-46, 2012). B and C) Loss of GFP expression is observed in the fin rays of the anal fin and the dorsal fin of the same fish at 1 hpa. B' and C' are close-views of the red boxes in B and C, respectively. Arrows indicate the GFP disappearance in the non-amputated fin rays. The asterisk indicates the auto fluorescence of the pigment cells (white cells).

3.4.3 Neutrophils response to half-fin amputation of the caudal fin

The causes or mechanisms for the loss of GFP expression in the non-amputated fin rays after half-fin amputation of the *Tg(fli1:EGFP)* and for the following tissue degeneration and regeneration were unknown. However, the loss of GFP expression in the non-amputated fin rays was observed as early as 10 mins post amputation (mpa) of the *Tg(fli1:EGFP)* (Figure 3.10), suggesting that immediate internal cue(s) after half-fin amputation were induced and acted on the non-amputated fin rays. In order to describe and characterize this immediate injury response, we started to investigate the response of neutrophils after local injury because neutrophils are the first immune cells that respond to the inflammation and that arrive to the sites of injury (Serhan *et al.*, 2007; Li *et al.*, 2012). We used the zebrafish transgenic line *Tg(mpx:GFP)* that express GFP in the neutrophils to help characterize the dynamics of the neutrophil response (Richardson *et al.*, 2013). *mpx* is the myeloid-specific peroxidase gene that is used as a marker for neutrophils (Renshaw *et al.*, 2006).

After half-fin amputation of the dorsal lobe of the fin, neutrophils remained at a constant level at 10 mpa and 1 hpa in both the amputated and non-amputated fin rays (Figure 3.10 A, B, C, E, F, G). By 8 hpa, a higher level of GFP expression was observed, indicating an infiltration by neutrophils in both the amputated and non-amputated fin rays in 18/28 *Tg(mpx:GFP)* fish (Figure 3.14 H, I, J). Between 8-24 hpa, the number of neutrophils was dramatically decreased in the amputated fin rays, shown by the diffusion of GFP-expressing cells, suggesting that neutrophils function during the early inflammatory response to the wound was finished (Figure 3.14 L). However, in the non-amputated fin rays of the ventral lobe, infiltration by neutrophils continued until 24 hpa, when the maximum appearance of neutrophils was observed (Figure 3.14 M). This observation suggested that requirements for neutrophils in the non-amputated fin rays seemed to be higher and the removal of neutrophils

delayed compared to the wounded area. By 48 hpa, neutrophils were maintained at a constant level without any infiltration as shown by GFP diffusion in both the amputated and non-amputated fin rays, suggesting that neutrophils had finished their function in the non-amputated fin rays as well (Figure 3.14 O, P). This result indicated that inflammation was activated or induced not only in the amputated fin rays, but also in the non-amputated fin rays of the caudal fin.

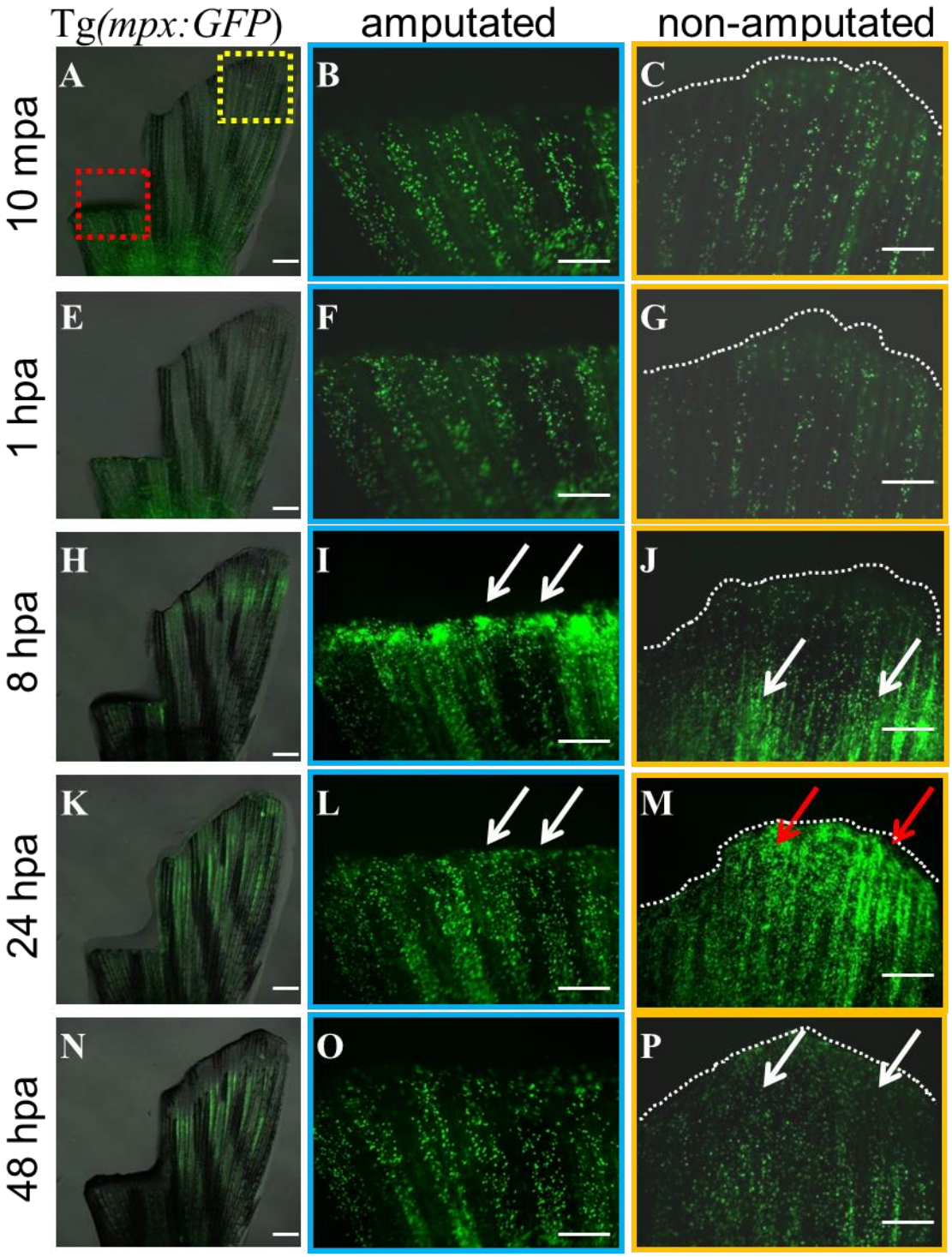
Tg(mpx:GFP)
amputated
non-amputated
10 mpa
1 hpa
8 hpa
24 hpa
48 hpa
A
B
C
E
F
G
H
I
J
K
L
M
N
O
P

Figure 3.14 Time course analysis of the neutrophils response, shown by GFP expression, at the distal tips of the caudal fin after half-fin amputation of the *Tg(mpx:GFP)*.

GFP expression is observed at 10 mpa (A-C), at 1 hpa (E-G), at 8 hpa (H-J), at 24 hpa (K-M), and at 48 hpa (N-P). Observations are made on the entire caudal fin of the same fish (A, E, H, K, N). Higher magnification of the amputated fin rays (the red box in A) and the non-amputated fin rays (the yellow box in A) are shown in (B, F, I, L, O), (C, G, J, M, P), respectively. White arrowheads in (I, L) and (J, P) indicate the same fin rays of the amputated lobe and in the non-amputated lobe, respectively. White dotted lines indicate the distal epidermis and distal edge of the fin. At 10 mpa and 1 hpa, no obvious recruitment of neutrophils is observed in the amputated fin rays of the dorsal lobe and non-amputated fin rays of the ventral lobe (B, F, C, G). Infiltration of neutrophils is observed at 8 hpa in the amputated and non-amputated fin rays (I, J), shown by the white arrows. Note neutrophils accumulate in a more proximal region in the non-amputated fin rays (indicated by white arrows in (J)) than in the amputated rays. At 24 hpa, neutrophils start to diffuse in the amputated fin rays (L), but in the non-amputated fin rays, neutrophils are still present in high number, and they are now present in the distal region, indicated by red arrows in (M). At 48 hpa, neutrophils number stays at a constant level at the amputated site (O), and neutrophils are dramatically diminished at the non-amputated site (P). Scale bars in (A, E, H, K, N): 1 mm. Scale bars in (B, C, F, G, I, J, L, M, O, P): 200 μm.

3.4.4 Thrombocytes response to half-fin amputation of the caudal fin

After half-fin amputation, blood flow was absent in the distal ends of the non-amputated fin rays of the opposite (ventral) lobe and blood flow was stopped in a more proximal region, suggesting that blood vessels at the distal ends were dysfunctional and hemostasis or a blood clot might be present in the more proximal region to prevent blood flow at the tip of the fin. Zebrafish thrombocytes serve as the coagulation regulator in hemostasis and can be visualized with GFP expression of the *Tg(CD41:GFP)* line, which is ideal for *in vivo* tracking of the dynamics of thrombocytes during fin regeneration (Lin *et al.*, 2005; Jagadeeswaran *et al.*, 1999; Kim *et al.*, 2012). CD41 is the α subunit of the platelet integrin CD41/CD61 (α_{IIb}/β_3, glycoprotein IIb [GPIIb]/GPIIIa) complex and the marker for thrombocytes and prothrombocyte precursors (Ferkowicz *et al.*, 2003; Mikkola *et al.*, 2002; Khandekar *et al.*, 2012).

After half-fin amputation of the dorsal lobe, infiltration of thrombocytes was observed by a higher level of GFP expression in both the amputated and non-amputated fin rays by 1 hpa in 14/20 *Tg(CD41:GFP)* fish. However, the recruited thrombocytes in the non-amputated lobe did not accumulate at the distal ends of the fin rays as in the amputated fin rays (Figure 3.15), but they accumulated in a more proximal region (Figure 3.15), suggesting that the blood clot might be formed in this more proximal region. Between 1-8 hpa, the infiltration by thrombocytes was still observed in both the amputated and non-amputated fin rays (Figure 3.15 E, F), but thrombocytes had disappeared by 24 hpa, as shown by the diffusion of GFP expression (Figure 3.15 H, I). In addition, tissue damage and bone damage were observed in the non-amputated fin rays at 24 hpa (Figure 3.15 I). The tissue damage were likely caused by the formation of blood clot in the more proximal region of the rays, where blood supply

failed to reach the distal ends of each fin ray, resulting in hypoxia and in a nutrient deprivation situation.

Tg (CD41:EGFP)
amputated
non-amputated
1 hpa
8 hpa
24 hpa
A
B
C
D
E
F
G
H
I
*

Figure 3.15 Time course analysis of the thrombocytes response, shown by GFP expression, at the distal tips of the caudal fin after half-fin amputation of the *Tg(CD41:GFP)*.

GFP expression is observed at 1 hpa (A-C), at 8 hpa (D-F), and at 24 hpa (G-I). Observations are made on the entire caudal fin of the same fish (A, D, G). Higher magnification of the amputated fin rays (the red box in A) and the non-amputated fin rays (the yellow box in A) are shown in (B, E, H), (C, F, I), respectively. White arrowheads in (B, E, H) indicate the same fin rays of the amputated lobe. B, E, H) Thrombocytes are recruited at 1 hpa, continue to be present at 8 hpa, but diminish by 24 hpa in the amputated fin rays. C, F, I) In the non-amputated fin rays, the recruitment of thrombocytes starts at 1 hpa, reaches the maximum at 8 hpa, and diminished by 24 hpa. Note white arrows in C and F indicate thrombocytes that are recruited in a more proximal region in the non-amputated fin rays by 8 hpa, and the white arrow in I shows that these recruited thrombocytes have disappeared by 24 hpa. The red arrow in I indicates the tissue damage and the bone damage. The asterisk indicates the auto fluorescence of the pigment cells (white cells). Scale bars in (A, D, G): 1 mm. Scale bars in (B, C, E, F, H, I): 200 μm.

3.4.5 Nerve fibers response to half-fin amputation of the caudal fin

As shown above, endothelial cells of blood vessels, neutrophils, and thrombocytes all responded to the half-fin amputation of the dorsal lobe in an organ-wide manner. Next, we examined the effect on the nerve fibers, another type of tissue that can quickly respond to injury. To observe the dynamics on the nerve fibers, the Zn-12 antibody that specifically labels the nerve fibers was used for immunostaining of the caudal fin of the *Tg(fli1:EGFP)*. The use of the *Tg(fli1:EGFP)* also allowed the observation of the endothelial cells of blood vessels.

After the half-fin amputation of the dorsal lobe of the caudal fin of *Tg(fli1:EGFP)* fish, some fish (13/31) showed a loss of GFP expression and some fish (18/31) had intact GFP expression in the non-amputated fin rays. Regardless the integrity of GFP expression, Zn-12 antibody staining was performed at 10 mpa, 1 hpa, and 8 hpa. Immunostaining on intact control (non-amputated) fin rays of the *Tg(fli1:EGFP)* showed that the nerve fibers extended towards the end of the fin rays distal to the blood vessels (Figure 3.16 A, A'). At 10 mpa, the loss of GFP expression was observed in the non-amputated fin rays of the intact lobe, indicated by the breakdown of the bridge between the artery and the vein. In addition, the nerve fibers at the distal tips of these fin rays were damaged as observed by the collapse of the nerve fibers (Figure 3.16 B, B'). At 1 hpa or at 8 hpa, although in some fins (13/31) no GFP disappearance was observed, nerve fibers were damaged (12/13) (Figure 3.16 C, C', D, D'). This result suggests that the nerve fibers are more sensitive to injury than blood vessels and can serve as an early response marker in the non-amputated fin rays to the local amputation of the caudal fin. Furthermore, the damage of nerve fibers immediately after half-fin amputation may be the cause of the following thrombocytes infiltration, of neutrophils recruitment, and of tissue damage.

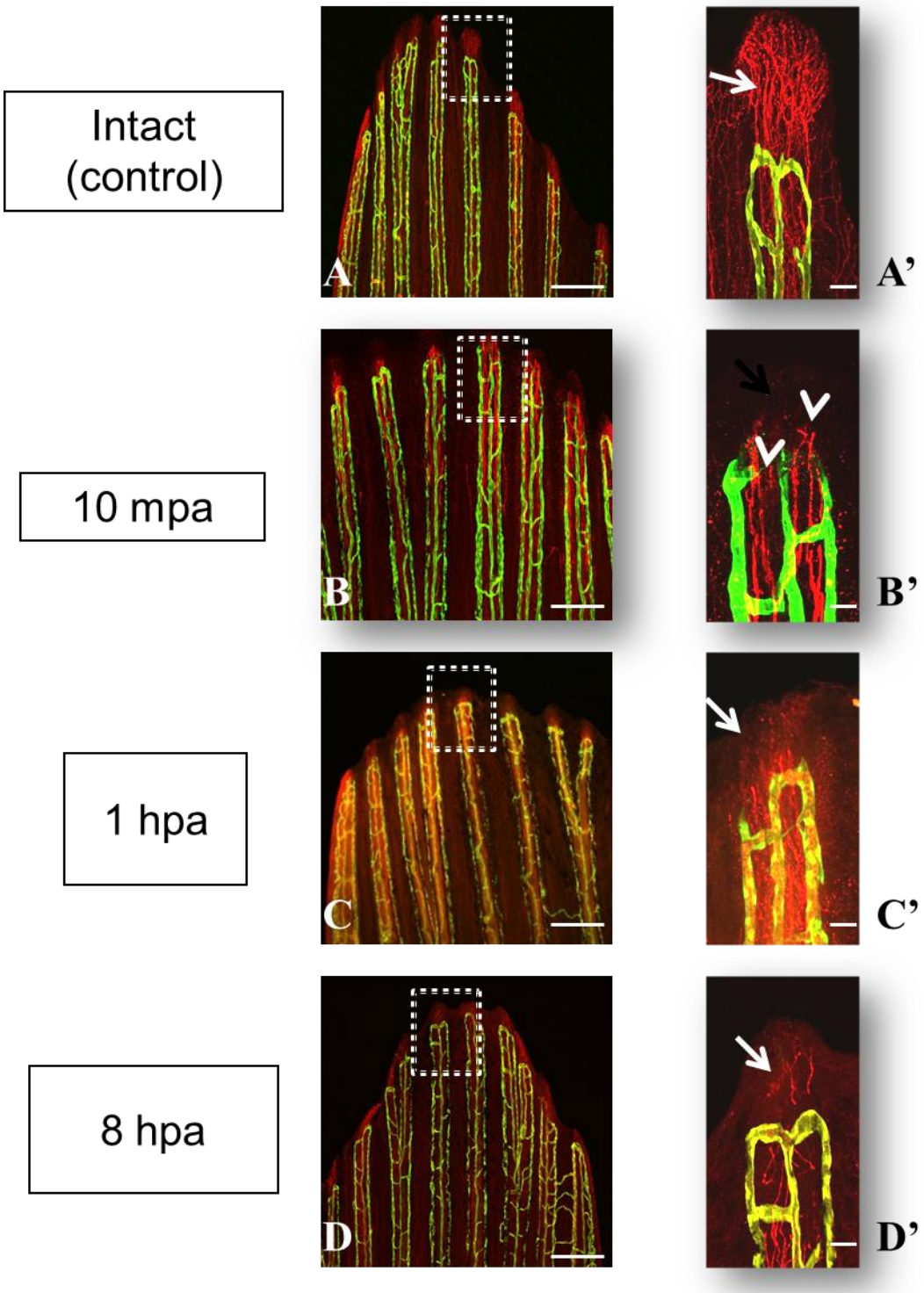
Intact
(control)
10 mpa
1 hpa
8 hpa
A
A'
B
B'
C
C'
D
D'

Figure 3.16 Nerve fibers response in the non-amputated fin rays after half-fin amputation of the caudal fin of the *Tg(fli1:EGFP)*.

A-D) Four different fins of the *Tg(fli1:EGFP)* were used for Zn-12 antibody staining for nerve fibers (shown in the red). Higher magnification of the non-amputated fin rays (the white boxes in A-D) are shown in (A'-D'). A, A') The intact (control) fin rays present an intact shape of the nerve fibers and intact blood vessels (yellow) in the distal ends of fin rays. The white arrow in A' indicates the intact nerve fibers. B, B') After half-fin amputation, at 10 mpa, the loss of GFP expression and the damage of nerve fibers are observed at the tips of the non-amputated fin rays, indicated by white arrowheads. C, C', D and D') After half-fin amputation, at 1 hpa and 8 hpa, the damage of nerve fibers is seen at the distal tips in the non-amputated fin rays (indicated by white arrows), but in the same fin, blood vessels are intact. Scale bars in (A-D): 200 μm. Scale bars in (A'-D'): 20 μm.

3.4.6 Systemic response to injury or organ-specific response to injury

After the observations of the dynamics of the endothelial cells of blood vessels, nerve fibers, neutrophils, and thrombocytes following half-fin amputation of the caudal fin, we wanted to test if the damage observed in the non-amputated fin rays was a systemic response to injury that would result from any kind of injury of the zebrafish, or if these responses were only the result from the local injury of the caudal fin.

To test for the systemic response to injury, various types of injury were performed. These injuries included stab lesion in the brain, abdominal injection, removal of scales, amputation of the pectoral or pelvic fins, or of the dorsal fin, and incision wounding (See Materials and Methods) and they were independently conducted on the *Tg(fli1:EGFP)* fish (ranging from 5-14 fish per group). However, none of the methods of injury stated above were able to induce GFP disappearance in the fin rays of the caudal fin, except for one fish after dorsal fin amputation (Table 6). The dorsal fin amputation resulted in the loss of GFP expression in the fin rays of the caudal fin; this effect resembled the inverse situation mentioned earlier, when half-fin amputation of the caudal fin showed the loss of GFP expression in the dorsal fin or the anal fin of the *Tg(fli1:EGFP)*. These results suggest that the response (e.g. loss of GFP, tissue damage) in the non-amputated fin rays after local injury of the caudal fin is not a systemic response to injury, but more likely an organ-wide response to injury.

Table 6. Tests of systematic injury response in adult *Tg(fli1:EGFP)* caudal fin

Injury methods	No. of fish showed GFP loss in the caudal fin	No. of fish showed no GFP loss in the caudal fin
Stab lesion in the brain	0	7
Abdominal injection	0	5
Removal of scales	0	5
Amputation of pelvic and pectoral fins	0	14
Amputation of the dorsal fin	1	5
Incision wounding	0	9

3.5 Discussion

In the caudal fin of the *Tg(2.4shha:GFP-ABC)*, GFP is expressed in the distal region of each fin ray and this expression recapitulates the endogenous expression of *shha* (Zhang *et al.*, 2012). The initial finding of GFP disappearance in the intact tissues of the *Tg(2.4shha:GFP-ABC)* after local injury of one fin ray in the caudal fin, set up the start point of this project (Figure 3.3). Many questions were raised regarding this initial finding. How a local injury can affect the area where no damage is induced? Why the loss of GFP expression is not seen simultaneously in all the fin rays of the caudal fin? What are the subsequent consequences of the GFP disappearance in the non-amputated fin rays?

3.5.1 The immediate GFP disappearance in the non-amputated tissues after local injury

To answer the questions regarding the loss of GFP expression in the non-amputated fin rays after local injury of the caudal fin, we first ruled out the possibility that the manipulation of the fish was the cause of the GFP disappearance. Next, we confirmed that the loss of GFP expression in the non-amputated fin rays was not a systemic injury response but an organ-wide response since injury from other organs could not induce GFP disappearance in the caudal fin. However, one fish showed the loss of GFP expression in the caudal fin after amputation of the dorsal fin (Table 6), which inversely corresponded to our findings that local injury of the caudal fin could induce the GFP disappearance in the dorsal fin or the anal fin. One potential explanation for these observations is that the dorsal, the anal and the caudal fins originally differentiate from a unique embryonic caudal fin fold (Smith *et al.*, 1994; Van Eeden *et al.*, 1996) which, later, during the larval stage locally regresses to give the three

individual and separate unpaired fins. Therefore, from this common embryonic origin, the three fins may be considered as one organ in zebrafish and can respond to local injury in the caudal fin in an organ-wide manner.

Taking advantages of the zebrafish transgenic lines *Tg(2.4shha:GFP-ABC)* and *Tg(fli1:EGFP),* we tested the effect of a local injury induced in these transgenic fish by amputation of less than one segment or of six segments in one fin ray, or amputation of one segment in the middle part of a fin ray. As a result, after all types of local injury, by 8 hpa, 47.7% (42/88) fish showed a GFP disappearance at the distal tips of the entire caudal fin. The loss of GFP expression was followed by tissue damage and bone damage in some of the fish (Figure 3.17, Figure 3.18, Yan Li, unpublished data), then by the re-expression of GFP and tissue regeneration. Interestingly, similar observations of an organ-wide response following a local injury, are seen in the regenerating zebrafish heart (Raya *et al.*, 2003; Lepilina *et al.*, 2006) and brain (my observations from data reported in publications Kishimoto *et al.*, 2012; Kizil *et al.*, 2012). After a local amputation of the adult zebrafish heart, embryonic gene programs are activated in the entire heart, and are not limited to the site of injury during the regeneration of the organ between 1-7 dpa (Lepilina *et al.*, 2006). Similarly, after a local stab lesion of adult zebrafish brain, the number of proliferating cells is increased and the injury induces the expression of the pro-regenerative factor *gata3* in the entire brain, again not only at the site of injury by 3 days post injury (Kishimoto *et al.*, 2012; Kizil *et al.*, 2012). So far, it is not clear why and how injury signals from the wound site transmit to the non-injured site and activate the embryonic gene programs in the entire organ. However, it has been postulated that the unique process of "searching for" and "identifying the injury site" in the regenerating organs is responsible for the organ-wide response to local injury, and such process contributes to the regenerative ability of the organs (Poss, 2010).

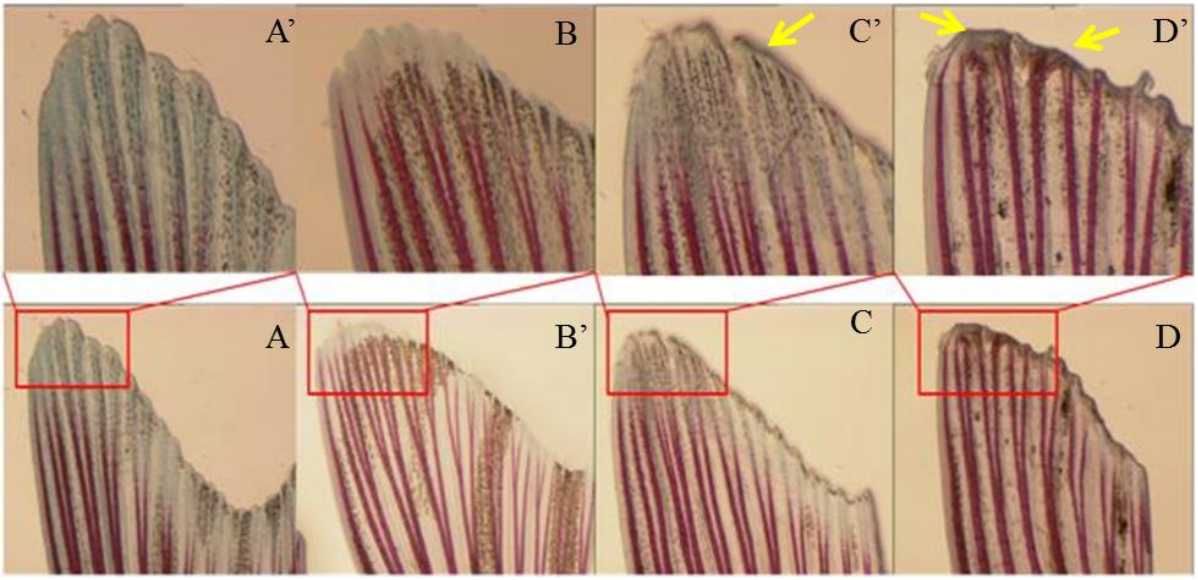
A’
B
C’
D’
A
B’
C
D

Figure 3.17 Bone staining using alcian blue and alizarin red of the non-amputated fin rays three days after half-fin amputation of the caudal fin (Modified from Yan Li, unpublished data).

Four different representative fins of wild type fish are shown. A', B', C', and D' are close-views of A, B, C, and D, respectively. A, A') Control (intact, non-amputated) fin shows no tissue damage or bone damage. At 3 dpa after half-fin amputation, the non-amputated fin rays can be categorized into three groups: B, B'), no tissue or bone damage. C, C') tissue damage (epidermal tissue and pigment loss and damage at the tip of the fin). D, D') tissue damage and bone damage. The yellow arrow in C' indicates the epidermal tissue damage. Yellow arrows in D' indicate the tissue damage and bone damage.

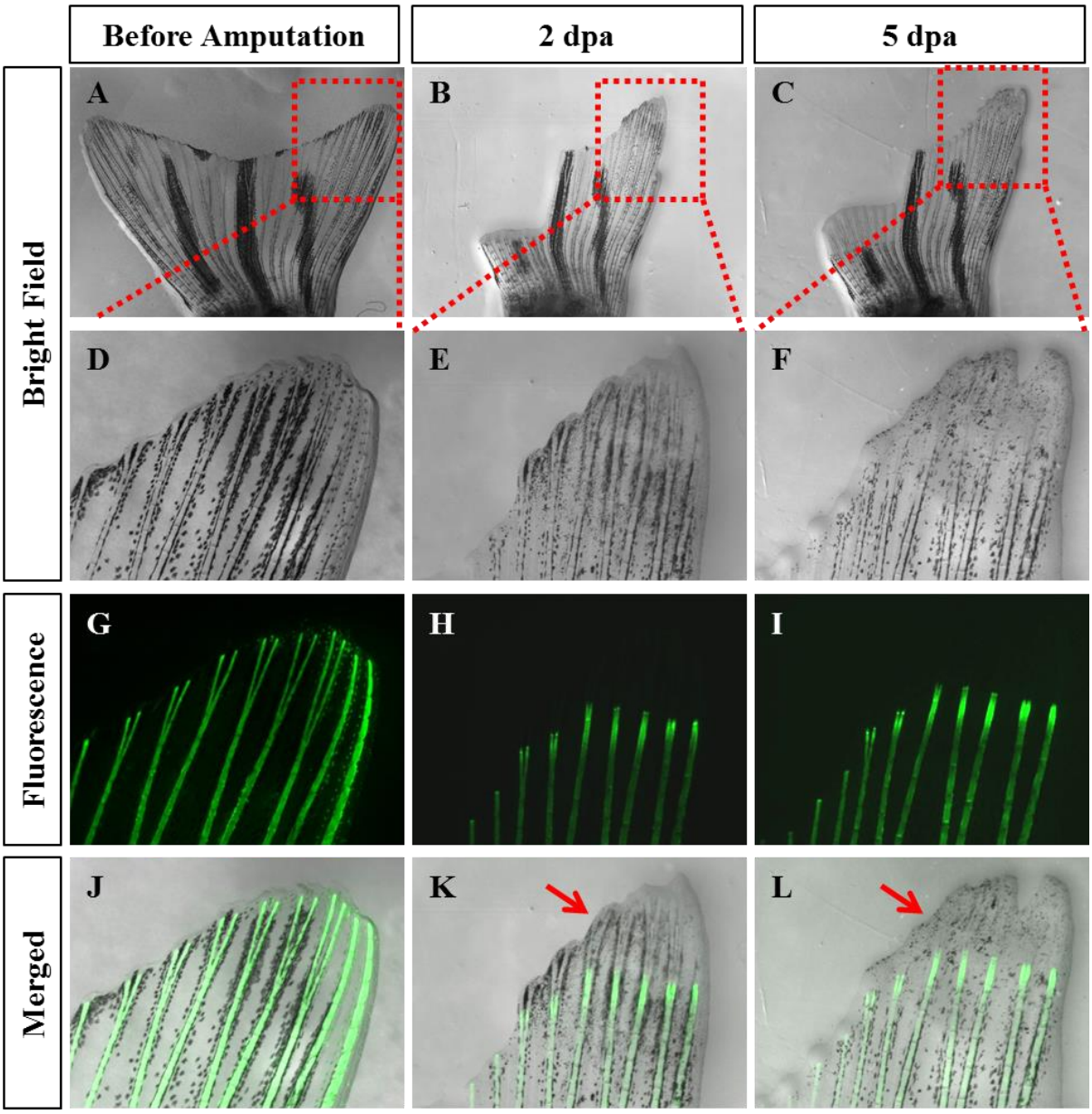
Before Amputation
2 dpa
5 dpa
Bright Field
Fluorescence
Merged
A
B
C
D
E
F
G
H
I
J
K
L

Figure 3.18 Bone staining using *in vivo* calcein staining in the half-fin amputated caudal fin (Modified from Yan Li, unpublished data).

Images of the same caudal fin were taken before amputation (A, D, G, J), at 2 dpa (B, E, H, K), and at 5 dpa (C, F, I, L). A, B, and C shows the entire caudal fin. D, E, and F are close-views of A, B, and C, respectively. G, H, and I are taken using fluorescence microscope with green filter. The merged photos (J, K, and L) are created by merging bright-field photos with green fluorescent photos using Adobe Photoshop. A, D, G, J) Before amputation, no bone damage is observed as shown by the green fluorescence. B, E, H, K) At 2 dpa, the loss of the green fluorescence indicating bone damage and loss of tissues (epidermal tissue and pigment loss and damage at the tip of the fin) are observed at the distal tips of the non-amputated fin rays. C, F, I, L) At 5 dpa, the loss of the green fluorescence indicating bone damage and a more severe loss of tissues are observed. Red arrows in K and L indicate the damages.

Yan Li (Honour's student in our laboratory) tested the possibility that the GFP disappearance in the non-amputated tissues is due to the microbial infection after the local injury. Indeed, severe infection in fins can lead to fin rot, which starts at the edge of the fins and destroys more and more tissue until it reaches the base of the fin (Kent *et al.*, 2012). To test this possibility, fish were treated with erythromycin, an antibiotic that has a broad antimicrobial spectrum (Zhanel *et al.*, 2001), for six days before half-fin amputation, with the aim of preventing fin infection and propagation at the time of amputation. After amputation, injured fish were also treated with erythromycin for another five days. Two erythromycin solutions with final concentrations of 0.25 mg/L and 0.5 mg/L were tested on *Tg(fli1:EGFP)* fish. As a result, 6/6 intact (control) fish showed no GFP expression loss throughout the duration of the experiment (data not shown), whereas 2/6 experimental fish (half-fin amputated) showed the loss of GFP expression in the non-amputated tissues after the local injury (Figure 3.19, Yan Li, unpublished data). These preliminary results suggest that microbial infection is unlikely to have contributed to the damages observed in the non-amputated lobe (Yan Li, unpublished data). However, a larger number of fish, other erythromycin doses and other antibiotics need to be tested before ruling out the possibility that the microbial infection may be at the origin of the organ wide response to local injury.

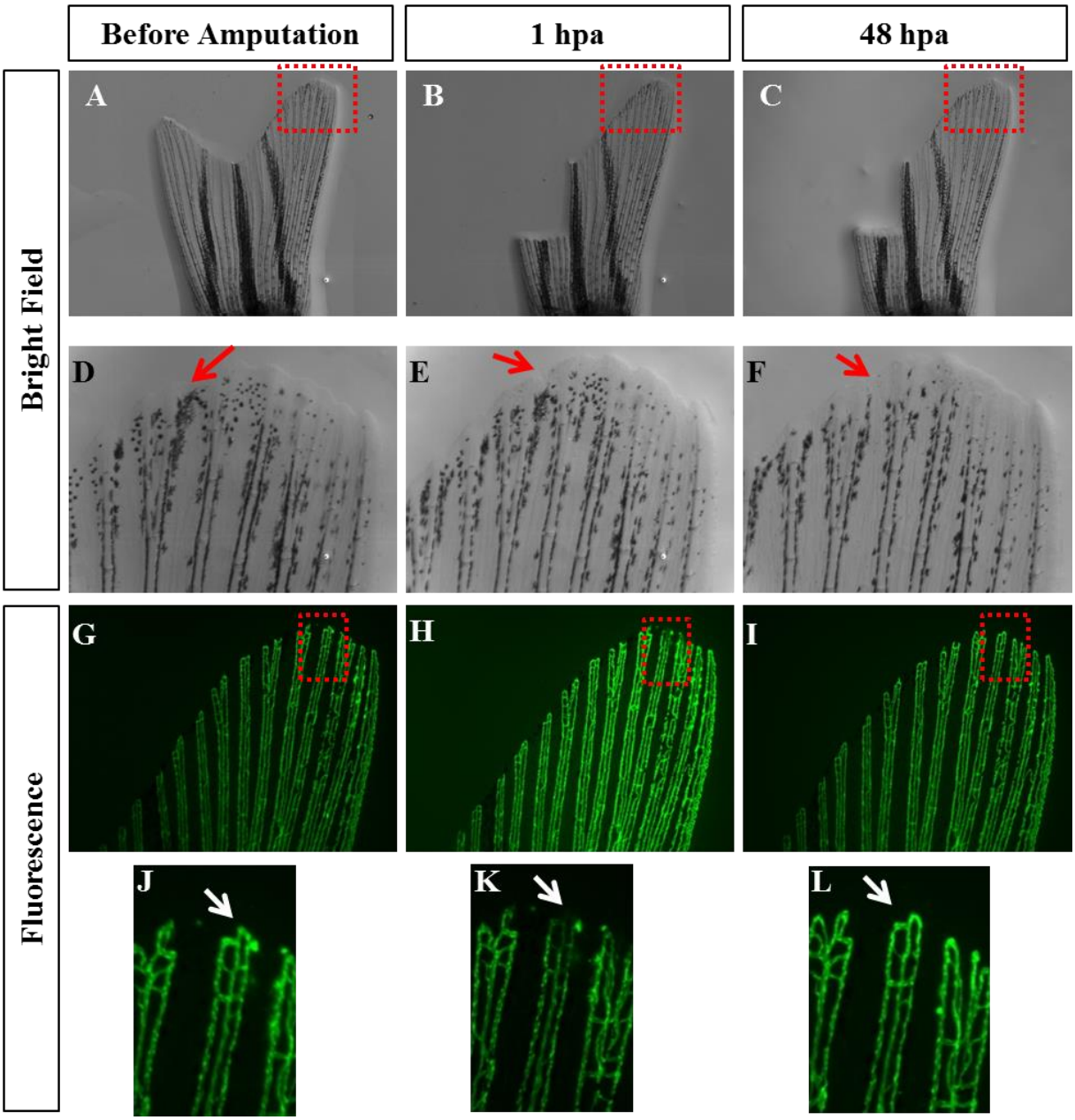
Before Amputation
1 hpa
48 hpa
Bright Field
Fluorescence
A
B
C
D
E
F
G
H
I
J
K
L

Figure 3.19 Treatment with erythromycin of non-amputated fin rays after half-fin amputation (Modified from Yan Li, unpublished data).

Tg(fli1:EGFP) fish were used in this experiment. Half-fin amputation was carried out on the fish following pre-treatment with 0.5 mg/L erythromycin for six days. After amputation, images of the same caudal fin were taken before amputation (A, D, G, J), at 1 hpa (B, E, H, K), and at 48hpa (C, F, I, L). D, E, and F are close-views of A, B, and C, respectively. J, K, and L are close-views of G, H, and I, respectively. A, D, G, J) Before amputation, no loss of GFP expression is observed. B, E, H, K) At 1 hpa, the loss of GFP expression is observed at the distal tips of the non-amputated fin rays. C, F, I, L) At 48 hpa, GFP is re-expressed in the fin ray. The red arrows in D, E, and F indicate the loss of pigment cells. The white arrows in J, K, and L indicate the loss of GFP expression in the non-amputated fin rays of the intact (ventral) lobe of the caudal fin.

3.5.2 Proposed scenario of the response following local injury

After local injury of one fin ray, we observed a very rapid, almost immediate regression of nerve fibers and blood vessels in the non-amputated tissues. This observation indicates that internal signals from the fish caused the tissue damage in the non amputated tissues, not the external sources, such as amputation. We have shown that following local injury, inflammatory cells and thrombocytes are recruited and running into every artery and vein in the caudal fin, and this recruitment most likely induces the formation of a blood clot at the distal end of each fin ray. It is possible that inflammatory cells recruited to the non-injured tissues respond to the false signal of a wound and attack cells/ tissues, resulting in GFP disappearance of endothelial cells and subsequently tissue damage and bone loss.

We also have observed that the local injury triggers the regression of the nerve bundles at the tip of the rays. This observation is similar to that described following amputation or denervation by laser axotomy of the zebrafish larval tail fin and that showed a severe degeneration of the peripheral sensory axon branches close to the wound margin (Rieger and Sagasti, 2011). Furthermore, previous studies have shown that injury on one side of a limb can damage the axons on the opposite (contralateral) side of the limb in both the newt and axolotl, resulting in the delay of the axonal flow and subsequently the neuronal degeneration (Tweedle, 1971; Kleinschnitz *et al.*, 2005; Suzuki *et al.*, 1993; Knecht *et al.*, 1996). It is possible that, in a similar transneuronal manner, the local injury damages the peripheral nerve in the caudal fin, which leads to the nerve fibers damage in the contralateral side (opposite lobe) of the caudal fin.

Thus, a possible scenario is that the local injury may induce a delay or affect the axonal flow or axonal integrity of the other lobe, resulting in the nerve fibers damage and subsequently blood vessels damage and tissue loss. In turn, these damages will activate the regeneration programs that will regulate the inflammatory response and start the re-construction of the damaged tissue. In the future, in order to verify the sequence of the proposed events, it would be interesting using the various fluorescent reporter transgenic lines available in zebrafish (such as *Tg(fli1:EGFP); Tg(mpx:GFP); Tg(CD41:GFP)* and *Tg(2.4shha:GFP-ABC)*) to test the effects of denervation of the adult zebrafish caudal fin and of denervation of a few fin rays on blood vessels, inflammatory cells and other cell types.

3.5.3 Reconsider "One half for control, the other half for experimentation"

The adult zebrafish caudal fin is considered to be an excellent system to study the molecular programs that regulate the regeneration process. Many labs have done extensive research to dissect essential signaling pathways that are activated after the caudal fin injury. In several experimental procedures, such as anti-sense morpholino oligonucleotides injection to knock-down gene(s) of interest (Thummel *et al.*, 2006; Hyde *et al.*, 2012; Thatcher *et al.*, 2008), laser cell ablation (Zhang *et al.*, 2012), or comparison of injury response and regeneration response (Sousa *et al.*, 2012), one of the lobes of the caudal fin is used as the internal control, whereas the other lobe is used for the experimental uses. Our results indicate that, in studies involving experimental manipulation on the fin rays of one lobe, the best control may not be the opposite lobe, especially when analyzing the early effects of the experimentation.

In our study, we present, for the first time, the immediate organ-wide response characterized by the damage of blood vessels and nerve fibers on the non-amputated tissues after local injury in the adult zebrafish caudal fin, suggesting the caudal fin can sense the local injury and response in an organ-wide manner, rather than a locally response to the wound site. This organ-wide response to local injury can also be observed in the adult zebrafish heart (Poss, 2010) and brain (my observations in the published papers), although little is known about the mechanisms that regulate this global injury response in an organ. It is known that injury-induced regeneration programs in multiple organs share some degree of commonality in term of the signaling pathways involved in these programs (Tal *et al.*, 2010). For example, the Fgf signaling pathway is activated and is known to be essential in both the regenerating brain and the regenerating caudal fin (Whitehead *et al.*, 2005; Koster and Fraser, 2006). It is therefore possible that programs responsible for the organ-wide response to local injury may also exist in these organs.

Here, we established that the adult zebrafish caudal fin may serve as an excellent model for the study of the organ-wide response to local injury, due to its extraordinary regenerative ability and to the fact that injury in the caudal fin does not impair the survival of the fish, and for the characterization of the molecular and cellular pathways involved in this response.

3.5.4 Perspectives for regenerative medicine

In 2010, Poss claimed that the injury response is dynamic and regeneration can involve organ- or organism-wide events rather than a locally response in the wound site (Poss, 2010). Evidence from various sources supports this notion. For example, in planarian, an invertebrate animal model, either a local injury in the head region or the tail region can

activate the apoptotic, mitotic and stem cells responses in the organism-wide manner (Pellettieri *et al.*, 2010; Wenemoser and Reddien, 2010; Guedelhoefer and Alvarado, 2012); in mammals, removal of part of the liver (partial hepatectomy) can activate the proliferation of compensatory hepatocytes from the rest of the liver and results in hyperplasia through factors such as interleukin-6, hepatocyte growth factor (Taub, 2004); in zebrafish, injury of approximately 20% of the heart by transection can activate embryonic developmental programs in the rest of the heart (Lepilina *et al.*, 2006).

No previous reports have indicated or documented the organ- or organism-wide response to local injury in the adult zebrafish caudal fin. Our study supports Poss's comment that (2010) "regeneration is not an isolated developmental event, but can control (and be controlled by) the physiology of the entire organ and/or animal". Meanwhile, our data provide new insights into the field of the regenerative medicine, because the regenerative medicine may become more complex, since one has to take into account the fact that stimulating regeneration locally may trigger responses in unintended locations.

References

Affolter M, Zeller R, Caussinus E. Tissue remodelling through branching morphogenesis. *Nat Rev Mol Cell Biol*. 2009; 10(12):831-842.

Akimenko MA, Mari-Beffa M, Becerra J, Geraudie J. Old questions, new tools, and some answers to the mystery of fin regeneration. *Dev Dyn*. 2003; 226(2):190-201.

Almuedo-Castillo M, Sureda-Gomez M, Adell T. Wnt signaling in planarians: New answers to old questions. *Int J Dev Biol*. 2012; 56(1-3):53-65.

Andersson ER, Lendahl U. Regenerative medicine: A 2009 overview. *J Intern Med*. 2009; 266(4):303-310.

Andersson O, Adams BA, Yoo D, et al. Adenosine signaling promotes regeneration of pancreatic beta cells in vivo. *Cell Metab*. 2012; 15(6):885-894.

Andreasen EA, Mathew LK, Lohr CV, Hasson R, Tanguay RL. Aryl hydrocarbon receptor activation impairs extracellular matrix remodeling during zebra fish fin regeneration. *Toxicol Sci*. 2007; 95(1):215-226.

Antos CL, Brand M. Regeneration of Organs and Appendages in Zebrafish: A Window into Underlying Control Mechanisms. *Encyclopedia of Life Sciences.* 2010; doi:10.1002/9780470015902.a0022101

Ariga J, Walker SL, Mumm JS. Multicolor time-lapse imaging of transgenic zebrafish: Visualizing retinal stem cells activated by targeted neuronal cell ablation. *J Vis Exp*. 2010; (43); doi(43):10.3791/2093.

Avaron F, Hoffman L, Guay D, Akimenko MA. Characterization of two new zebrafish members of the hedgehog family: Atypical expression of a zebrafish indian hedgehog gene in skeletal elements of both endochondral and dermal origins. *Dev Dyn*. 2006; 235(2):478-489.

Aza-Blanc P, Lin HY, Ruiz i Altaba A, Kornberg TB. Expression of the vertebrate gli proteins in drosophila reveals a distribution of activator and repressor activities. *Development*. 2000; 127(19):4293-4301.

Azevedo AS, Grotek B, Jacinto A, Weidinger G, Saude L. The regenerative capacity of the zebrafish caudal fin is not affected by repeated amputations. *PLoS One*. 2011; 6(7):e22820.

Bardet SM, Ferran JL, Sanchez-Arrones L, Puelles L. Ontogenetic expression of sonic hedgehog in the chicken subpallium. *Front Neuroanat*. 2010; 4:10.3389/fnana.2010.00028.

Becerra J, Montes GS, Bexiga SR, Junqueira LC. Structure of the tail fin in teleosts. *Cell Tissue Res*. 1983; 230(1):127-137.

Beck CW, Izpisua Belmonte JC, Christen B. Beyond early development: Xenopus as an emerging model for the study of regenerative mechanisms. *Dev Dyn*. 2009; 238(6):1226-1248.

Becker CG, Becker T. Repellent guidance of regenerating optic axons by chondroitin sulfate glycosaminoglycans in zebrafish. *J Neurosci*. 2002; 22(3):842-853.

Becker CG, Lieberoth BC, Morellini F, Feldner J, Becker T, Schachner M. L1.1 is involved in spinal cord regeneration in adult zebrafish. *J Neurosci*. 2004; 24(36):7837-7842.

Bellusci S, Furuta Y, Rush MG, Henderson R, Winnier G, Hogan BL. Involvement of sonic hedgehog (shh) in mouse embryonic lung growth and morphogenesis. *Development*. 1997; 124(1):53-63.

Bellusci S, Henderson R, Winnier G, Oikawa T, Hogan BL. Evidence from normal expression and targeted misexpression that bone morphogenetic protein (bmp-4)

plays a role in mouse embryonic lung morphogenesis. *Development*. 1996; 122(6):1693-1702.

Benazet JD, Zeller R. Vertebrate limb development: Moving from classical morphogen gradients to an integrated 4-dimensional patterning system. *Cold Spring Harb Perspect Biol*. 2009; 1(4):a001339.

Bernhardt RR, Tongiorgi E, Anzini P, Schachner M. Increased expression of specific recognition molecules by retinal ganglion cells and by optic pathway glia accompanies the successful regeneration of retinal axons in adult zebrafish. *J Comp Neurol*. 1996; 376(2):253-264.

Bridgewater JA, Knox RJ, Pitts JD, Collins MK, Springer CJ. The bystander effect of the nitroreductase/CB1954 enzyme/prodrug system is due to a cell-permeable metabolite. *Hum Gene Ther*. 1997; 8(6):709-717.

Bridgewater JA, Springer CJ, Knox RJ, Minton NP, Michael NP, Collins MK. Expression of the bacterial nitroreductase enzyme in mammalian cells renders them selectively sensitive to killing by the prodrug CB1954. *Eur J Cancer*. 1995; 31A (13-14):2362-2370.

Burglin TR. The hedgehog protein family. *Genome Biol*. 2008; 9(11):241-2008-9-11-241.

Buttitta L, Mo R, Hui CC, Fan CM. Interplays of Gli2 and Gli3 and their requirement in mediating shh-dependent sclerotome induction. *Development*. 2003; 130(25):6233-6243.

Chen CF, Chu CY, Chen TH, Lee SJ, Shen CN, Hsiao CD. Establishment of a transgenic zebrafish line for superficial skin ablation and functional validation of apoptosis modulators in vivo. *PLoS One*. 2011; 6(5):e20654.

Chin HJ, Fisher MC, Li Y, et al. Studies on the role of Dlx5 in regulation of chondrocyte differentiation during endochondral ossification in the developing mouse limb. *Dev Growth Differ*. 2007; 49(6):515-521.

Choi KY, Kim HJ, Lee MH, et al. Runx2 regulates FGF2-induced Bmp2 expression during cranial bone development. *Dev Dyn*. 2005;233(1):115-121.

Choi RY, Engbretson GA, Solessio EC, et al. Cone degeneration following rod ablation in a reversible model of retinal degeneration. *Invest Ophthalmol Vis Sci*. 2011; 52(1):364-373.

Chuang PT, Kornberg TB. On the range of hedgehog signaling. *Curr Opin Genet Dev*. 2000; 10(5):515-522.

Curado S, Anderson RM, Jungblut B, Mumm J, Schroeter E, Stainier DY. Conditional targeted cell ablation in zebrafish: A new tool for regeneration studies. *Dev Dyn*. 2007; 236(4):1025-1035.

Curado S, Stainier DY, Anderson RM. Nitroreductase-mediated cell/tissue ablation in zebrafish: A spatially and temporally controlled ablation method with applications in developmental and regeneration studies. *Nat Protoc*. 2008; 3(6):948-954.

Currie PD, Ingham PW. Induction of a specific muscle cell type by a hedgehog-like protein in zebrafish. *Nature*. 1996; 382(6590):452-455.

Davies JA. Do different branching epithelia use a conserved developmental mechanism? *Bioessays*. 2002; 24(10):937-948.

De Vrieze E, Sharif F, Metz JR, Flik G, Richardson MK. Matrix metalloproteinases in osteoclasts of ontogenetic and regenerating zebrafish scales. *Bone*. 2011; 48(4):704-712.

Denny PC, Ball WD, Redman RS. Salivary glands: A paradigm for diversity of gland development. *Crit Rev Oral Biol Med*. 1997; 8(1):51-75.

Detrich HW, 3rd, Westerfield M, Zon LI. Overview of the zebrafish system. *Methods Cell Biol*. 1999; 59:3-10.

Du SJ, Frenkel V, Kindschi G, Zohar Y. Visualizing normal and defective bone development in zebrafish embryos using the fluorescent chromophore calcein. *Dev Biol*. 2001;238(2):239-246.

Echelard Y, Epstein DJ, St-Jacques B, et al. Sonic hedgehog, a member of a family of putative signaling molecules, is implicated in the regulation of CNS polarity. *Cell*. 1993; 75(7):1417-1430.

Ekker SC, Ungar AR, Greenstein P, et al. Patterning activities of vertebrate hedgehog proteins in the developing eye and brain. *Curr Biol*. 1995; 5(8):944-955.

Elliott SA, Alvarado AS. The history and enduring contributions of planarians to the study of animal regeneration. *Dev Biol.* 2012; 2(3):301-326.

Eltzschig HK, Collard CD. Vascular ischaemia and reperfusion injury. *Br Med Bull*. 2004; 70:71-86.

Ferkowicz MJ, Starr M, Xie X, et al. CD41 expression defines the onset of primitive and definitive hematopoiesis in the murine embryo. *Development*. 2003; 130(18):4393-4403.

Fernandes AM, Fero K, Arrenberg AB, Bergeron SA, Driever W, Burgess HA. Deep brain photoreceptors control light-seeking behavior in zebrafish larvae. *Curr Biol*. 2012; 22(21):2042-2047.

Ferrari D, Kosher RA. Dlx5 is a positive regulator of chondrocyte differentiation during endochondral ossification. *Dev Biol*. 2002; 252(2):257-270.

Fuse N, Maiti T, Wang B, et al. Sonic hedgehog protein signals not as a hydrolytic enzyme but as an apparent ligand for patched. *Proc Natl Acad Sci U S A*. 1999; 96(20):10992-10999.

Gjorevski N, Nelson CM. Branch formation during organ development. *Wiley Interdiscip Rev Syst Biol Med*. 2010; 2(6):734-741.

Godwin JW, Pinto AR, Rosenthal NA. Macrophages are required for adult salamander limb regeneration. *Proc Natl Acad Sci U S A*. 2013.

Goldsmith MI, Fisher S, Waterman R, Johnson SL. Saltatory control of isometric growth in the zebrafish caudal fin is disrupted in long fin and rapunzel mutants. *Dev Biol*. 2003; 259(2):303-317.

Goodrich LV, Scott MP. Hedgehog and patched in neural development and disease. *Neuron*. 1998; 21(6):1243-1257.

Gray RS, Cheung KJ, Ewald AJ. Cellular mechanisms regulating epithelial morphogenesis and cancer invasion. *Curr Opin Cell Biol*. 2010; 22(5):640-650.

Grindley JC, Bellusci S, Perkins D, Hogan BL. Evidence for the involvement of the gli gene family in embryonic mouse lung development. *Dev Biol*. 1997; 188(2):337-348.

Guedelhoefer OC, 4th, Sanchez Alvarado A. Amputation induces stem cell mobilization to sites of injury during planarian regeneration. *Development*. 2012; 139(19):3510-3520.

HAAS HJ. Studies on mechanisms of joint and bone formation in the skeleton rays of fish fins. *Dev Biol*. 1962; 5:1-34.

Hacohen N, Kramer S, Sutherland D, Hiromi Y, Krasnow MA. Sprouty encodes a novel antagonist of FGF signaling that patterns apical branching of the drosophila airways. *Cell*. 1998; 92(2):253-263.

Hadzhiev Y, Lele Z, Schindler S, et al. Hedgehog signaling patterns the outgrowth of unpaired skeletal appendages in zebrafish. *BMC Dev Biol*. 2007; 7:75.

Hale LV, Ma YF, Santerre RF. Semi-quantitative fluorescence analysis of calcein binding as a measurement of in vitro mineralization. *Calcif Tissue Int.* 2000: 67(1):80-4.

Han M, Yang X, Taylor G, Burdsal CA, and Anderson RA, Muneoka K. Limb regeneration in higher vertebrates: Developing a roadmap. *Anat Rec B New Anat*. 2005; 287(1):14-24.

Harunaga J, Hsu JC, Yamada KM. Dynamics of salivary gland morphogenesis. *J Dent Res*. 2011; 90(9):1070-1077.

Heim R, Tsien RY. Engineering green fluorescent protein for improved brightness, longer wavelengths and fluorescence resonance energy transfer. *Curr Biol*. 1996; 6(2):178-182.

Henry KM, Loynes CA, Whyte MK, Renshaw SA. Zebrafish as a model for the study of neutrophil biology. *J Leukoc Biol.* 2013.

Ho L, Alman B. Protecting the hedgerow: P53 and hedgehog pathway interactions. *Cell Cycle*. 2010; 9(3):506-511.

Howe K, Clark MD, Torroja CF, et al. The zebrafish reference genome sequence and its relationship to the human genome. *Nature*. 2013; 496(7446):498-503.

Hsu CC, Hou MF, Hong JR, Wu JL, Her GM. Inducible male infertility by targeted cell ablation in zebrafish testis. *Mar Biotechnol (NY)*. 2010; 12(4):466-478.

Huang CC, Lawson ND, Weinstein BM, Johnson SL. Reg6 is required for branching morphogenesis during blood vessel regeneration in zebrafish caudal fins. *Dev Biol*. 2003; 264(1):263-274.

Huang J, McKee M, Huang HD, Xiang A, Davidson AJ, Lu HA. A zebrafish model of conditional targeted podocyte ablation and regeneration. *Kidney Int*. 2013.

Hyde DR, Godwin AR, Thummel R. In vivo electroporation of morpholinos into the regenerating adult zebrafish tail fin. *J Vis Exp*. 2012;(61). Doi(61):10.3791/3632.

Hynes M, Stone DM, Dowd M, et al. Control of cell pattern in the neural tube by the zinc finger transcription factor and oncogene gli-1. *Neuron*. 1997; 19(1):15-26.

Ingham PW, McMahon AP. Hedgehog signaling in animal development: Paradigms and principles. *Genes Dev*. 2001; 15(23):3059-3087.

"International Innovation". 2012; 43-46. http://www.unifr.ch/zoology/assets/files/Current%20Research_full.pdf

Iovine MK, Johnson SL. Genetic analysis of isometric growth control mechanisms in the zebrafish caudal fin. *Genetics*. 2000; 155(3):1321-1329.

Irvin BC, Tassava RA. Effects of peripheral nerve implants on the regeneration of partially and fully innervated urodele forelimbs. *Wound Repair Regen*. 1998; 6(4):382-387.

Itou J, Kawakami H, Burgoyne T, Kawakami Y. Life-long preservation of the regenerative capacity in the fin and heart in zebrafish. *Biol Open*. 2012; 1(8):739-746.

Jaillon O, Aury JM, Brunet F, et al. Genome duplication in the teleost fish tetraodon nigroviridis reveals the early vertebrate proto-karyotype. *Nature*. 2004; 431(7011):946-957.

Johnson RL, Laufer E, Riddle RD, Tabin C. Ectopic expression of sonic hedgehog alters dorsal-ventral patterning of somites. *Cell*. 1994; 79(7):1165-1173.

Johnson RL, Tabin C. The long and short of hedgehog signaling. *Cell*. 1995; 81(3):313-316.

Johnson SL, Weston JA. Temperature-sensitive mutations that cause stage-specific defects in zebrafish fin regeneration. *Genetics*. 1995; 141(4):1583-1595.

Johnson CK, Voss SR. Salamander paedomorphosis: linking thyroid hormone to life history and life cycle evolution. *Curr top dev biol*. 2013; 103:229-58.

Kaiser LR. The future of multihospital systems. *Top Health Care Financ*. 1992; 18(4):32-45.

Karlsson J, von Hofsten J, Olsson PE. Generating transparent zebrafish: A refined method to improve detection of gene expression during embryonic development. *Mar Biotechnol (NY)*. 2001; 3(6):522-527.

Katoh Y, Katoh M. Hedgehog signaling pathway and gastrointestinal stem cell signaling network (review). *Int J Mol Med*. 2006; 18(6):1019-1023.

Kent ML, Harper C, Wolf JC. Documented and potential research impacts of subclinical diseases in zebrafish. *ILAR J*. 2012; 53(2):126-134.

Khandekar G, Kim S, Jagadeeswaran P. Zebrafish thrombocytes: Functions and origins. *Adv Hematol*. 2012; 857058.

Kimmel CB, DeLaurier A, Ullmann B, Dowd J, McFadden M. Modes of developmental outgrowth and shaping of a craniofacial bone in zebrafish. *PLoS One*. 2010; 5(3):e9475.

Kishimoto N, Shimizu K, Sawamoto K. Neuronal regeneration in a zebrafish model of adult brain injury. *Dis Model Mech.* 2012:5(2): 200–209.

Kizil C, Kyritsis N, Dudczig S, et al. Regenerative neurogenesis from neural progenitor cells requires injury-induced expression of Gata3. *Dev Cell*. 2012; 23(6):1230-1237.

Kleinschnitz C, Brinkhoff J, Sommer C, Stoll G. Contralateral cytokine gene induction after peripheral nerve lesions: Dependence on the mode of injury and NMDA receptor signaling. *Brain Res Mol Brain Res*. 2005; 136(1-2):23-28.

Knecht S, Henningsen H, Elbert T, et al. Reorganizational and perceptional changes after amputation. *Brain*. 1996; 119 (Pt 4):1213-1219.

Knopf F, Hammond C, Chekuru A, et al. Bone regenerates via dedifferentiation of osteoblasts in the zebrafish fin. *Dev Cell*. 2011; 20(5):713-724.

Knox RJ, Boland MP, Friedlos F, Coles B, Southan C, Roberts JJ. The nitroreductase enzyme in walker cells that activates 5-(aziridin-1-yl)-2, 4-dinitrobenzamide (CB 1954) to 5-(aziridin-1-yl)-4-hydroxylamino-2-nitrobenzamide is a form of NAD(P)H dehydrogenase (quinone) (EC 1.6.99.2). *Biochem Pharmacol*. 1988; 37(24):4671-4677.

Koster RW, Fraser SE. FGF signaling mediates regeneration of the differentiating cerebellum through repatterning of the anterior hindbrain and reinitiation of neuronal migration. *J Neurosci*. 2006; 26(27):7293-7304.

Krauss S, Concordet JP, Ingham PW. A functionally conserved homolog of the drosophila segment polarity gene hh is expressed in tissues with polarizing activity in zebrafish embryos. *Cell*. 1993; 75(7):1431-1444.

Kroehne V, Freudenreich D, Hans S, Kaslin J, Brand M. Regeneration of the adult zebrafish brain from neurogenic radial glia-type progenitors. *Development*. 2011; 138(22):4831-4841.

Laforest L, Brown CW, Poleo G, et al. Involvement of the sonic hedgehog, patched 1 and bmp2 genes in patterning of the zebrafish dermal fin rays. *Development*. 1998; 125(21):4175-4184.

Lam CS, Marz M, Strahle U. gfap and nestin reporter lines reveal characteristics of neural progenitors in the adult zebrafish brain. *Dev Dyn.* 2009:238: 475–486.

Lanzky PF, Halling-Sorensen B. The toxic effect of the antibiotic metronidazole on aquatic organisms. *Chemosphere*. 1997; 35(11):2553-2561.

Lawson ND, Weinstein BM. In vivo imaging of embryonic vascular development using transgenic zebrafish. *Dev Biol*. 2002;248(2):307-318.

Lee Y, Hami D, De Val S, et al. Maintenance of blastemal proliferation by functionally diverse epidermis in regenerating zebrafish fins. *Dev Biol*. 2009; 331(2):270-280.

Lepilina A, Coon AN, Kikuchi K, et al. A dynamic epicardial injury response supports progenitor cell activity during zebrafish heart regeneration. *Cell*. 2006; 127(3):607-619.

Levesque M, Feng Y, Jones RA, Martin P. Inflammation drives wound hyperpigmentation in zebrafish by recruiting pigment cells to sites of tissue damage. *Dis Model Mech*. 2013; 6(2):508-515.

Li X, Montgomery J, Cheng W, Noh JH, Hyde DR, Li L. Pineal photoreceptor cells are required for maintaining the circadian rhythms of behavioral visual sensitivity in zebrafish. *PLoS One*. 2012; 7(7):e40508.

Lin G, Chen Y, Slack JM. Imparting regenerative capacity to limbs by progenitor cell transplantation. *Dev Cell*. 2013; 24(1):41-51.

Lopez-Schier H, Hudspeth AJ. Supernumerary neuromasts in the posterior lateral line of zebrafish lacking peripheral glia. *Proc Natl Acad Sci U S A*. 2005;102(5):1496-1501.

Mailleux AA, Tefft D, Ndiaye D, et al. Evidence that SPROUTY2 functions as an inhibitor of mouse embryonic lung growth and morphogenesis. *Mech Dev*. 2001; 102(1-2):81-94.

Major RJ, Poss KD. Zebrafish heart regeneration as a model for cardiac tissue repair. *Drug Discov Today Dis Models*. 2007; 4(4):219-225.

Marigo V, Roberts DJ, Lee SM, et al. Cloning, expression, and chromosomal location of SHH and IHH: Two human homologues of the drosophila segment polarity gene hedgehog. *Genomics*. 1995; 28(1):44-51.

Marigo V, Scott MP, Johnson RL, Goodrich LV, Tabin CJ. Conservation in hedgehog signaling: Induction of a chicken patched homolog by sonic hedgehog in the developing limb. *Development*. 1996; 122(4):1225-1233.

Marti E, Takada R, Bumcrot DA, Sasaki H, McMahon AP. Distribution of sonic hedgehog peptides in the developing chick and mouse embryo. *Development*. 1995; 121(8):2537-2547.

März M, Chapouton P, Diotel N, Vaillant C, Hesl B, Takamiya M, Lam CS, Kah O, Bally-Cuif L, Strahle U. Heterogeneity in progenitor cell subtypes in the ventricular zone of the zebrafish adult telencephalon. Glia. 2010:58: 870–888.

Melet F, Motro B, Rossi DJ, Zhang L, Bernstein A. Generation of a novel fli-1 protein by gene targeting leads to a defect in thymus development and a delay in friend virus-induced erythroleukemia. *Mol Cell Biol*. 1996; 16(6):2708-2718.

Metcalfe WK, Myers PZ, Trevarrow B, Bass MB, Kimmel CB. Primary neurons that express the L2/HNK-1 carbohydrate during early development in the zebrafish. *Development*. 1990; 110(2):491-504.

Metzger RJ, Klein OD, Martin GR, Krasnow MA. The branching programme of mouse lung development. *Nature*. 2008; 453(7196):745-750.

Mikkola HK, Fujiwara Y, Schlaeger TM, Traver D, Orkin SH. Expression of CD41 marks the initiation of definitive hematopoiesis in the mouse embryo. *Blood*. 2003; 101(2):508-516.

Miller LA, Wert SE, Clark JC, Xu Y, Perl AK, Whitsett JA. Role of sonic hedgehog in patterning of tracheal-bronchial cartilage and the peripheral lung. *Dev Dyn*. 2004; 231(1):57-71.

Ming JE, Roessler E, Muenke M. Human developmental disorders and the sonic hedgehog pathway. *Mol Med Today*. 1998; 4(8):343-349.

Minowada G, Jarvis LA, Chi CL, et al. Vertebrate sprouty genes are induced by FGF signaling and can cause chondrodysplasia when overexpressed. *Development*. 1999; 126(20):4465-4475.

Monaghan JR, Athippozhy A, Seifert AW, et al. Gene expression patterns specific to the regenerating limb of the Mexican axolotl. *Biol Open*. 2012; 1(10):937-948.

Montgomery JE, Parsons MJ, Hyde DR. A novel model of retinal ablation demonstrates that the extent of rod cell death regulates the origin of the regenerated zebrafish rod photoreceptors. *J Comp Neurol*. 2010; 518(6):800-814.

Morgan TH. Regeneration and liability to injury. *Science*. 1901; 14(346):235-248.

Moss JB, Koustubhan P, Greenman M, Parsons MJ, Walter I, and Moss LG. Regeneration of the pancreas in adult zebrafish. *Diabetes*. 2009; 58(8):1844-1851.

Munch J, Gonzalez-Rajal A, de la Pompa JL. Notch regulates blastema proliferation and prevents differentiation during adult zebrafish fin regeneration. *Development*. 2013; 140(7):1402-1411.

Murciano C, Fernandez TD, Duran I, et al. Ray-interray interactions during fin regeneration of danio rerio. *Dev Biol*. 2002; 252(2):214-224.

Nachtrab G, Czerwinski M, Poss KD. Sexually dimorphic fin regeneration in zebrafish controlled by androgen/GSK3 signaling. *Curr Biol*. 2011; 21(22):1912-1917.

Nachtrab G, Poss KD. Toward a blueprint for regeneration. *Development*. 2012; 139(15):2639-2642.

Nemtsas P, Wettwer E, Christ T, Weidinger G, Ravens U. Adult zebrafish heart as a model for human heart? An electrophysiological study. *J Mol Cell Cardiol*. 2010; 48(1):161-171.

Ochoa-Espinosa A, Affolter M. Branching morphogenesis: From cells to organs and back. *Cold Spring Harb Perspect Biol*. 2012; 4(10):10.1101/cshperspect.a008243.

Odent S, Atti-Bitach T, Blayau M, et al. Expression of the sonic hedgehog (SHH) gene during early human development and phenotypic expression of new mutations causing holoprosencephaly. *Hum Mol Genet*. 1999; 8(9):1683-1689.

Pellettieri J, Fitzgerald P, Watanabe S, Mancuso J, Green DR, Sanchez Alvarado A. Cell death and tissue remodeling in planarian regeneration. *Dev Biol*. 2010; 338(1):76-85.

Pepicelli CV, Lewis PM, McMahon AP. Sonic hedgehog regulates branching morphogenesis in the mammalian lung. *Curr Biol*. 1998; 8(19):1083-1086.

Phillips GJ. Green fluorescent protein--a bright idea for the study of bacterial protein localization. *FEMS Microbiol Lett*. 2001; 204(1):9-18.

Pisharath H, Parsons MJ. Nitroreductase-mediated cell ablation in transgenic zebrafish embryos. *Methods Mol Biol*. 2009; 546:133-143.

Pisharath H, Rhee JM, Swanson MA, Leach SD, Parsons MJ. Targeted ablation of beta cells in the embryonic zebrafish pancreas using E. coli nitroreductase. *Mech Dev*. 2007; 124(3):218-229.

Poleo G, Brown CW, Laforest L, Akimenko MA. Cell proliferation and movement during early fin regeneration in zebrafish. *Dev Dyn*. 2001; 221(4):380-390.

Poss KD, Keating MT, Nechiporuk A. Tales of regeneration in zebrafish. *Dev Dyn*. 2003; 226(2):202-210.

Poss KD, Shen J, Nechiporuk A, et al. Roles for fgf signaling during zebrafish fin regeneration. *Dev Biol*. 2000; 222(2):347-358.

Poss KD, Wilson LG, Keating MT. Heart regeneration in zebrafish. *Science*. 2002; 298(5601):2188-2190.

Poss KD. Advances in understanding tissue regenerative capacity and mechanisms in animals. *Nat Rev Genet.* 2010:11:710-22.

Puchtler, H, Meloan SN, Terry MS. "On the History and Mechanism of Alizarin Red S Stains for Calcium". *J. Histochem. Cytochem.* 1969:17 (2): 110–124.

Quint E, Smith A, Avaron F, et al. Bone patterning is altered in the regenerating zebrafish caudal fin after ectopic expression of sonic hedgehog and bmp2b or exposure to cyclopamine. *Proc Natl Acad Sci U S A*. 2002; 99(13):8713-8718.

Raya A, Consiglio A, Kawakami Y, Rodriguez-Esteban C, Izpisua-Belmonte JC. The zebrafish as a model of heart regeneration. *Cloning Stem Cells*. 2004; 6(4):345-351.

Reimschuessel R. A fish model of renal regeneration and development. *ILAR J*. 2001; 42(4):285-291.

Rennert RC, Sorkin M, Garg RK, Gurtner GC. Stem cell recruitment after injury: Lessons for regenerative medicine. *Regen Med*. 2012; 7(6):833-850.

Renshaw SA, Loynes CA, Trushell DM, Elworthy S, Ingham PW, Whyte MK. A transgenic zebrafish model of neutrophilic inflammation. *Blood*. 2006:108(13):3976-8.

Ribes V, Balaskas N, Sasai N, et al. Distinct sonic hedgehog signaling dynamics specify floor plate and ventral neuronal progenitors in the vertebrate neural tube. *Genes Dev*. 2010; 24(11):1186-1200.

Richardson R, Slanchev K, Kraus C, Knyphausen P, Eming S, Hammerschmidt M. Adult zebrafish as a model system for cutaneous wound-healing research. *J Invest Dermatol*. 2013; 133(6):1655-1665.

Rieger S, Sagasti A. Hydrogen peroxide promotes injury-induced peripheral sensory axon regeneration in the zebrafish skin. *PLoS Biol*. 2011; 9(5):e1000621.

Risau W. Mechanisms of angiogenesis. *Nature*. 1997; 386(6626):671-674.

Robbins DJ, Fei DL, Riobo NA. The Hedgehog Signal Transduction Network. *Sci. Signal.* 2012; 5(246):6.

Roelink H, Augsburger A, Heemskerk J, et al. Floor plate and motor neuron induction by vhh-1, a vertebrate homolog of hedgehog expressed by the notochord. *Cell*. 1994; 76(4):761-775.

Sadler KC, Krahn KN, Gaur NA, Ukomadu C. Liver growth in the embryo and during liver regeneration in zebrafish requires the cell cycle regulator, uhrf1. *Proc Natl Acad Sci U S A*. 2007; 104(5):1570-1575.

Sanchez Alvarado A. Q&A: What is regeneration, and why look to planarians for answers? *BMC Biol*. 2012; 10:88-7007-10-88.

Sanchez Alvarado A. Regeneration and the need for simpler model organisms. *Philos Trans R Soc Lond B Biol Sci*. 2004; 359(1445):759-763.

Santamaria JA, Mari-Beffa M, Becerra J. Interactions of the lepidotrichial matrix components during tail fin regeneration in teleosts. *Differentiation*. 1992; 49(3):143-150.

Sasaki H, Nishizaki Y, Hui C, Nakafuku M, Kondoh H. Regulation of Gli2 and Gli3 activities by an amino-terminal repression domain: Implication of Gli2 and Gli3 as primary mediators of shh signaling. *Development*. 1999; 126(17):3915-3924.

Scherz PJ, McGlinn E, Nissim S, Tabin CJ. Extended exposure to sonic hedgehog is required for patterning the posterior digits of the vertebrate limb. *Dev Biol*. 2007; 308(2):343-354.

Seifert AW, Voss SR. Revisiting the relationship between regenerative ability and aging. *BMC Biology*. 2013:11:2.

Serhan CN, Brain SD, Buckley CD, et al. Resolution of inflammation: State of the art, definitions and terms. *FASEB J*. 2007; 21(2):325-332.

Singer M. The influence of the nerve in regeneration of the amphibian extremity. *Q Rev Biol*. 1952; 27(2):169-200.

Singh SP, Holdway JE, Poss KD. Regeneration of amputated zebrafish fin rays from de novo osteoblasts. *Dev Cell*. 2012; 22(4):879-886.

Sire JY, Girondot M, Babiar O. Marking zebrafish, danio rerio (cyprinidae), using scale regeneration. *J Exp Zool*. 2000; 286(3):297-304.

Smith A, Avaron F, Guay D, Padhi BK, Akimenko MA. Inhibition of BMP signaling during zebrafish fin regeneration disrupts fin growth and scleroblasts differentiation and function. *Dev Biol*. 2006; 299(2):438-454.

Sousa S, Valerio F, Jacinto A. A new zebrafish bone crush injury model. *Biol Open*. 2012; 1(9):915-921.

Starnes TW, Huttenlocher A. Neutrophil reverse migration becomes transparent with zebrafish. *Adv Hematol.* 2012:398640.

Streisinger G, Walker C, Dower N, Knauber D, Singer F. Production of clones of homozygous diploid zebra fish (brachydanio rerio). *Nature*. 1981; 291(5813):293-296.

Suzuki T, Takano Y. Comparative immunohistochemical studies of p53 and proliferating cell nuclear antigen expression and argyrophilic nucleolar organizer regions in pancreatic duct cell carcinomas. *Jpn J Cancer Res*. 1993; 84(10):1072-1077.

Tal TL, Franzosa JA, Tanguay RL. Molecular signaling networks that choreograph epimorphic fin regeneration in zebrafish - a mini-review. *Gerontology*. 2010; 56(2):231-240.

Tassava RA, Olsen-Winner CL. Responses to amputation of denervated ambystoma limbs containing aneurogenic limb grafts. *J Exp Zool A Comp Exp Biol*. 2003; 297(1):64-79.

Taub R. Liver regeneration: From myth to mechanism. *Nat Rev Mol Cell Biol*. 2004; 5(10):836-847.

Tefft JD, Lee M, Smith S, et al. Conserved function of mSpry-2, a murine homolog of drosophila sprouty, which negatively modulates respiratory organogenesis. *Curr Biol*. 1999; 9(4):219-222.

Thatcher EJ, Paydar I, Anderson KK, Patton JG. Regulation of zebrafish fin regeneration by microRNAs. *Proc Natl Acad Sci U S A*. 2008; 105(47):18384-18389.

Thompson MA, Ransom DG, Pratt SJ, et al. The cloche and spadetail genes differentially affect hematopoiesis and vasculogenesis. *Dev Biol*. 1998; 197(2):248-269.

Thummel R, Bai S, Sarras MP, Jr, et al. Inhibition of zebrafish fin regeneration using in vivo electroporation of morpholinos against fgfr1 and msxb. *Dev Dyn*. 2006; 235(2):336-346.

Towers M, Mahood R, Yin Y, Tickle C. Integration of growth and specification in chick wing digit-patterning. *Nature*. 2008; 452(7189):882-886.

Trevarrow B, Marks DL, Kimmel CB. Organization of hindbrain segments in the zebrafish embryo. *Neuron*. 1990; 4(5):669-679.

Tu S, Johnson SL. Fate restriction in the growing and regenerating zebrafish fin. *Dev Cell*. 2011; 20(5):725-732.

Tweedle C. Transneuronal effects on amphibian limb regeneration. *J Exp Zool*. 1971; 177(1):13-29.

Van Eeden FJ, Granato M, Schach U, et al. Genetic analysis of fin formation in the zebrafish, danio rerio. *Development*. 1996; 123:255-262.

Varjosalo M, Taipale J. Hedgehog: Functions and mechanisms. *Genes Dev*. 2008; 22(18):2454-2472.

Wenemoser D, Reddien PW. Planarian regeneration involves distinct stem cell responses to wounds and tissue absence. *Dev Biol*. 2010; 344(2):979-991.

Westerfield M. 2000. The zebrafish Book. University of Oregon Press.

White YA, Woods DC, Wood AW. A transgenic zebrafish model of targeted oocyte ablation and de novo oogenesis. *Dev Dyn*. 2011; 240(8):1929-1937.

Whitehead GG, Makino S, Lien CL, Keating MT. Fgf20 is essential for initiating zebrafish fin regeneration. *Science*. 2005; 310(5756):1957-1960.

Xu Q, Guo L, Moore H, Waclaw RR, Campbell K, Anderson SA. Sonic hedgehog signaling confers ventral telencephalic progenitors with distinct cortical interneuron fates. *Neuron*. 2010; 65(3):328-340.

Yokoyama H. Initiation of limb regeneration: The critical steps for regenerative capacity. *Dev Growth Differ*. 2008; 50(1):13-22.

Yuasa T, Kataoka H, Kinto N, et al. Sonic hedgehog is involved in osteoblast differentiation by cooperating with BMP-2. *J Cell Physiol*. 2002; 193(2):225-232.

Zhang J, Jeradi S, Strahle U, Akimenko MA. Laser ablation of the sonic hedgehog-a-expressing cells during fin regeneration affects ray branching morphogenesis. *Dev Biol*. 2012; 365(2):424-433.

Zhang J, Wagh P, Guay D, et al. Loss of fish actinotrichia proteins and the fin-to-limb transition. *Nature*. 2010; 466(7303):234-237.

Zhao XF, Ellingsen S, Fjose A. Labelling and targeted ablation of specific bipolar cell types in the zebrafish retina. *BMC Neurosci*. 2009; 10:107-2202-10-107.

Zhu H, Bendall AJ. Dlx5 is a cell autonomous regulator of chondrocyte hypertrophy in mice and functionally substitutes for Dlx6 during endochondral ossification. *PLoS One*. 2009;4(11):e8097.

Zunich SM, Douglas T, Valdovinos M, et al. Paracrine sonic hedgehog signalling by prostate cancer cells induces osteoblast differentiation. *Mol Cancer*. 2009; 8:12-4598-8-12.

Zupanc GK. Adult neurogenesis and neuronal regeneration in the central nervous system of teleost fish. *Brain Behav Evol*. 2001; 58(5):250-275.

Zupanc GK, Sirbulescu RF. Teleost fish as a model system to study successful regeneration of the central nervous system. *Curr Top Microbiol Immunol*. 2013; 367:193-233.

Appendix I

List of primers for the PCR reaction

1. **CFP-NTR (for 1380 bp DNA fragment):**

   Forward primer: AAGGGCGAGGAGCTGTTCA

   Reverse primer: TAAGGTGATGTTTTGCGGCAGA

2. **CFP (for 653 bp DNA fragment):**

   Forward primer: GCGACGTAAACGGCCACAAG

   Reverse primer: TACAGCTCGTCCATGCCGAG